

Cover Page



Universiteit Leiden



The handle <http://hdl.handle.net/1887/138643> holds various files of this Leiden University dissertation.

Author: Zhang, Z.

Title: Group benefits from genomic instability: A tale of antibiotic warriors in *Streptomyces*

Issue date: 2020-12-14

Group benefits from genomic instability

a tale of antibiotic warriors in *Streptomyces*

Zheren Zhang

张哲人

Ph.D. thesis, Leiden University, 2020

Zheren Zhang was supported by the China Scholarship Council.

Cover design: Lianru Zhang

Illustrated abstracts: Shraddha Shitut

Layout: Zheren Zhang

ISBN: 978-94-6416-328-5

Copyright © 2020 by Zheren Zhang

Group benefits from genomic instability

a tale of antibiotic warriors in *Streptomyces*

Proefschrift

ter verkrijging van
de graad van Doctor aan de Universiteit Leiden,
op gezag van Rector Magnificus prof. mr. C.J.J.M. Stolker,
volgens besluit van het College voor Promoties
te verdedigen op maandag 14 December 2020
klokke 16:15 uur

door

Zheren Zhang
geboren te Xinyang, China
in 1991

Promotoren:

Dr. D. E. Rozen
Prof. dr. D. Claessen
Prof. dr. G. P. van Wezel

Promotiecommissie:

Prof. dr. P. G. L. Klinkhamer (voorzitter)
Prof. dr. B. E. Snaar-Jagalska (secretaris)
Dr. K. Riebel
Prof. dr. D. K. Aanen
Prof. dr. P. Hoskisson

Table of contents

Chapter 1	7
General introduction	
Chapter 2	13
Understanding microbial divisions of labor	
Chapter 3	26
Antibiotic production is organized by a division of labor in <i>Streptomyces</i> through terminal genomic differentiation	
Chapter 4	44
Mutational meltdown of microbial altruists in <i>Streptomyces coelicolor</i> colonies	
Chapter 5	60
Proteomic and metabolomic changes driven by spontaneous genomic rearrangements in <i>Streptomyces coelicolor</i>	
Chapter 6	75
General discussion	
Nederlandse samenvatting	82
References	84
Appendix I Supplementary materials for Chapter 2	105
Appendix II Supplementary materials for Chapter 3	109
Appendix III Supplementary materials for Chapter 4	125
Appendix IV Supplementary materials for Chapter 5	139
Curriculum vitae	153
List of publications	154

Chapter 1

General introduction

Although invisible to our eyes, bacteria constitute the largest and most biodiverse domain of life on earth (1, 2). Similar to animals and plants, bacteria also display a broad diversity of morphologies, ranging from unicellular species with different shapes to multicellular groups taking distinct forms and manners of organization (3, 4). The physiology and morphology of bacteria reflect how they adapt to their living environment, offering a gigantic repository for microbiologists to study. Within the diversity of bacteria, *Streptomyces* are particularly noteworthy because of several exceptional features. The filamentous *Streptomyces* are a large genus within the phylum Actinobacteria. *Streptomyces* predominantly live in soil but can also be found in aquatic sediments (5, 6). Different from many other bacteria, *Streptomyces* produce spores that germinate to produce branching vegetative mycelia. Hyphae extend into the soil, growing from their tips, and secrete a large repertoire of proteases, cellulases and chitinases that allow these bacteria to break down insoluble organic materials arising from the decay of fungi, plants and animals. When these resources are exhausted, mycelia undergo a developmental shift from vegetative growth to aerial growth, followed by sporulation leading to another cycle of life (7–9) (Fig. 1). This shift is accompanied by the production of an enormous diversity of secreted secondary metabolites (10, 11), including many antimicrobial compounds; indeed, *Streptomyces* antibiotics and antifungals include a majority of the antimicrobials used in clinical practice (12, 13). For example, streptomycin, produced by *Streptomyces griseus*, was one of the first discovered antibiotics in this genus (14). Daptomycin which is used as one of the last resort antibiotics is also produced by *Streptomyces roseosporus* (15). Although these antimicrobials have important value in human medicine, they are also ecologically important for the bacteria that make them. They provide advantages for ecologically invasion and defense (16). But as this thesis will show, antibiotics are metabolically expensive to produce which has led to novel evolutionary strategies to mitigate these costs.

Both because of their multicellular lifestyle as well as their prolific production of secondary metabolites, streptomycetes are of unique fundamental and applied importance. However, an important challenge to continue the commercial exploitation of these organisms is the fact that streptomycetes display enormous genomic instability, an attribute that can lead to the alteration of functions that are relevant to their economic value, especially the production of antibiotics (17–20).

Phenotypic heterogeneity due to genomic instability has been recognized for more than half a century (21). This was initially identified through observation of frequent loss of certain phenotypes, including formation of aerial hyphae and sporulation, pigmentation, antibiotic resistance and amino acid synthesis. Instability occurs spontaneously at a frequency of higher than 0.1% per spore in numerous species (22), while DNA damaging agents can further increase it several-fold (23, 24). This latter aspect suggested that phenotypic changes were caused by underlying genetic changes. Later, the development

of more modern molecular methods (e.g., pulsed-field gel electrophoresis and DNA hybridization) allowed scientists to directly associate phenotypic changes with genomic rearrangements, often revealed to be massive amplifications and deletions to the genome (25–32). Studies since the 1980s highlighted hotspots where amplifications tend to arise, named as the amplifiable unit of DNA (AUD) (33). These AUD structures exist in many different species and can be amplified to a few to thousands of copies designated as amplified DNA sequences (ADS), which regularly coincide with extensive deletions at the edges of genome (25–30). At the beginning of the 21st century, the advances of whole genome sequencing improved our understanding of the linear nature of *Streptomyces* chromosomes (34, 35). The ~9Mb linear chromosome in *Streptomyces* contains a centrally located origin of replication and core functions and two arms on the two sides that contain more dispensable functions. At the end of the two arms, terminal inverted repeats (TIRs) are found that bear covalently bound terminal proteins (TPs). These arms are typically where the gross genomic rearrangements occur (36). Other than the general description of the fact that genomic instability arises from extensive genomic rearrangements, the precise mechanisms that either trigger or suppress these diverse phenomena remain unknown, thereby placing limits on our ability to control these processes for commercial gain. Moreover, until the work in this thesis, there has been very little effort to understand these phenomena in evolutionary or ecological terms.

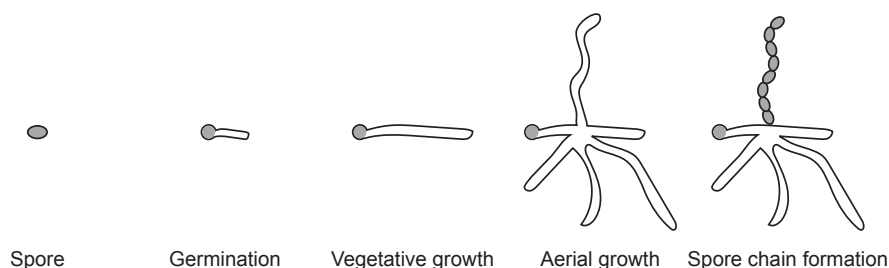


Fig. 1. A schematic representation of the *Streptomyces* life cycle on solid surfaces.

A spore germinates to form vegetative mycelia which extend into the substrate to absorb nutrients. Afterwards, aerial mycelia grow out from the vegetative mycelia. During this transition, secondary metabolites including antibiotics are produced for their ecological benefits. Aerial hyphae will eventually form spore chains that stay dormant until the next life cycle.

Beyond earlier studies focusing on commercially important streptomycetes, we have found that bacteria freshly isolated from the soil (37) also display genomic instability (Fig. 2). This implies that the genomic instability seen in an industrial setting is not an artifact of this condition and leads to the question of the natural role of the exceptionally high rates of phenotypic heterogeneity and genomic rearrangements in streptomycetes.

More specifically, what are the evolutionary and ecological consequences of genomic instability in these bacteria? Both theory and experiments have shown that bacterial mutation rates can evolve (38–40). On the one hand, because most new mutations are likely to be deleterious, natural selection will tend to reduce the mutation rate (41, 42). This occurs by increasing the accuracy and efficiency of mechanisms of DNA replication and repair (43). On the other hand, mutations are the ultimate source of adaptive change, thus an increased mutation rate can sometimes be adaptive because this will facilitate the fixation of beneficial mutations (44, 45). This is best exemplified in a medical setting where many bacterial pathogens evolve mutator genotypes, leading to more rapid evolution of antibiotic resistance (46). However, the rates of mutation, even in these mutators, are several orders of magnitude lower than genomic instability appears to be in wild-type streptomycetes (47, 48). Why are these bacteria so prone to variation? Does genomic instability offer benefits and in which ecological contexts? And what are the costs of this instability?

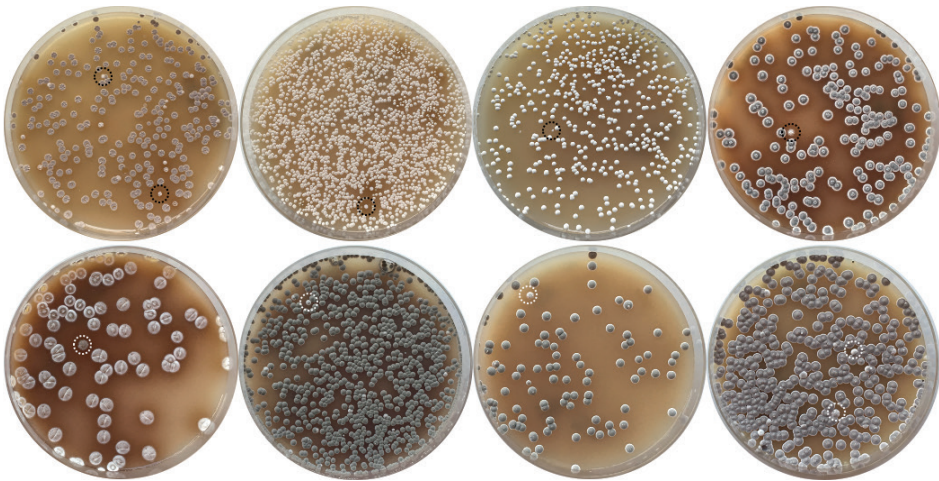


Fig. 2. Genomic instability is common in freshly isolated actinomycetes from soil. Plates show colonies of eight individual actinomycete strains after 3–4 days of growth. While the majority of colonies shows a wild-type morphology, aberrant phenotypes with altered growth and / or pigmentation are present at a high frequency (indicated by white and black cycles).

Understanding genomic instability in streptomycetes therefore sits at the intersection of many important applied and fundamental questions in microbiology. The aim of this thesis is to elucidate the evolutionary functions, mechanisms and consequences of genomic instability in *Streptomyces*, by focusing on the model species *Streptomyces coelicolor*.

Division of labor is used in multicellular organisms to coordinate mutually incompatible functions and to increase group efficiency. It is defined as the situation where individual cells within a body or sub-populations within societies perform complementary tasks to increase fitness of the organism or colony (49–52). This definition ideally requires identifying the extent and causes of preexisting phenotypic variation, cooperation and/or altruism and a quantitative estimate of adaptative benefits (50). Microbes offer unique opportunities to assess these features, and the last several years have seen a significant increase in cases of microbial division of labor. To understand this concept better, and to frame our later discussion of division of labor in *Streptomyces* colonies, in **Chapter 2**, we review recent articles and discuss causes and implications of division of labor in microbes. First by focusing on multicellularity as a representative example of germ:soma division of labor in *Myxococcus* and *Dictyostelium*, we debate how the idea of caste ratios in social insects can be compared to spore production in microbes and how kin selection can work as a mechanism in maintaining cooperation against cheating. Later, we consider division of labor in patterned multicellular bacteria, using examples from cyanobacteria and streptomycetes. This is followed by a more general discussion of additional possibilities for division of labor in *Streptomyces* and how these types of studies have been performed in other bacteria.

Hyperpigmentation is frequently observed in colony variants of *S. coelicolor* generated due to genomic instability. The few known antibiotics produced by *S. coelicolor* are pigmented. We therefore investigated the hypothesis that instability coordinated a division of labor related to antibiotic production in *S. coelicolor*. Through utilizing diverse techniques from microbial evolution and different omics approaches, **Chapter 3** provides a new insight into how antibiotic production is coordinated in *S. coelicolor* through terminal differentiation of their genome. We show that the emergence of mutants, at a rate of approximately 1%, creates variants that have reduced fitness but elevated amounts and diversity of antibiotics. These changes scale with the size of genome deletions, resulting in a clear trade-off between antibiotic production and fitness. By performing competition experiments in a mixture of mutants and wild-type cells, we confirmed that a division of labor occurs between mutants and wild-type that increases colony-wide fitness.

Since mutants are less fit than their parental wild-type, they are rapidly eliminated in the colony by competition. In **Chapter 4**, in order to learn the genetic fate of mutants after their emergence, we extended our study to a series of transfers to simulate spore-to-spore reproduction happening across colonies. Results show that mutants with initial genome deletions continue to suffer from further deletions. This reveals the same trade-off, as above, namely that continued deletions to both left and right chromosome arms reduce the fitness of strains, by decreasing spore production markedly. Mutants also tend to become mutators which accelerates the base-substitution mutation rate, and therefore the rate of deleterious mutations. Taken together, these results suggest that mutants in

Chapter 1

S. coelicolor are similar to sterile castes in social insects. Due to diverse and continuous genomic damage, they are readily eliminated during colony growth and therefore need to be reestablished anew in every developing colony. These data add a new dimension to the idea of mutational meltdown, since gross genomic deletions work together with the emergence of increased mutation rates and competitive declines to guarantee that mutant lineages rapidly go extinct.

In **Chapter 5** we used mass spectrometry-based proteomics and metabolomics to study the effects of genomic rearrangements in *S. coelicolor*. We confirmed that the increased antibacterial activity is caused by overproduction of their antibiotics. More specifically, we observed upregulation of many proteins in three known antibiotic biosynthetic gene clusters. Additionally, several key developmental proteins are downregulated in mutants, leading to their reduced fitness. This chapter provides detailed molecular information of how the trade-off between antibiotics and fitness is mediated by genomic differentiation, which helps us to better understand the division of labor in *S. coelicolor* colonies

Results obtained in the other chapters are discussed in **Chapter 6** as are future perspectives for studying genomic instability in *Streptomyces* and other multicellular bacteria.

Chapter 2

Understanding microbial divisions of labor

Zheren Zhang, Dennis Claessen and Daniel E. Rozen
Institute of Biology, Leiden University, Leiden, the Netherlands

Published in
Frontiers in Microbiology (2016).
DOI: 10.3389/fmicb.2016.02070

Abstract

Divisions of labor are ubiquitous in nature and can be found at nearly every level of biological organization, from the individuals of a shared society to the cells of a single multicellular organism. Many different types of microbes have also evolved a division of labor among its colony members. Here we review several examples of microbial divisions of labor, including cases from both multicellular and unicellular microbes. We first discuss evolutionary arguments, derived from kin selection, that allow divisions of labor to be maintained in the face of non-cooperative cheater cells. Next we examine the widespread natural variation within species in their expression of divisions of labor and compare this to the idea of optimal caste ratios in social insects. We highlight gaps in our understanding of microbial caste ratios and argue for a shift in emphasis from understanding the maintenance of divisions of labor, generally, to instead focusing on its specific ecological benefits for microbial genotypes and colonies. Thus, in addition to the canonical divisions of labor between e.g., reproductive and vegetative tasks, we may also anticipate divisions of labor to evolve to reduce the costly production of secondary metabolites or secreted enzymes, ideas we consider in the context of streptomycetes. The study of microbial divisions of labor offers opportunities for new experimental and molecular insights across both well-studied and novel model systems.

Introduction

It is often stated that there is “strength in numbers”. Bigger armies tend to conquer smaller ones, while giant flocks of starlings migrate more efficiently than a single bird on its own. But what is the source of the added value in having more individuals? In some cases it is pure power, e.g., a pride of lions that is more effective at subduing large prey through the simple benefit of added strength. However, in many other examples, the benefit of numbers derives from the fact that larger groups of individuals can segregate tasks, thereby allowing them to diversify into teams of coordinated specialists that can accomplish more together than the simple sum of their parts. The understanding of this “division of labor” has its origin in studies of human economics, but the central idea is of equal importance across the diversity of life and at virtually every scale of biological organization (49, 50, 53). Social insects clearly exemplify divisions of labor at the level of a society of individuals (53). Within a colony of leaf cutter ants, potentially containing millions of individuals, there are soldiers who defend the nest, foragers that travel far and wide gathering leaves, gardeners of many types to tend to the specialized fungal gardens these ants require for nourishment, and nurses to rear offspring, among many others (54). Narrowing our view to the level of a single individual, multicellular organisms also are characterized by a division of labor among distinct cell and tissue types that each play specialized roles in maintaining the fitness of the whole organism. However, divisions of labor are not the unique privilege of animals. As we discuss below, many microbes also divide tasks among clone-mates, and these divisions can have far-reaching effects for colony-level fitness.

In the interest of space, we only briefly discuss the evolutionary advantages of a division of labor and instead refer interested readers to the numerous excellent reviews on the topic in multicellular organisms or microbes (49, 50, 53). However, we review several key features in order to guide the remaining text. Divisions of labor in a society or a single organism require the coexistence of multiple types, or subpopulations, that interact and are specialized to carry out complementary tasks (49). In microbial colonies, each sub-type can be derived from a single parental cell in response to environmental change (e.g., starvation) via deterministic or stochastic processes (55). Differentiation into functionally distinct cell types, whether it arises from genetic or regulatory changes, requires cooperation among these types, which is maintained by their shared evolutionary interests via kin selection, whereby individuals sacrifice individual fitness for the sake of related individuals (50). Importantly, differentiated colonies have higher fitness than those lacking a division of labor. This benefit typically results from the added efficiency of dividing tasks between cells rather than a single cell either switching between these tasks or carrying them out simultaneously, although other advantages can be envisioned (49, 50, 56–58). In addition, it is important to note that phenotypic diversification does not necessarily represent a division of labor, as heterogeneity among cells can provide

individual benefits that may have no effects on the group or even reduce colony fitness. Accordingly, by our strict definition, divided complementary tasks must increase population fitness to be identified as a division of labor. As made clear in table S1, these criteria have only been experimentally verified in a handful of cases, although divisions of labor are nevertheless often assumed to be present. In examples we discuss below, e.g., the division of labor between vegetative growth and sporulation, differentiated tasks are mutually incompatible and cannot be carried out by a single cell at once. Using these generalized features, we next consider specific examples of divisions of labor before focusing our attention on streptomycetes.

Divisions of labor in multicellular microbes

Although microbes often live solitary lives, many phylogenetically divergent groups have independently evolved different levels of coordinated or patterned multicellularity (59). These can be facultative, in the case of biofilms that develop from the aggregation and proliferation of independent cells, or can be an obligate component of the microbial life-cycle. The latter group, microbes that display obligate patterned multicellularity, offer the most dramatic examples of divisions of labor. This is because these groups are characterized by terminal differentiation into reproductive and non-reproductive cells that mimic the divisions between germ and soma in plants or animals (59–62). In addition to offering insights into the evolution of microbial multicellularity and a division of labor, the examples we consider also provide the best evidence of the central factors that ensure that these divisions are stably maintained. Here, there is necessary overlap with conditions that maintain cooperative behaviors against “cheats” more generally (63–66).

Maintaining divisions of labor with aggregative multicellularity

Myxobacteria are social bacteria with a multicellular lifestyle (56, 59). When growing in the presence of abundant resources, vegetative cells in the best studied species, *Myxococcus xanthus*, hunt socially via the coordinated secretion of lytic enzymes that digest bacterial and fungal prey (56, 67, 68). Upon starvation, they undergo a dramatic transition where individual cells migrate together to create fruiting bodies containing $\sim 10^5$ cells. Fruiting bodies in *Myxococcus xanthus* contain three differentiated cell types: spores, which comprise around 10% of the fruiting body, peripheral rods that comprise another 10–30%, and then the rest that die and lyse during development via a process assumed to be programmed cell death (PCD) (59, 60, 69).

Spores are the most easily understood of the myxobacterial cell types, as these are the cells that persist through environmental deprivation and stress. Moreover, the benefit of their survival is direct and immediate. By contrast, any benefits of coordinated development for the other cell types are likely to be indirect, especially for the 60–80% of cells fated to die. If the death of these cells is caused by PCD, what explains their altruistic self-

sacrifice? The simplest explanation is kin selection: as stalk cells are the clone mates of spores, their sacrifice is repaid indirectly when related spores survive (56). Accordingly, it is assumed that PCD in these stalk cells directly increases spore numbers or the probability of spore survival, although the mechanisms by which this might occur remain unclear (70). One possibility is that stalk cells aid in spore dispersal, perhaps by elevating them above the substrate. Another argument is that material from lysed cells, e.g. lipid bodies, is incorporated into the spore or spore coat which works to increase spore hardness (71, 72). Despite suggestive evidence for both possibilities, neither option has been validated experimentally.

It could be argued that a detailed understanding of the mechanisms by which stalk or peripheral rod cells contribute to spore survival is not needed, as we can already adequately explain the evolutionary maintenance of a division of labor among clonal groups of cells by kin selection. However, two areas of research would benefit from a fuller understanding of these mechanisms: (i) the division of labor in non-clonal groups, an area that has already been studied extensively, and (ii) explaining the relative frequencies of cell types within and across genotypes, a topic that has been largely neglected. Why, for example, do 10% of cells become spores instead of 5%, 50% or even 100%? Is this value fixed across strains or do strains vary in their allocation to spores or stalk cells? And can cell type frequencies for any given strain respond adaptively to environmental contingencies? Analogous questions have long been posed in the context of social insects using the terminology of the caste ratio (73, 74). We believe a similar framework would be valuable for microbes. We address each of these areas in turn.

Labile divisions of labor

Altruism among clone-mates can be explained by kin selection. However, both in the lab and in nature, there is evidence that myxobacterial fruiting bodies can be comprised of mixed genotypes where the benefits of altruistic behaviors are strongly reduced (56, 75, 76). Where relatedness among strains in fruiting bodies is low, there is strong selection for the evolution of “cheats” that seek to benefit at the expense of others by increasing their own representation within the population of spores (75, 77, 78). In one study, socially defective mutants that arose during selection for rapid growth lost the ability to sporulate in isolation; however, when these cells were mixed with wild-type clones they were able to increase in frequency, potentially by utilizing the developmental signals of wild-type cells, although the mechanisms are not fully understood (76, 79, 80). Natural isolates also show significant variation in spore output across several orders of magnitude, and as with laboratory evolved clones, these wild-type variants can also exploit one another in chimeric fruiting bodies (56, 75, 81). These cheats have led to the evolution of diverse mechanisms to distinguish kin from non-kin (82, 83), an issue we will consider later on. Interestingly, these interactions also provide suggestive evidence that the division of

labor in myxobacteria is socially contingent; whereas strains in isolation produce a fixed number of spores, this value can vary during competitive interactions. However, at present, it remains unclear how competitive interactions affect the allocation behavior of different genotypes to different cell types, the caste ratio, and if this is dependent on the identity of competing strains. For example, it is possible that exploitative strains grown as chimeras increase their individual spore output by decreasing allocation to peripheral cells or cells that die via PCD; in other words, competition leads to an adaptive change in the caste ratio. Alternatively, the caste ratio of these strains may remain unchanged, even while total spore number increases, if these strains are able to increase total cell numbers at the expense of their competitors. The key issue with respect to divisions of labor is to distinguish how cells behave in isolation from their behavior in mixtures. Does the caste ratio change, and if so, does it change in both competitors or in one competitor at the expense of the other? Additionally, it is crucial to quantify how these changes influence spore survival—the presumed reason these cells divide labor at all.

Some of these questions have been considered in an analogous microbial system: the social eukaryote *Dictyostelium discoideum*. Like myxobacteria, dictyostelids live as asocial bacterivores that, upon starvation, aggregate together and differentiate into a multicellular fruiting body containing spores and altruistic stalk cells (plus several other minority cell types) (84, 85). When genetically different strains are mixed together to form chimeric fruiting bodies, one strain often appears to gain unfair representation in the spores (86–88). While these “winner” strains have been labeled cheaters, alternative explanations, not based on exploitation, could lead to the same outcome. Like myxobacteria, there is extensive natural variation among *Dictyostelium* genotypes for caste ratios (86). Cells of some strains primarily differentiate into spores during development, while in other strains, most cells in fruiting bodies differentiate into stalk cells. When strains of these two extremes are mixed, it is easy to see that the former would produce the majority of spores. However, this may not be the result of changes to caste ratios, as maintaining a “fixed” strategy—behaving in mixtures just as you would when alone—also leads to competitive differences between strains. Indeed, knowing the caste ratio of a strain grown in isolation is almost perfectly predictive of its spore production in chimeric fruiting bodies (86). This predictability makes clear, in a way that has not yet been possible in myxobacteria, that deviations in divisions of labor can have dramatic consequences for microbial social behaviors and interactions.

If *Dictyostelium* strains that differentiate a greater fraction of cells into spores are apparently socially dominant, why don't all strains utilize a similar division of labor? The answer, it turns out, lies in the fact that allocation decisions are coupled to trade-offs in spore size, number and viability. Strains with high proportions of spore:stalk, those that “win” during social competition, tend to make many smaller spores that individually have reduced viability (89). By contrast, strains that divide labor by differentiating a greater fraction of cells into

stalk, tend to make fewer larger spores that each have higher viability. Accordingly, what “winners” gain in terms of spore numbers, they lose in terms of spore viability, and this leads to an overall equivalence in the fitness of strains. Of course, this equivalence leads back to the original question of why different strategies exist—and here there are no clear answers, because we simply lack an understanding of why these microbes divide labor to begin with. Recent work in *Dictyostelium* focusing on a third type of cell that remains vegetative and fails to aggregate during starvation, has suggested that variance in starvation times (i.e., seasonality) can allow for the coexistence of different division of labor strategies (90, 91). By this mechanism one could envision that if spores of different sizes also differ in the duration of dormancy or their sensitivity to cues required to exit dormancy, then different divisions of labor could arise across a heterogeneous landscape. At present, this remains untested. It does, however, emphasize the need to supplement kin selection arguments for the evolutionary maintenance of microbial divisions of labor with a more detailed understanding of the ecological factors that lead to the coexistence of different division of labor strategies in nature.

Cheating and kin recognition

Whether via fixed strategies, as outlined above, or via “facultative” adjustments to caste ratios (86), it is clear that microbial divisions of labor can have profound effects on social interactions between strains. In response to this, many microbes have evolved mechanisms of kin discrimination to ensure that altruistic behaviors are preferentially directed towards clone mates (61, 83, 92). In multicellular microbes like myxobacteria or *Dictyostelium*, both active and passive mechanisms (93, 94) work to keep different genotypes apart. Highly polymorphic cell-surface-mediated matching systems in both microbes allow strains to distinguish self from non-self. While some of the genes underlying these responses are known (e.g., *tra* or *tgr* loci in myxobacteria or *Dictyostelium*, respectively) (83, 92, 95) it is also apparent that mechanisms of exclusion can evolve rapidly via diverse mechanistic routes (82). In other cases, strains can remain spatially segregated by passive means if the migration of cells is highly restricted or if population sizes remain low, thus reducing the encounter rate of different strains (93, 94). Regardless of the mechanisms used by strains to insulate themselves from social exploitation, it is clear that these mechanisms are effective; fruiting bodies of both myxobacteria and *Dictyostelium* are most often clonal in nature (75, 96, 97). Thus, it is likely that the different divisions of labor that distinguish strains are maintained for reasons that may have little to do with social challenges, but rather because of ecological benefits to specific strategies that are contingent on the environment where strains are growing.

Divisions of labor in patterned multicellularity

Several groups of multicellular microbes display forms of patterned multicellularity where divisions of labor arise following the outgrowth of a single cell, much like the

2 multicellularity that characterizes animals or plants (59). In contrast to the aggregative multicellular microbes discussed above, cells in these species are physically attached to one another and form filaments with semi-permeable cross-walls and growth at the filament tips. These features, which ensure clonality, largely insulates these groups from social exploitation from within. In addition, because of their high relatedness, microbial colonies with patterned multicellularity tend to contain more cells/biomass as well as a larger diversity of cell types (98).

In filamentous cyanobacteria, photosynthetic microbes responsible for a large fraction of our planet's primary production, some species have evolved strategies to differentiated into two cell types that segregate chemically incompatible tasks – photosynthesis and nitrogen fixation (99). Some of them, e.g., *Anabaena* spp. terminally differentiate around 5-10% of their cells into specialized cells, called heterocysts, that carry out nitrogen fixation. As with myxobacterial cells that undergo PCD, heterocysts in *Anabaena* are unable to divide and are thus reproductively sterile (100). Alternatively, in some non-heterocystous species, e.g., *Plectonema boryanum*, a temporal division of labor is employed to allow cells to pursue both photosynthesis and nitrogen fixation by switching between both functions on the basis of an externally driven circadian rhythm. Mathematical studies have suggested that compared to temporal divisions of labor, spatially segregating incompatible tasks, such as in *Anabaena*, can overcome biochemical constraints between distinct pathways and thereby maximize the production of biomass from the available light or nitrogen (57). In addition, this physical division of labor offsets time or resource costs associated with alternating between two distinct metabolic systems, while theoretical studies have suggested that the ratio of heterocysts to vegetative cells has evolved to maximize carrying capacity under conditions of high light (100). Interestingly, cyanobacterial divisions of labor are labile and can be regulated depending on environmental conditions. For example, in the presence of a utilizable nitrogen source, thus reducing the requirement for endogenous nitrogen fixation, the filaments of *Anabaena* or *Nostoc* form homogenous filaments of vegetative cells that remain undifferentiated (99, 101). Such flexibility is analogous to the flexible caste ratios seen in social insects, e.g., in the ant *Pheidole pallidula*, where the production of soldier pupae and adult soldiers both increase under threat of foreign workers from unrelated colonies (73). Filamentous cyanobacteria generate several other classes of differentiated cell types, such as akinetes, that act as durable spores and arise during conditions of starvation (99, 102). However, it is as yet unclear how the fraction of cells that adopt these states is determined.

Another example of a division of labor in patterned microbial multicellularity can be found in streptomycetes which are filamentous spore-forming bacteria that are widespread in terrestrial and aquatic environments (9, 59). Streptomycete colonies arise following the germination of a single spore which gives rise to a multi-chromosomal mycelium that superficially resembles that of filamentous fungi (10). These multicellular

organisms forage on complex organic materials that are converted into small molecules using secreted proteases, cellulases and chitinases (11). Upon nutrient depletion behind an actively growing colony front, a developmental program is initiated allowing these bacteria to escape harsh environmental conditions (8, 9). This leads to the formation of aerial hyphae that differentiate into uni-genomic spores. The energetic burden associated with the formation of these reproductive structures is thought to be supported by the partial degradation of the vegetative mycelium via PCD (103, 104). Because streptomycete colonies are physically attached to one another and are the clonal products of division and growth from a single spore, kin selection can also explain this apparently altruistic PCD (105). In addition, the architecture of streptomycete colonies appears to largely insulate strains from mutations that give rise to less PCD or from exploitation from strains via colony fusion (106, 107). PCD within streptomycete colonies is coupled to the production of numerous secondary metabolites, some of which have strong antimicrobial properties (10). As starvation is an environmental cue for sporulation, these antimicrobials are thought to prevent competitive soil bacteria in the same nutrient-deprived environment from benefiting from the nutrients released during PCD (108, 109). The central molecular mechanism that connects PCD to antibiotic production is the pleiotropic transcriptional repressor DasR, which prevents antibiotic production during vegetative growth. Colony dismantling during PCD leads to the extracellular accumulation of cell wall-derived *N*-Acetylglucosamine (GlcNAc) around the colony periphery. Internalization and modification of GlcNAc subsequently yields glucosamine-6-phosphate (GlcN-6P), which can allosterically bind to DasR thereby relieving its repressing activity (110). As such, this switch is considered a robust timing mechanism to maximize the colony-wide benefits while reducing the potential harm of PCD (108, 109).

The vegetative and reproductive growth phases in streptomycetes represent a clear example of a division of labor: the vegetative hyphae are programmed to forage, while the reproductive hyphae lead to stable spores that can persist through starvation and potentially migrate to more fruitful resource patches (10). Notably, these processes are also mutually incompatible due to their distinct physical positions in the colony itself. Unlike vegetative hyphae which grow radially from a colony center through the substrate, aerial hyphae are physically separated from potential nutritional resources. Instead, they emerge from the colony surface and protrude up into the air (111). To achieve this, they become enveloped by a hydrophobic surface layer that possibly serves two roles: it maximizes successful spore dispersal, but also prevents hyphae from growing back into the substrate. The vegetative hyphae, on the other hand, have a more hydrophilic nature which may make them better suited to thrive in soils, whose natural minerals, such as silica, are hydrophilic (111).

Divisions of labor beyond sporulation

2 In parallel with the myxobacteria or *Dictyostelium*, the most obvious divisions of labor in streptomycetes concern those arising during sporulation. However, both in this and other systems, additional divisions of labor are likely to arise if colony-wide benefits can be obtained at the expense of a small fraction of cells (49, 50). In particular, we expect these to be found for secreted products, like antibiotics or enzymes, whose effects can be shared by producers and non-producers alike and whose production is metabolically costly. Thus, by differentiating a subset of specialized cells dedicated to production at the cost of their own replication, colonies can potentially increase overall efficiency. Antibiotic production in *Streptomyces* offers a clear test of this possibility. The species in this genus are prolific antibiotic producers that are responsible for some 70% of all antibiotics used in human and veterinary medicine (9). Because antibiotic biosynthesis is metabolically costly and can trade-off with growth, it is conceivable that production and secretion by only a fraction of the hyphae would offer resource savings, yet be sufficient to provide benefits to the entire colony. Concomitantly, the antibiotic non-producing hyphae could continue foraging while transporting nutrients to other parts of the colony. At present, there are few data to support the existence of a trade-off between growth and secretion nor data on the form this trade-off takes (112), either for antibiotics or other secreted products; however, we suspect this is more for lack of looking than true absence. Indeed, in similarly structured filamentous networks of fungal hyphae, increasing evidence supports the idea that there is considerable heterogeneity across the colony in the production of costly secreted enzymes (113–116). Gene expression and translational activity in *Aspergillus* is spatially variable leading to subclasses of differentiated hyphae that adopt distinct functional roles (115). At the colony periphery, minority fractions of hyphae highly express secreted proteins, including glucoamylase, acid amylase, α -glucuronidase and feruloyl esterase, that are essential for resource acquisition. This apparent division of labor enables a small fraction of the total colony biomass to focus on enzyme secretion and foraging, while the majority remains in a so-called “battery-saving” transcriptional status (116, 117). Convincing experiments have clarified that hyphal heterogeneity in *Aspergillus oryzae* is regulated by restrictions to cytoplasmic streaming, regulated by Woronin bodies that transiently block septa between fungal compartments (117). Although further work is required to quantify the potential ecological advantages of this division of labor, as well as the form of the trade-offs that may govern it (112), it has been argued that it facilitates colony-wide responses to unpredictable environmental stress (118). Additionally, it remains unclear which environmental factors serve as cues for differentiation, and whether different strains vary in these responses to these cues. Despite the considerable differences between filamentous bacteria and fungi, their convergent morphologies suggest that similar divisions of labor may have evolved in both groups to reduce the costs and increase the efficiency of secreted products, especially given recent results conclusively demonstrating effective cytoplasmic streaming in streptomycetes (119, 120).

As research into microbial divisions of labor expand, more examples are identified, even in species that lack the types of patterned multicellularity outlined above. For example, in *Bacillus subtilis* biofilms, flagellum-independent migration can be conducted by the collective action of two cell types: surfactin-producing cells and those that produce matrix (121). While surfactin production works as a lubricant to reduce the obstruction between cells and substrate, matrix producing cells assemble themselves into so-called van Gogh bundles that can migrate over greater distances than would be possible without this division of labor. During this process, *srfA*, which coordinates surfactic production, is up-regulated via quorum sensing, which in turn triggers the up-regulation of *tapA* resulting in the production of matrix. Importantly, there are strong trade-offs between *srfA* and *tapA*, which likely underpins why cells segregate tasks in this system (121).

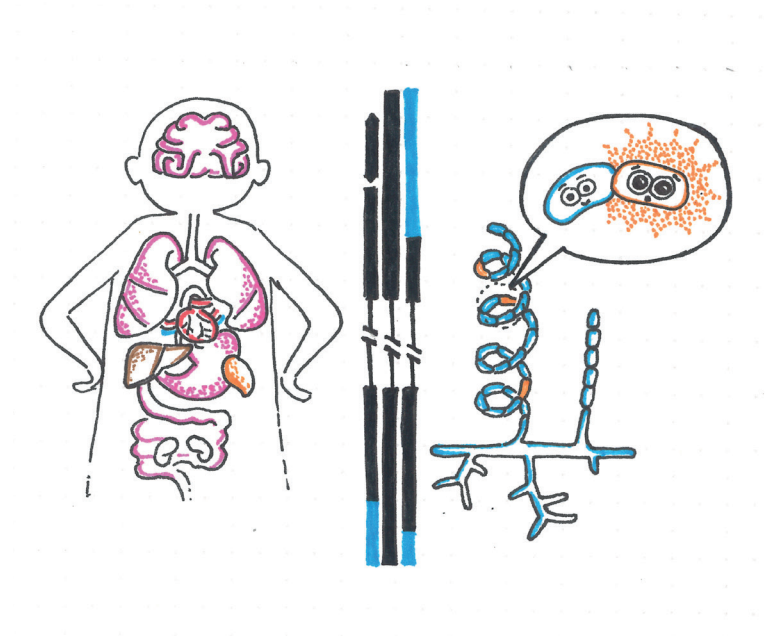
In a more recent study using *Pseudomonas fluorescens*, similar cooperative interactions evolved that affected migration and led to increased colony-wide mobility and fitness (58, 122). Notably, the cooperative division of labor that was seen in these experiments arose *de novo* during laboratory evolution, indicating that divisions of labor can appear stably with relative ease over very short evolutionary timeframes. Here, rather than surfactin and matrix production, D-cells, corresponding to a “dry” morphotype, evolved from an otherwise homogeneous parental M-cell that expressed a mucoid morphology. While D-cells grew within the center of the colony, forming a fan-like structure, M-cells were pushed towards the colony edge. This led to increased mobility of the entire colony, greater acquisition of territory, and presumably increased access to resources at the colony edge. Amazingly, the evolution of this division of labor required only a single nucleotide mutation for D-cells to arise, which altered the concentrations of the intracellular messenger cyclic-di-GMP and thereby potentially changed the expression of hundreds of genes directly or indirectly regulated by this second messenger. This result underscores the fact that although divisions of labor can result in highly complex and tightly orchestrated phenotypes, they can arise by very few mutational events, although these mutations may be accompanied by highly pleiotropic effects (58). In addition, we anticipate that this type of experimental study will be instrumental in helping to identify the ecological conditions that facilitate the emergence of microbial divisions of labor.

Conclusions and perspectives

Microbial divisions of labor have been best studied in the more general context of microbial sociality and multicellularity. The diverse examples presented above and shown in table S1 from different systems and functional roles highlight that divisions of labor rely on high relatedness and kin selection. However, although kin selection provides a powerful explanation for how divisions of labor are maintained, this approach is less able to explain the extensive variation observed in divisions of labor across different genotypes

Chapter 2

within species. Equally, it is limited in its ability to explain the conditions under which divisions of labor arise. ESS (evolutionarily stable strategy) models may help to resolve these questions (50), an effort that must be further informed by a greater understanding of the ecological benefits of divisions of labor in the conditions where they evolved. Finally, given the apparent ease with which divisions of labor evolve in the laboratory (58), experimental evolution offers unparalleled opportunities to address these questions mechanistically and phenotypically in highly tractable experimental systems.



Chapter 3

Antibiotic production in *Streptomyces* is organized by a division of labor through terminal genomic differentiation

Zheren Zhang¹, Chao Du¹, Frédérique de Barsy¹, Michael Liem¹, Apostolos Liakopoulos¹, Gilles P. van Wezel¹, Young Hae Choi^{1,2}, Dennis Claessen¹ and Daniel E. Rozen¹

1. Institute of Biology, Leiden University, Leiden, the Netherlands

2. College of Pharmacy, Kyung Hee University, Seoul, Republic of Korea

Published in

Science Advances (2020).

DOI: 10.1126/sciadv.aay5781

Abstract

One of the hallmark behaviors of social groups is division of labor, where different group members become specialized to carry out complementary tasks. By dividing labor, cooperative groups increase efficiency, thereby raising group fitness even if these behaviors reduce individual fitness. We find that antibiotic production in colonies of *Streptomyces coelicolor* is coordinated by a division of labor. We show that *S. coelicolor* colonies are genetically heterogeneous because of amplifications and deletions to the chromosome. Cells with chromosomal changes produce diversified secondary metabolites and secrete more antibiotics; however, these changes reduce individual fitness, providing evidence for a trade-off between antibiotic production and fitness. Last, we show that colonies containing mixtures of mutants and their parents produce significantly more antibiotics, while colony-wide spore production remains unchanged. By generating specialized mutants that hyper-produce antibiotics, streptomycetes reduce the fitness costs of secreted secondary metabolites while maximizing the yield and diversity of these products.

Introduction

Social insects provide some of the most compelling examples of division of labor, with extremes in morphological differentiation associated with highly specialized functions and reproductive sterility in all colony members, except the queen (123). However, conditions that select for division of labor are not limited to animals, and it has become increasingly clear that microbes offer unique opportunities to identify and study the mechanistic underpinnings of divisions of labor (49–51, 58, 121, 124, 125). First, microbes are typically clonal, which helps ensure that a division of labor is favored by kin selection (50). Second, microbial populations are highly social, often cooperating to carry out coordinated behaviors such as migration or biofilm formation that require the secretion of metabolically expensive public goods that can be shared among clonemates (66, 126). If these conditions are met, and investment in public good secretion trades off with fitness, divisions of labor are predicted to evolve (50, 127).

Here, we describe the cause and evolutionary benefits of a unique division of labor that has evolved in colonies of the filamentous actinomycete *Streptomyces coelicolor*. After germinating from uni-chromosomal spores, these bacteria establish multicellular networks of vegetative hyphae, reminiscent of fungal colonies (8, 9, 59). Vegetative hyphae secrete a broad variety of public goods, such as chitinases and cellulases that are used to acquire resources, as well as a chemically diverse suite of antibiotics that are used to kill or inhibit competing organisms (10, 11, 128). Streptomyces are prolific producers of antibiotics and are responsible for producing more than 50% of our clinically relevant antibiotics (13). Although the terminal differentiation of *Streptomyces* colonies into vegetative hyphae (soma) and viable spores (germ) is well understood (129–131), no other forms of division of labor in these multicellular bacteria are known. However, opportunities for phenotypic differentiation are possible, because although colonies begin clonally, they can become genetically heterogeneous because of unexplained high-frequency rearrangements and deletions in their large, ~9-Mb linear chromosome (22, 26, 27, 29). The work we describe shows that these two phenomena are intertwined. Briefly, we find that genomic instability causes irreversible genetic differentiation within a subpopulation of growing cells. This differentiation, in turn, gives rise to a division of labor that increases the productivity and diversity of secreted antibiotics and increases colony-wide fitness.

Results

Genomic instability and phenotypic heterogeneity are coupled

Genomic instability and phenotypic heterogeneity have been observed in several *Streptomyces* species (17, 20, 132–136), but there are no explanations for the evolution or functional consequences of this extreme mutability. To begin addressing this question, we quantified the phenotypic heterogeneity arising within 81 random single colonies of *S.*

3 *coelicolor* M145 by harvesting the spores of each of these colonies and then replating the collected spores onto a new agar surface. Although most progeny are morphologically homogeneous and similar to the wild-type (WT), notably aberrant colonies arise at high frequencies ($0.79 \pm 0.06\%$, mean \pm SEM, ranging from 0 to 2.15%, $n = 81$) (Fig. 1A). Similarly high rates were obtained on two minimal media (MM: $2.13 \pm 0.14\%$; MM + casamino acids: $5.13 \pm 0.37\%$; mean \pm SEM; $n = 30$ and $n = 40$, respectively) (fig. S1), thereby ruling out the possibility that these mutations are an artifact of rapid growth on rich resources. The differences we observed on these two media types also suggest that the mutant frequencies we estimated based on spore counts may underestimate their values within growing colonies, given that mutants may be compromised in growth or sporulation (as we confirm below). This is supported by the nearly two-fold difference in mutant frequencies on MM + casamino acids compared to unsupplemented MM, where auxotrophs arising by mutation would be unable to persist. To determine the heritability of these aberrant phenotypes, we restreaked 15 random colonies from different plates onto a new agar plate, which revealed remarkable variability in colony morphology (Fig. 1B). Rather than reverting to the WT morphology, as would be anticipated if the initial heterogeneity was due to phenotypic plasticity or another form of bistability, the colonies derived from mutant colonies are themselves hypervariable, giving rise to up to nine diverse phenotypes from any single colony. Thus, in the course of two cycles of colony outgrowth, an array of colony types that differ in size, shape, and color emerged (Fig. 1B). Because our ability to discern colony heterogeneity is limited to only a few visually distinct phenotypic characters, we assume that these estimates of diversity are lower than their true level of occurrence.

Using whole-genome sequencing of eight random mutants, we confirmed that these isolates contained profound chromosomal changes. As shown in Fig. 2A, large genome deletions were observed at the chromosome ends in all eight strains. In three cases, we found an ~ 297 -kb amplification on the left chromosomal arm flanked by the Insertion Sequence *IS1649*, encoded by SCO0091 and SCO0368. Average sequence coverage of the amplified region suggests that it contains between 2 and 15 copies of this amplification (Fig. 2A and fig. S2). Sequencing results were expanded using pulsed-field gel electrophoresis (PFGE) analysis of 30 mutant isolates (Fig. 2B and fig. S3). Consistent with our sequencing results, this analysis revealed that mutants contain variably sized deletions of up to ~ 240 or ~ 872 kb on the left chromosome arm and up to 1.6 Mb on the right chromosome arm, deleting more than 1000 genes. In addition, 8 of 30 strains contained the same large amplification between copies of *IS1649* as noted above. These strains are conspicuously yellow, which might be caused by the overproduction of carotenoids due to the amplification of the *crt* gene cluster (SCO0185-0191) (35, 137, 138). In addition to this and other phenotypic effects associated with these changes that are discussed below, deletions to the right chromosome arm cause the loss of two loci, *argG* (SCO7036) and *cmlR1* (SCO7526)/*cmlR2* (SCO7662), that result in two easily scorable phenotypes: arginine

auxotrophy and chloramphenicol susceptibility, respectively. Scoring these phenotypes allows rapid determination of the minimal size of the deletion on the right chromosome arm in the absence of molecular characterization. Chloramphenicol susceptibility indicates a deletion of at least 322 kb, while the addition of arginine auxotrophy indicates a deletion of at least 843 kb (Fig. 2B).

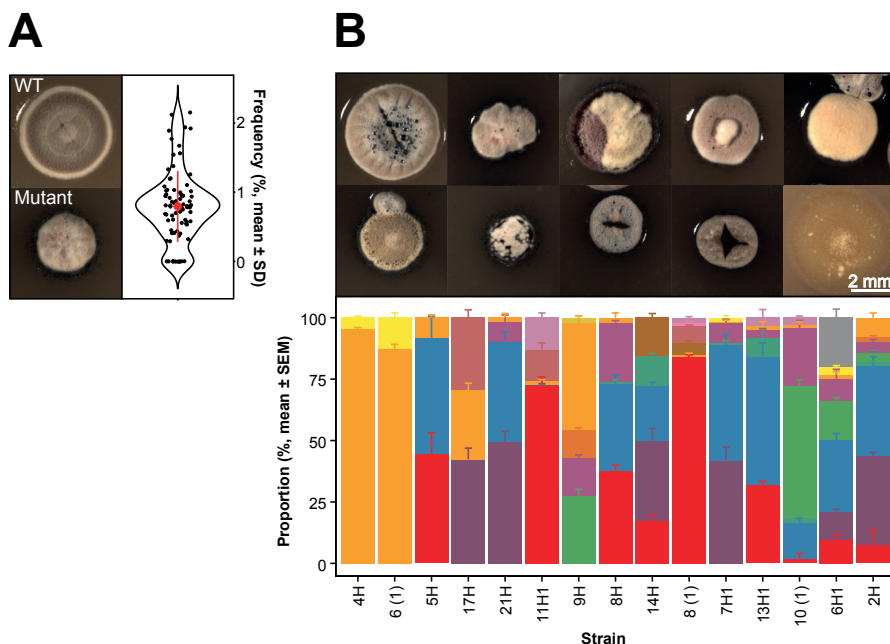
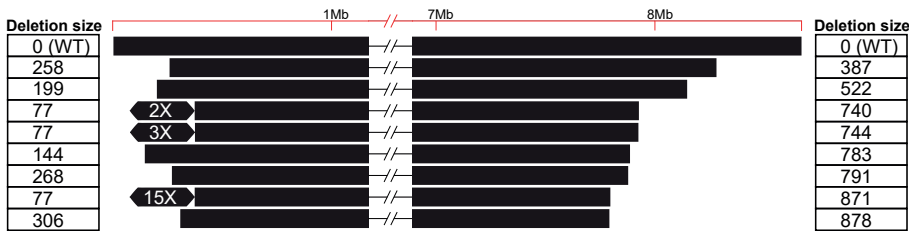


Fig. 1. Emergence of phenotypic heterogeneity in colonies of *S. coelicolor*. (A) WT (top) and mutant (bottom) colonies and the frequency that mutants emerge from WT colonies on SFM agar (right). (B) Phenotypically diverse progeny (top) emerge after restreaking mutant colonies that vary in size, shape, and pigmentation. Representative colonies are shown. The bottom graph depicts the range of distinct morphologies that emerge after restreaking 15 random colonies. Each color represents a distinct colony phenotype.

Mutants increase the production and diversity of antibiotics

Mutant strains were conspicuously pigmented when compared to their parental WT strains (Fig. 1). Because several antibiotics produced by *S. coelicolor* are pigmented, namely, actinorhodin, prodigines, and coelimycin P1, which are blue, red, and yellow, respectively, we tested whether mutant strains had altered secondary metabolite and inhibitory profiles. Secreted metabolites from mutant and WT strains grown on agar surfaces were analyzed using quantitative ^1H nuclear magnetic resonance (NMR) profiling (139, 140).

A



B

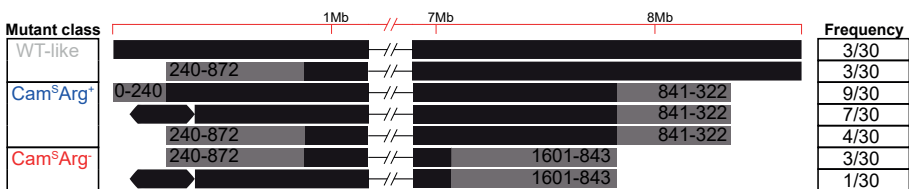


Fig. 2. Genome diversity of mutant colonies determined from whole-genome sequencing and PFGE. Values in (A) correspond to the size (in kilobases) of genome deletions, while the hexagons represent an ~297-kb genome amplification. Each line in (B) depicts the range of deletion sizes (gray) in each mutant class, together with their respective frequencies from 30 sampled mutant strains.

Principal components analysis (Fig. 3A) supports the partition of strains into three well separated groups: WT and WT-like strains and then two clusters of mutant isolates. In each case, groupings corresponded to the size of genomic lesions mentioned above. More specifically, strains grouping in the WT and WT-like cluster were chloramphenicol resistant (Cam^R) and arginine prototrophic (Arg⁺), while those clustering within the blue ellipse were chloramphenicol susceptible (Cam^S) and arginine prototrophic (Arg⁺), and those in the red ellipsed cluster were chloramphenicol susceptible (Cam^S) and arginine auxotrophic (Arg⁻). To assess whether genomic deletions affected antibiotic biosynthesis, we used mass spectrometry (MS)-based quantitative proteomics on five representative strains from the two mutant clusters. This analysis revealed that the biosynthetic pathways for actinorhodin, coelimycin P1, and calcium-dependent antibiotic were significantly upregulated in all mutants (Fig. 3, B and C; fig. S4; and table S1). Because the expression level of biosynthetic enzymes directly correlates with antibiotic production (141), these MS results are consistent with increased antibiotic production in these strains (Fig. 3, B to D; fig. S4; and table S1). In addition to antibiotic biosynthesis clusters, pathways regulating arginine and pyrimidine biosynthesis were also increased in both arginine auxotrophic

strains (fig. S4B and table S1) (142). No antibiotic-related proteins were downregulated in this analysis.

We next asked whether these different metabolic and proteomic profiles translated to differences in biological activity, specifically the ability to inhibit the growth of other bacteria. Thirty mutant strains were grown on agar plates and then covered with a soft agar overlay containing *Bacillus subtilis*. Inhibition was visualized as an absence of growth surrounding the mutant colony, and the extent of inhibition was determined from the size of the inhibition zone. As shown in Fig. 3D, mutant strains produced significantly larger zones of inhibition than the WT strain (26 of 30; one-tailed one-sample *t* tests, all $P < 0.05$). In addition, we observed significant heterogeneity among mutant strains in halo size [one-way analysis of variance (ANOVA), $F_{29,90} = 5.45$, $P < 0.001$].

To test whether the increased inhibition we observed against *B. subtilis* was correlated with the ^1H NMR profiles, we used a partial least-squares regression (Fig. 3E) (140). This confirmed that the separation into different groups significantly correlates with the halo size ($Q^2 = 0.879$), which was further validated by both permutation tests and ANOVA of crossvalidated residuals (CV-ANOVA, $F_{8,116} = 104.443$, $P < 0.001$). To identify possible compounds that are overproduced in mutants compared to WT, we identified several ^1H NMR signals that varied across strains and strongly correlated with the size of the zone of inhibition against *B. subtilis* (table S2); notable among these are several aromatic signals, which correspond to actinorhodin, consistent with our proteomic analyses (Fig. 3, B and C; fig. S4; and table S1).

Phenotypic results indicate that mutant strains produce more antibiotics than their WT parent when assayed against a single bacterial target, as anticipated given our NMR and proteomic results. However, they do not distinguish whether strains can be further partitioned on the basis of which other species they inhibit. Score plots of principal components analysis based on ^1H NMR signals reveal clear separation between mutant clones within and between clusters (Fig. 3A), suggesting that their inhibitory spectra may vary. In addition, quantitative proteomic data show that different strains vary in their production of known antimicrobials. To test this, we measured the ability of four mutant clones to inhibit 48 recently isolated *Streptomyces* strains (37). *Streptomyces* targets were chosen because these are likely to represent important competitors for other streptomycetes in soil environments. At least one of the four mutant strains produced a significantly larger halo than the WT strain against 40 of 48 targets, indicating increased inhibition (Fig. 3F). For these 40 targets, we observed significant differences between the mutant strains themselves. We found differences in the size of the zone of inhibition on different target species (two-way ANOVA, $F_{39,117} = 21.21$, $P < 0.001$) as well as a significant interaction between mutant strain and the target species (two-way ANOVA, $F_{117,320} = 5.83$, $P < 0.001$), indicating that the inhibitory profile of each mutant strain is distinct from the



Fig. 3. Secondary metabolite production in mutant strains determined by ^1H NMR, quantitative proteomics, or zones of inhibition on *B. subtilis* or 40 different natural streptomycete isolates. (A) Principal components (PC) analysis plot of ^1H NMR data. Each cluster enclosed in a colored ellipse (with 95% confidence interval) corresponds to a mutant class with a different phenotype and degree of genomic instability: WT-like strains (gray), Cam^SArg⁺ strains (blue), and Cam^SArg⁻ strains (red). (B and C) Volcano plots of MS-based quantitative proteomics of two representative strains 9H1A (Cam^SArg⁻) (B) and 9H1B (Cam^SArg⁺) (C). Protein level is indicated by the size of the dot, and genes with ≤ 2 -fold change and/or $P \geq 0.05$ are grayed out. (D) Zones of inhibition of each strain when grown with a *B. subtilis* soft agar overlay. Colors represent the same mutant classes as in (A). The large dot represents the mean of four replicates, while error bars represent the SE. (E) Partial least-squares (PLS) plot of ^1H NMR data partitioned by the same clusters as in (A). The heat map indicates the size of the zone of inhibition on *B. subtilis*. (F) Zones of inhibition of four representative mutant strains with an overlay of 40 different natural streptomycetes, each represented by a different line. Statistics are given in the main text.

others. Together, these results reveal that mutants arising within colonies not only are more effective at inhibiting other strains but also are diversified in who they can inhibit because their inhibition spectra do not overlap. They also suggest that the beneficiary of diversified antibiotic secretion is the parent strain, because competing bacteria are unlikely to be resistant to this broadened combination of secreted antimicrobials.

Antibiotic production is coordinated by a division of labor

Having shown that *Streptomyces* colonies differentiate into distinct subpopulations that vary in their antibiotic production, we next asked how this differentiation affects colony fitness. To answer this, we measured the fitness of each mutant strain by quantifying the number of spores they produce when grown in isolation. As shown in Fig. 4A, mutants produce significantly fewer spores than the WT strain (28 of 30; two-sample t tests, $P < 0.05$) and, in extreme cases, as much as 10000-fold less, with significant heterogeneity among strains (one-way ANOVA, $F_{29,59} = 132.57$, $P < 0.001$). The reduction in spore production is significantly negatively correlated with antibiotic production ($F_{1,29} = 26.58$, $r^2 = 0.478$, $P < 0.001$) (fig. S5A). This provides evidence that antibiotic production is costly to *S. coelicolor* and that there is a direct trade-off between antibiotic production and reproductive capacity, possibly because energy is redirected from development to antibiotic production (143). In addition, we observed a significant negative correlation between the size of the genome deletion and colony-forming unit (CFU) ($F_{1,7} = 12.32$, $r^2 = 0.638$, $P = 0.0099$) and a positive correlation between the deletion size and bioactivity against *B. subtilis* ($F_{1,7} = 37.97$, $r^2 = 0.844$, $P < 0.001$), suggesting that these phenotypes scale with the magnitude of genomic changes (Fig. 4B).

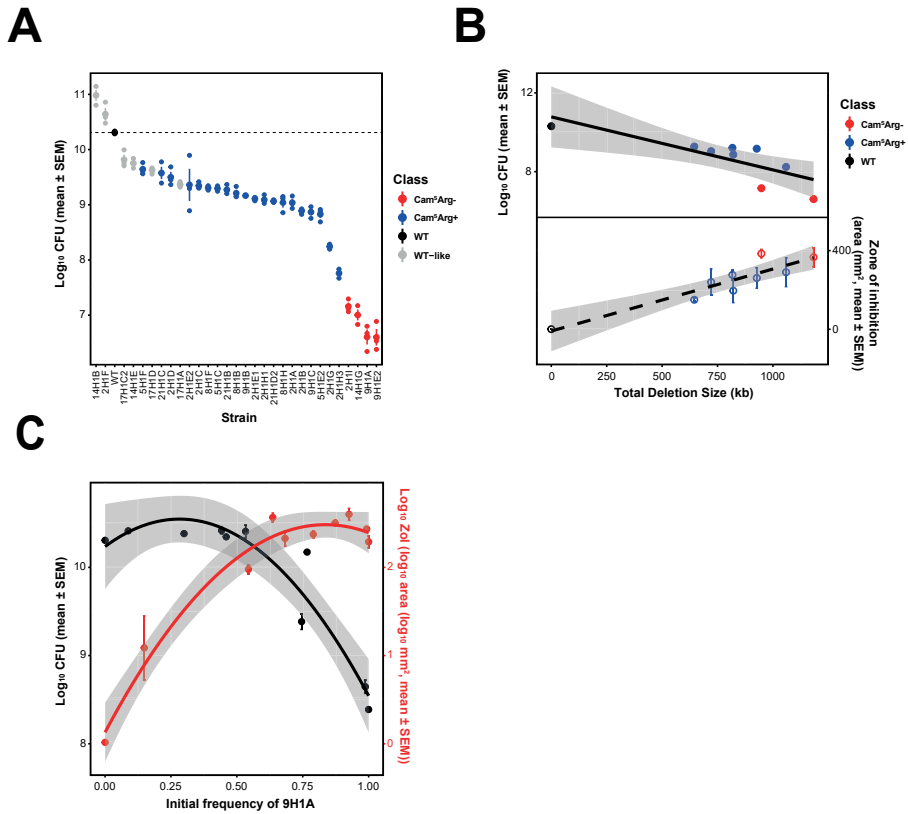


Fig. 4. Fitness of mutant strains grown alone or during coculture with the WT strain and the effects of genome deletions on fitness and antibiotic production. (A) Fitness [colony-forming unit (CFU)] of mutant strains. **(B)** Decreases in genome size negatively correlate with fitness (top) and positively correlate with antibiotic production (bottom). **(C)** Division of labor during coculture of the WT and strain 9H1A at different starting frequencies. Increasing frequencies of 9H1A cause increased antibiotic production ($F_{2,7} = 107.7$, $r^2 = 0.969$, $P < 0.001$) (red) but only negatively affect colony fitness at frequencies $> \sim 50\%$ ($F_{2,7} = 37.95$, $r^2 = 0.916$, $P < 0.001$) (black). Quadratic regression lines include the 95% confidence interval.

To examine the effects of mutant strains on the colony as a whole, we mixed mutant strains with their WT parent at increasing frequencies and quantified colony-wide spore production and the ability of these mixtures to kill *B. subtilis*. We measured responses across a broad range of initial mutant frequencies to reflect the large variation in these values across media types and colonies and to also address uncertainties in their frequencies and spatial distribution during colony growth. Results of these experiments, shown in Fig. 4C, support two important conclusions: (i) Increasing fractions of mutants

lead to increased antibiotic production, and (ii) although mutant strains have individually reduced fitness (fig. S5B), their presence within colonies has no effect on colony-wide spore production, until the mutant frequency exceeds >50% of the total. We carried out the same assay with three additional mutant clones, but at fewer frequencies, to estimate spore production and observed concordant results (fig. S6): Up to a frequency of ~50%, mutant strains have no effect on colony-wide spore production, while each incremental increase in the frequency of these strains enhances colony-wide antibiotic output. These results indicate that the benefits of producing cells with chromosomal lesions are evident across a broad range of frequencies, but that even with extremely high mutation rates, the costs to colony-wide fitness are minimal or entirely absent.

Discussion

Streptomycetes are prolific producers of antibiotics, with genomes typically containing more than 20 secondary metabolite gene clusters that comprise more than 5% of their entire genome (35, 144, 145). They invest heavily in these products, and their biosynthesis and secretion are costly. Our results suggest that, by limiting antibiotic production to a fraction of the colony through division of labor, *S. coelicolor* can eliminate the overall costs of biosynthesis while maximizing both the magnitude and diversity of their secreted antibiotics. Although this comes at a large individual cost, it increases group fitness by improving the ability for *S. coelicolor* to inhibit their competitors. Moreover, our results reveal that the range of conditions that select for a division of labor are quite broad, because colony-wide fitness is unaffected, even if mutant strains are as frequent as ~50%.

Division of labor is predicted to be favored in this system for several reasons. First, *Streptomyces* colonies emerge from a single spore and are clonal (129). This fact, together with their filamentous mode of growth, ensures that costly individual traits can be maintained because of their indirect fitness benefits (50, 51, 59). In addition, because resistance to the diversified antibiotic profile of mutant strains is unlikely to be present in competing strains, only the parent strain stands to benefit from their sacrifice. Second, the costs of antibiotic production via large and dedicated multistep biosynthetic pathways, e.g., nonribosomal peptide or polyketide synthases, are likely to be highest at the initiation of antibiotic production but diminish thereafter, meaning that producing cells become more efficient at making antibiotics through time (127); furthermore, we show that antibiotic production trades off with reproduction. Last, many antibiotics are secreted, so the entire colony, but not susceptible competitors, can benefit from the protection they provide (146).

Even if conditions predispose to a division of labor, there must still be a process that generates phenotypic heterogeneity. Our results show that, in *Streptomyces*, this is caused by genomic instability that creates a subpopulation of cells within colonies that contain large deletions or amplifications at the termini (26, 29, 136). These mutations are severe

and irreversible. Because strains, or portions of colonies, containing these deletions have significantly reduced fitness, they effectively behave like a sterile caste that provide direct benefits to the rest of the colony and receive little in return (123). Even when the initial frequency of mutants in mixed colonies approaches 80%, their final frequency declines to less than 1% after one cycle of colony growth (fig. S7). This suggests that the division of labor in *S. coelicolor* is reestablished independently and differently in each colony, a mechanism that may help to maximize the diversity of secreted antibiotics.

3 It remains unclear whether there are mechanisms regulating the size and frequency of chromosomal deletions and amplifications. One possibility is that these events are induced by external environmental conditions and that their rate is context dependent. Instability can be elevated by exposure to certain toxicants, e.g., mitomycin C or nitrous acid (24), although no explicit stress was added in the experiments we report, and it also varies with media type. It may also be increased during competition with other strains, a process that is known to alter the secretion of secondary metabolites (128, 147). Another possibility is that deletions and the benefits they bring for antibiotic production are a fortuitous by-product of the cell death that accompanies development (129). By this argument, chromosome degradation would be regulated but would not always be lethal. Although we have not confirmed this experimentally, it is likely that conserved amplifications result from the flanking copies of *IS1649*, which can facilitate intragenomic rearrangements (148). In either case, the expectation is that increased antibiotic production results from the deregulation of biosynthetic clusters following the deletion of hundreds of genes, many known to coordinate antibiotic biosynthesis (35). In addition, because deletions are stochastic, especially following the removal of protective telomeres at the ends of linear chromosomes, this would also cause antibiotic production to vary in different sections of the colony.

Our preliminary surveys have found similar levels of genomic instability in streptomycete strains that we have freshly isolated from soil, suggesting that the division of labor we describe here is general. We are limited, however, in our ability to detect polymorphisms; color changes are conspicuous and are invariably associated with changes to pigmented secondary metabolites, but other secreted public goods may also become modified in these multicellular bacteria. Understanding which, if any other, public goods vary in the ways shown here is crucial because it will help to identify conditions that lead to a genetically encoded division of labor as compared to other forms of regulation that allow complex multicellular microbial systems to coordinate their behaviors and maximize their fitness.

Materials and methods

Bacterial strains and growth conditions

S. coelicolor A3(2) M145 was obtained from the John Innes Centre strain collection. The strain was cultivated at 30°C on soya flour mannitol medium agar plates (SFM) for strain isolation and to quantify CFU (149). SFM contains mannitol (20 g liter⁻¹), agar (20 g liter⁻¹), and soya flour (20 g liter⁻¹). To examine antibiotic production and to extract secondary metabolites, we used MM supplied with 0.5% mannitol and casamino acids (740 µg ml⁻¹). MM contains asparagine (0.5 g liter⁻¹), K₂HPO₄ (0.5 g liter⁻¹), MgSO₄·7H₂O (0.2 g liter⁻¹), FeSO₄·7H₂O (0.01 g liter⁻¹), and agar (10 g liter⁻¹). For DNA extraction, strains were grown in liquid flasks shaken at 200 rpm at 30°C in TSBS:YEME (1:1, v:v) supplemented with 0.5% glycine and 5 mM MgCl₂. TSBS contains tryptic soya broth powder (30 g liter⁻¹) and sucrose (100 g liter⁻¹), and YEME contains 3 g of yeast extract, 5 g of peptone, 3 g of malt extract, 10 g of glucose, and 340 g of sucrose. *Escherichia coli* and *B. subtilis* were cultivated at 37°C in LB media with constant shaking or on LB agar plates.

All strains were derived from a single isolate of *S. coelicolor* A3(2) M145 (designed as WT). Briefly, samples from a frozen spore stock were diluted and plated onto SFM agar to obtain single colonies. After 5 days of growth, single colonies with WT morphology were diluted and plated onto another SFM plate. From each plate, single colonies with conspicuously mutant phenotypes were picked into sterile water and plated at appropriate dilutions onto SFM agar (n = 3 per colony), from which we estimated the frequency of different mutant phenotype classes. Each derived type was plated to confluence on SFM agar, and after 7 days of growth, spores were harvested to generate spore stocks, which were stored at -80°C in 20% glycerol. To quantify mutation frequency, single colonies were grown for 5 days on three different media, and then we picked the colonies with WT morphology, diluted, and plated them onto the corresponding media. Mutation frequency was scored on the basis of the phenotypes after 3 to 5 days. Table S3 provides strain designations and indicates which strains were examined in each set of assays.

Phenotypic scoring

Two phenotypes that are related to the loss of loci in the right arm were scored (n = 3 per strain). The arginine auxotrophs were identified by replicating 10³ CFUs of each strain on MM supplied with 0.5% mannitol with and without arginine (37 µg ml⁻¹) (24). After 5 days of growth, auxotrophs were identified as those strains that only grow on the media supplied with arginine. Chloramphenicol resistance was estimated by using the disk diffusion method. In detail, 2 × 10⁵ spores were spread onto MM supplemented with casamino acids (740 µg ml⁻¹) (24) in 120-mm square petri dishes, followed by placing a paper disk containing 25 µg of chloramphenicol on it. After 4 days, the radius of the inhibition zone around the disk was measured using ImageJ (150). Inhibition zones that

were smaller than 5 mm were scored as resistant, while those that are larger than 5 mm were scored as susceptible.

Antibiotic production

Spores of each strain were diluted to 10^5 CFU ml⁻¹ in Milli-Q water, and 1 µl was spotted onto MM + casamino acid agar plates (n = 4 per strain). After growth for 5 days at 30°C, plates were covered with 15 ml of LB soft agar (0.7%) containing 300 µl of a freshly grown indicator strain [optical density at 600 nm (OD_{600}) = 0.4 to 0.6]. After overnight incubation at 30°C, zones of inhibition around producing colonies were measured using ImageJ.

The bioactivity against *Streptomyces* isolates was tested for four strains: 2H1A, 8H1B, 9H1B, and 9H1A. Three milliliters of SFM agar was poured onto each well of a 100-mm square petri dish (Thermo Fisher Scientific, USA), after which we spotted 1 µl of each test strain containing $\sim 10^3$ total spores in the corner of each well. After 5-day growth, 500 µl of MM supplemented with 0.5% mannitol and casamino acids (740 µg ml⁻¹) containing $\sim 10^5$ spores of the target strain was overlaid on top. Zones of inhibition were measured 2 days later using ImageJ (150).

¹H NMR profiling and data analysis

Spores (2×10^5) were spread onto MM + casamino acids in 120-mm square petri dishes (n = 3 per strain, except n = 2 for one WT clone). After 5 days of incubation at 30°C, agar was chopped into small pieces using a sterile metal spatula and secreted compounds were extracted in 50 ml of ethyl acetate for 72 hours at room temperature. Next, the supernatant was poured off and evaporated at 37°C using a rotating evaporator. Pellets were obtained by drying at room temperature to remove extra solvents and then freeze-dried to remove remaining water. After adding 500 µl of methanol-*d*₄ to the dried pellets, the mixtures were vortexed for 30 s followed by a 10-min centrifugation at 16000 rpm. The supernatants were then loaded into a 3-mm NMR tube and analyzed using 60-MHz ¹H NMR (Bruker, Karlsruhe, Germany) (139, 140).

Data bucketing of NMR profiles was performed using AMIX software (version 3.9.12, Bruker BioSpin GmbH) set to include the region from δ 10.02 to 0.2 with a bin of 0.04 parts per million scaled to total intensity, while the signal regions of residual H₂O in methanol (δ 4.9 to 4.7) and methanol (δ 3.34 to 3.28) were excluded. Multivariate data analysis was performed with the SIMCA software (version 15, Umetrics, Sweden) (139).

MS-based quantitative proteomics

Spores (10^4) were spotted on SFM agar covered with cellophane and incubated for 5 days at 30°C. Colonies were scraped off and snap-frozen in liquid N₂ in tubes and then lysed three times in a precooled TissueLyser (Qiagen, The Netherlands). Proteins were dissolved

in lysis buffer [4% SDS, 100 mM tris-HCl (pH 7.6), 50 mM EDTA] and then precipitated using chloroform-methanol (151). The dried proteins were dissolved in 0.1% RapiGest SF surfactant (Waters, USA) at 95°C. Protein digestion steps were done according to van Rooden *et al.* (152). After digestion, trifluoroacetic acid was added for complete degradation and removal of RapiGest SF. Peptide solution containing 8 µg of peptide was then cleaned and desalted using the STAGE-Tipping technique (153). Final peptide concentration was adjusted to 40 ng µl⁻¹ with 3% acetonitrile solution containing 0.5% formic acid. Two hundred nanograms of digested peptide was injected and analyzed by reversed-phase liquid chromatography on a nanoACQUITY UPLC system (Waters) equipped with HSS-T3 C18 1.8 µm, 75 µm × 250 mm column (Waters). A gradient from 1 to 40% acetonitrile in 110 min was applied, and [Glu¹]-fibrinopeptide B was used as the lock mass compound and sampled every 30 s. Online MS/MS analysis was done using a Synapt G2-Si HDMS mass spectrometer (Waters) with an UDMS^E method setup as described (152).

Mass spectrum data were generated using ProteinLynx Global SERVER (PLGS, version 3.0.3), with MS^E processing parameters with charge 2 lock mass 785.8426. Reference protein database was downloaded from GenBank with the accession number NC_003888.3. The resulting data were imported to ISOQuant (154) for label-free quantification. TOP3 quantification result from ISOQuant was used in later data processing steps.

In total, of the 7767 proteins from the database, 2261 proteins were identified across all samples. For each sample, on average, 1435 proteins were identified. TOP3 quantification was filtered to remove identifications meeting both criteria: (i) identified in less than 70% of samples of each strain and (ii) the sum of TOP3 value less than 1×10^5 . This led to the removal of 297 protein quantification results. Proteins were considered significantly altered in expression when \log_2 fold change ≥ 1 and $P \leq 0.05$. Volcano plots were made from filtered data, with the four biosynthetic gene clusters highlighted.

CFU production

To quantify CFU, 10^4 spores of each strain were spread onto SFM agar ($n = 3$ per strain, except $n = 2$ for 9H1B) and left to grow for 7 days to confluence. After 7 days, spores were harvested by first adding 10 ml of Milli-Q water onto the plate and then using a cotton swab to remove spores and mycelial fragments from the plate surface. Next, the water suspension was filtered through an 18-gauge syringe plugged with cotton wool to remove mycelial fragments. After centrifuging the filtered suspension at 4000 rpm for 10 min, the supernatant was poured off and the spore pellet was dissolved in a total volume of 1 ml of 20% glycerol. CFU per plate was determined via serial dilution onto SFM agar.

DNA extraction and sequencing

Nine strains, including one WT and eight mutants, were selected for sequencing with the

Chapter 3

Sequel Systems from Pacific Biosciences (PacBio, USA). Roughly 10^8 spores were inoculated in 25 ml of TSBS:YEME (1:1, v:v) supplemented with 0.5% glycine and 5 mM MgCl_2 and cultivated at 30°C with 200 rpm shaking speed overnight. The pellet was then collected after centrifugation and washed twice with 10.3% sucrose. Samples were then resuspended in DNA/RNA Shield (Zymo Research, USA) with 10× volume at room temperature and sent to be commercially sequenced at BaseClear (Leiden, The Netherlands).

Subreads of the sequenced results shorter than 50 base pairs (bp) were filtered and stored in BAM format. The reference alignments were performed against *S. coelicolor* A3(2) genome (NC_003888.3) using BLASR (v5.3.2) (155). Resulting BAM files were then sorted and indexed using SAMtools (v1.9) (156). For the calculation of genome rearrangements, the depths were called and exported through the depth function in SAMtools. The edges of genome were identified by manually checking the break point where the coverage drops to zero. The size of the amplified region was defined by the markedly higher coverage compared to the adjacent sequences. All results were further confirmed by visualizing them in IGV (v2.4.15) (157, 158).

Pulsed-field gel electrophoresis

Approximately 10^8 spores were inoculated into 25 ml of TSBS:YEME (1:1, v:v) supplemented with 0.5% glycine and 5 mM MgCl_2 and cultivated overnight at 30°C at 200 rpm. After centrifuging the culture at 4000 rpm for 10 min, the pellet was resuspended in 400 μl of cell suspension buffer containing 100 mM tris:100 mM EDTA (pH 8.0) and lysozyme (1 mg ml^{-1}) and mixed with the same volume of 1% SeaKem Gold Agarose (Lonza, USA) in TE buffer containing 10 mM tris:1 mM EDTA (pH 8.0) with 1% SDS. This mixture was immediately loaded into the PFGE plug mold (Bio-Rad, USA). Next, plugs were lysed in 5 ml of cell lysis buffer containing 50 mM tris:50 mM EDTA (pH 8.0), 1% *N*-lauroylsarcosine sodium salt, and lysozyme (4 mg ml^{-1}) incubated for 4 hours at 37°C with gentle agitation. This was then followed by a 5-hour incubation in 5-ml cell lysis buffer containing proteinase K (0.1 mg ml^{-1} ; Qiagen, The Netherlands) at 56°C and 50 rpm. Last, the plug was washed twice in preheated Milli-Q water and four times in preheated TE buffer and incubated at 56°C for at least 15 min with gentle mixing. Plugs were sliced into 2-mm width pieces and presoaked in 200 μl of 1× NEBuffer 3.1 for at least 30 min. After replacing the buffer with 200 μl of 1× NEBuffer 3.1, 2 μl of the rare-cutter Ase I (New England Biolabs, UK) was added and incubated at 30°C overnight. Agarose (1%) was used for running fragments in 0.5× freshly prepared tris-borate-EDTA. *S. cerevisiae* chromosomal DNA (0.225 to 2.2 Mb; Bio-Rad, USA) and WT *S. coelicolor* DNA were used as size markers to estimate fragment sizes. Two electrophoresis conditions were applied to separate and visualize the smaller (<1016 kb) and larger (>1016 kb) fragments: (switch time: 2.2 to 75 s; voltage: 200 V; running time: 19 hours) and (switch time: 60 to 125 s; voltage: 200 V; running time: 20 hours), respectively.

PFGE results were compared to the Ase I restriction maps of the WT strain, which contains

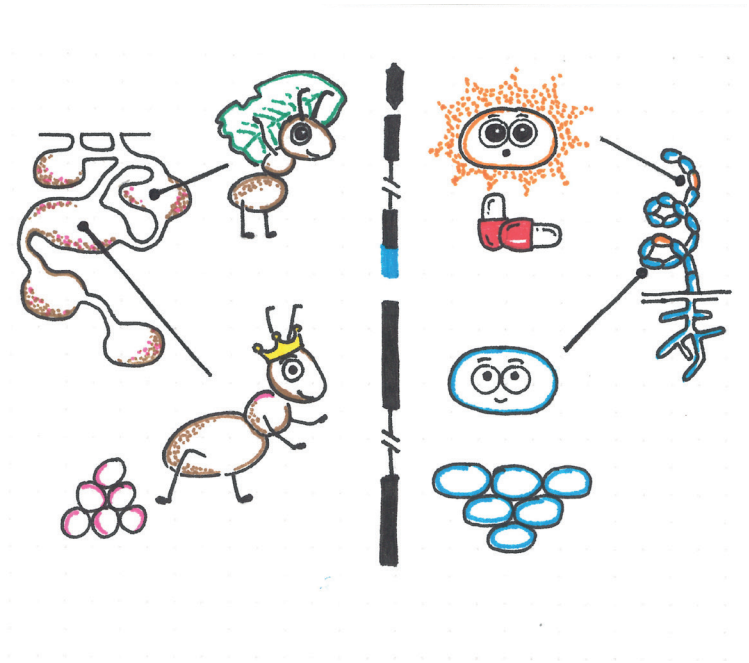
17 fragments ranging from 26 bp to 1601 kb (fig. S3). Two fragments, 240 and 632 kb, can be easily resolved if they are deleted from the left arm, while one large 1601-kb fragment can be affected when deletions occur in the right arm.

Fitness estimates

The relative fitness of four fully sequenced mutant isolates-2H1A, 8H1B, 9H1B, and 9H1A-was estimated during pairwise competition with the WT parent. To distinguish strains, we first transformed mutant and WT strains with the integrating plasmids pIJ82 and pSET152, which confer hygromycin B and apramycin resistance, respectively. Potential fitness effects of the markers were determined by generating two WT variants that were transformed with either single marker. No effects were observed in these control experiments (one-sample *t* test, $t = 2.029$, $P = 0.082$). Fitness assays were initiated by normalizing each strain to a density of 10^6 spores ml^{-1} and then mixing at different starting ratios of mutant:WT. One hundred microliters of this mixture, containing 10^5 spores, was plated as a lawn onto SFM agar and incubated at 30°C for 5 days, while another fraction of the sample was plated after serial dilution onto SFM containing either apramycin ($50 \mu\text{g ml}^{-1}$) or hygromycin B ($50 \mu\text{g ml}^{-1}$) to precisely quantify the densities of each strain. After 5 days of growth, bacteria were harvested as above and plated by serial dilution onto SFM containing either apramycin ($50 \mu\text{g ml}^{-1}$) or hygromycin B ($50 \mu\text{g ml}^{-1}$). Fitness was quantified, following Lenski *et al.* (159), by calculating the ratio of the Malthusian parameters of both strains. Values below 1 indicate that mutant strains have lower fitness than the WT strain. More detailed assays were carried out with strain 9H1A, where we simultaneously estimated the fitness of this strain at a broader range of frequencies from 10 to 99% and determined how the frequency of the mutant strain influenced antibiotic production, as measured by the size of the zone of inhibition against a *B. subtilis* indicator in a soft agar overlay.

Data availability

All data needed to evaluate the conclusions in the chapter are present in the paper and/or the Supplementary Materials. The MS proteomics data have been deposited to the ProteomeXchange Consortium via the PRIDE partner repository with the dataset identifiers PXD014413 and 10.6019/PXD014413 (160, 161). Raw data are available at Dryad (10.5061/dryad.bnzs7h462).



Chapter 4

Mutational meltdown of microbial altruists in *Streptomyces coelicolor* colonies

Zheren Zhang, Bart Claushuis, Dennis Claessen and Daniel E. Rozen
Institute of Biology, Leiden University, Leiden, the Netherlands

Available online in

bioRxiv (2020).

DOI: 10.1101/2020.10.20.347344

Abstract

In colonies of the filamentous multicellular bacterium *Streptomyces coelicolor*, a sub-population of cells arise that hyper-produce metabolically costly antibiotics, resulting in a division of labor that maximizes colony fitness. Because these cells contain large genomic deletions that cause massive reductions to individual fitness, their behavior is altruistic, much like worker castes in eusocial insects. To understand the reproductive and genomic fate of these mutant cells after their emergence, we use experimental evolution by serially transferring populations via spore-to-spore transfer for 25 cycles, reflective of the natural mode of bottlenecked transmission for these spore-forming bacteria. We show that, in contrast to wild-type cells, altruistic mutant cells continue to significantly decline in fitness during transfer while they delete larger and larger fragments from their chromosome ends. In addition, altruistic mutants acquire a roughly 10-fold increase in their base-substitution rates due to mutations in genes for DNA replication and repair. Ecological damage, caused by reduced sporulation, coupled with irreversible DNA damage due to point mutation and deletions, leads to an inevitable and irreversible type of mutational meltdown in these cells. Taken together, these results suggest that the altruistic cells arising in this division of labor are equivalent to reproductively sterile castes of social insects.

Introduction

Multicellular organisms show enormous variation in size and complexity, ranging from multicellular microbes to sequoias and whales, and from transient undifferentiated cellular clusters to stable individuals with highly specialized cell types. Despite their differences, a recent study showed that a central factor determining organismal complexity is the way in which multicellular organisms are formed (98). Clonal groups, where relatedness among cells is high, show more cellular specialization and an increased likelihood of expressing a reproductive division of labor between somatic and germ cells (50, 98, 162, 163). By contrast, groups with aggregative multicellularity like dictyostelid social amoebae or myxobacteria, which potentially have lower relatedness between cells if unrelated genotypes co-aggregate during development, tend to show reduced specialization (56, 96, 164). Thus, in analogy with sterile castes within colonies of social insects, the extreme altruism needed for reproductive sterility is facilitated by high relatedness (165).

In microbes, the requirement of high relatedness is most easily met if colonies are initiated from a single cell or spore. High relatedness during multicellular growth or development is even further guaranteed if the cells within colonies remain physically connected to each other, as observed in filamentous streptomycetes (51, 59). These bacteria have a well-characterized developmental program that leads to the formation of durable spores following a period of vegetative growth and the elaboration of spore-bearing aerial hyphae (7, 8). In addition, we recently showed that colonies are further divided into a sub-population of cells that hyper-produces antibiotics (166). Here we provide a detailed examination of the fate of these specialized cells and provide evidence that they represent a terminally differentiated altruistic cell type within these multicellular microbes.

Streptomyces are bacteria that live in the soil and produce a broad diversity of antibacterial and antifungal compounds, among other specialized metabolites (9, 13). Division of labor allows *Streptomyces coelicolor* colonies to partly offset the metabolic cost of producing these compounds. However, differentiation into this hyper-producing cell type is accompanied by huge fitness costs due to massive deletions of up to 1 Mb from the ends of their linear chromosomes. Examining independent mutant strains, we found a strong positive correlation between the size of genome deletions and the amount of antibiotics produced, as well as a strong negative correlation between the deletion size and spore production. In addition, competitive fitness assays revealed that mutant strains were strongly disadvantaged. Indeed, even when the initial frequency of mutants in mixed colonies was as high as ~80%, their final frequency declined to less than 1% after one cycle of colony growth (166). These results suggested that mutant strains would be quickly eliminated during competitive growth. We hypothesized that, like sterile insect workers, these altruistic cells represented a sterile microbial caste. However, as our results were based on static colonies, we lacked insight into the fate of these cells after they emerged.

To address this question, the current study tracked the fate and fitness of altruistic mutant and wild-type lineages during short-term experimental evolution. To reflect the manner of spore-to-spore reproduction in these bacteria, lineages were serially transferred via single colonies, similar to a mutation accumulation design (43) (Fig. 1A). In contrast to much longer-term experiments using this approach in other microbes, where fitness declines extremely slowly (42, 167), we observed massive fitness reductions, including extinction, in our mutant lineages after only 25 transfer cycles. These changes were not only associated with continued deletions to the chromosome ends, but also the tendency for lineages to become hypermutators likely due to errors in genes for DNA replication and repair (168, 169). Together these data support the idea that this specialized sub-population of cells within *Streptomyces* colonies is equivalent to a sterile caste and further highlights the idea that clonal propagation can give rise to a broad diversity of functionally specialized cells within bacterial colonies, beyond the binary distinction between spores and vegetative cells.

Results

Phenotypic changes during serial transfer

To track the fate of different mutant lineages harboring different spontaneous genomic deletions we transferred six WT (W1-W6) and six mutant (M1-M6) strains for 25 transfers cycles through single spore bottlenecks twice per week (Fig 1A). Consistent with our earlier results (166), we first confirmed that the starting competitive fitness of a subset of these mutants was significantly reduced compared to the WT ancestor (Fig 1B). Even when mutant lineages were inoculated at an initial frequency as high as roughly 80%, their final frequency during paired competition declined to less than 1%. In addition, the mutant strains that were used to initiate the MA experiment produced significantly fewer colony-forming unit (CFU) after clonal development than their WT counterparts (Wilcoxon rank-sum test, $P = 0.0022$, Fig. 3A). Strains were sampled every 5 transfers, with the exception of one WT lineage (W3) that was sampled more frequently after it acquired chromosome deletions, as explained below. One of the six mutant lineages (M2) acquired a bald morphology after the 5th transfer and became functionally extinct due to a total loss of spore production and was not included in fitness analyses (fig. S1).

To identify phenotypic changes in evolved lineages, we screened for two easily scored traits that are indicative of deletions to the right chromosome arm. Chloramphenicol susceptibility, due to the deletion of *cmlR1* (SCO7526)/*cmlR2* (SCO7662), indicates a deletion of at least 322 kb (170, 171) and arginine auxotrophy, due to the deletion of *argG* (SCO7036), corresponds to a deletion of at least 843 kb (172). In addition, we analyzed changes to resistance to three other antibiotics. As is evident in Fig. 2A, whereas the WT lineages remained resistant to chloramphenicol (except for W3, as noted above) the minimal inhibitory concentration (MIC) of mutant lineages were lower than the WT

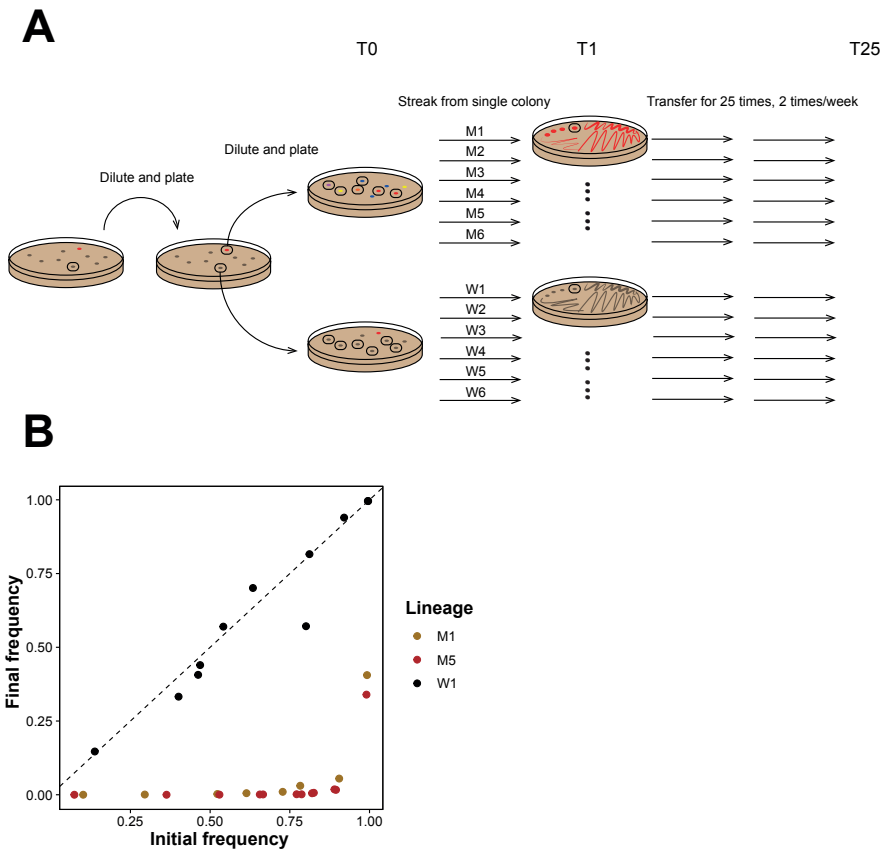


Fig. 1. Overview of the experimental design. (A) The schematic of our experimental setup. An ancestral WT colony was picked and plated to obtain individual colonies. One mutant and one WT colony were picked and plated to obtain six WT and six mutant clones. Lineages were subsequently transferred via single colony bottlenecks for 25 transfers. **(B)** Initial and final frequency of three T0 strains from different lineages during competition with the WT ancestor. The dashed line shows the expectation if initial and final frequencies are equal, as seen for the strain from the WT lineage (W1). By contrast, mutant fitness (M1 and M5) is dramatically lower than WT fitness, dropping to < 1% even when starting from as high as approximately 73% (M1) or 82% (M5).

or declined during the course of the experiment. On the basis of these results, W3 was hereafter analyzed as a mutant lineage, despite its WT origin. A trend towards increased arginine auxotrophy was also observed in mutant lineages (Fig. 2B), suggesting that continuous chromosome deletions occurred during the course of the experiment. Tests for susceptibility to other antibiotics (fig. S2) also showed similar trends as those found for chloramphenicol, with the exception of the bald populations from M2 that showed a 4-fold increase in the MIC for ciprofloxacin.

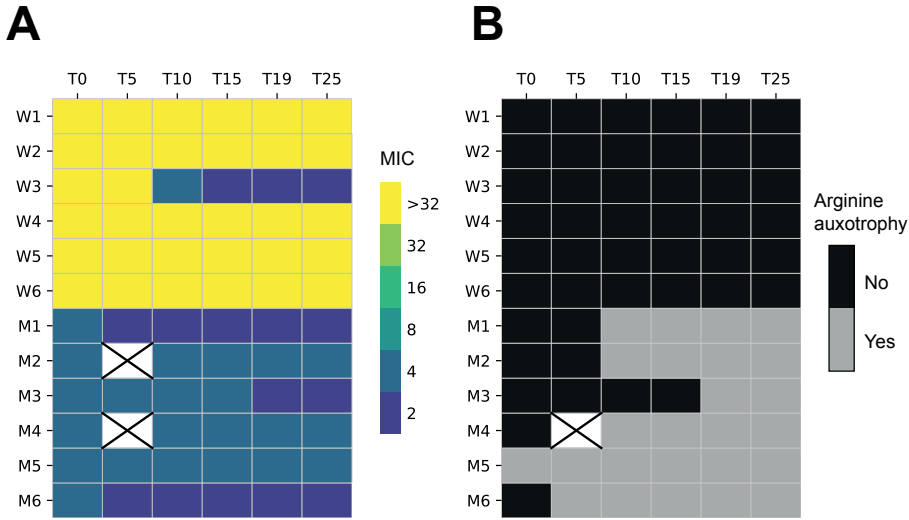


Fig. 2. Phenotypic results for transferred lineages based on two genetic makers on the right chromosome arm. (A) MIC ($\mu\text{g ml}^{-1}$) of chloramphenicol over time. **(B)** Arginine auxotrophy over time. The vertical axis indicates a lineage name while the horizontal axis indicates a time point during serial transfer.

Fitness rapidly declines in evolved populations

Results in Fig. 3A show that the CFU of mutant lineages declined continuously compared to WT lines. M2, that went extinct after the 5th transfer, was only evaluated for the first two time points, and W3 was treated as a mutant lineage from the 7th transfer. We compared the differences of CFU between the end and starting time point of the experiment within each lineage. Of the mutant lineages, all 7 showed significant reductions in CFU during the experiment (Welch's t tests, all $P < 0.01$), amounting to a 9.8-fold median decline (IQR 5.4-13.3; one-sample Wilcoxon signed-rank test, $P = 0.016$). By contrast, 4 of 6 WT lineages show small, but significant, increases in CFU (Welch's t tests, all $P < 0.05$), amounting to a 2.4-fold median fitness increase (IQR 1.6-2.8; one-sample Wilcoxon signed-rank test, $P = 0.031$). Accordingly, as shown in Fig 3B, the average CFU change of WT and mutant lineages are significantly different from each other (Wilcoxon rank-sum test, $P = 0.0012$).

Continuous deletions in mutant lineages but not wild-type lineages

To identify genetic changes that led to the rapid declines in mutant fitness, we used whole-genome sequencing to measure changes in genome size by mapping against a reference strain (fig. S3). As expected, no changes were observed in WT lineages (with the exception of W3). By contrast, as shown in Fig. 4A and fig. S3, mutant lineages continued to

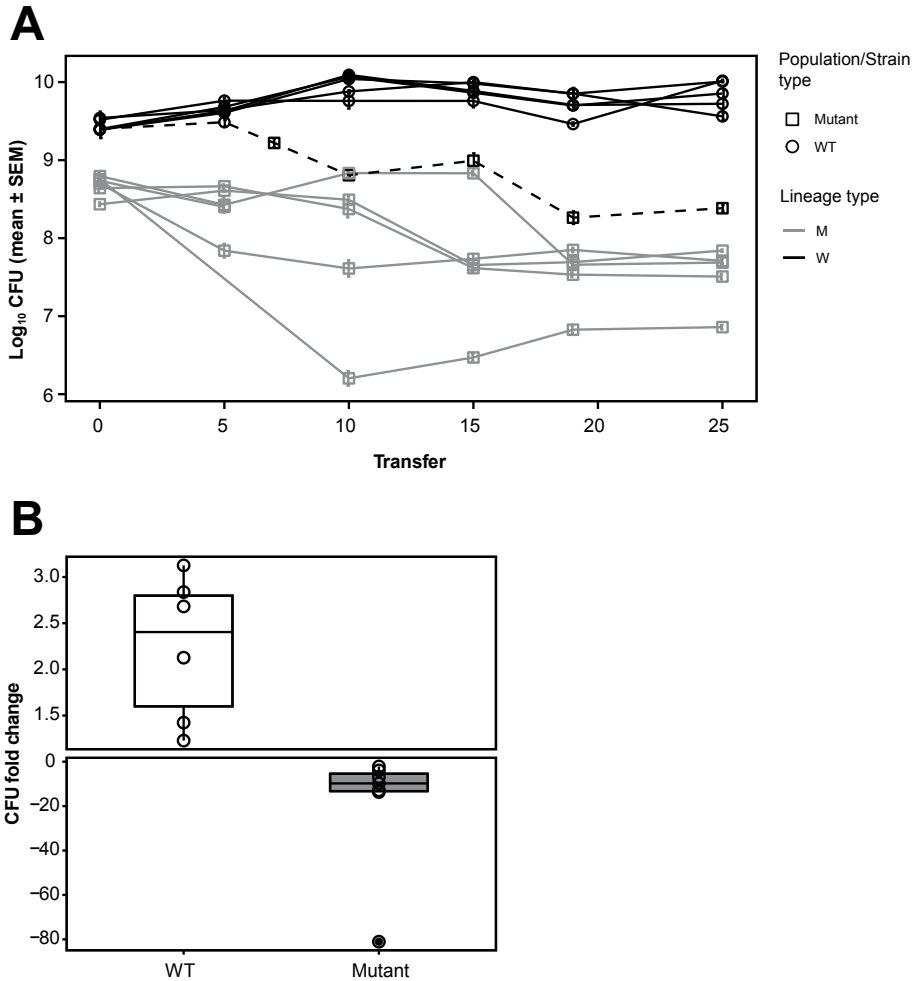


Fig. 3. Fitness changes in WT and mutant lineages. (A) The fitness (CFU) dynamics of each replicate lineage through time. WT lineages are shown in black while mutants are shown in gray. The WT lineage that became mutant after the 7th transfer is indicated by a dashed line (W3). (B) Median fold change of CFU of WT ($n = 6$) and mutant ($n = 7$) lineages during serial transfer.

accumulate large deletions to the left and right chromosome arms during serial transfer. Deletions to the left arm ranged from 0 to 882 kb, and in the right arm from 0 to 250 kb (Left arm: 289 ± 117 kb (mean \pm SE), $n = 7$; Right arm: 80 ± 30 kb (mean \pm SE), $n = 7$). The total deletion sizes of these strains ranged from 0 to 924 kb (369 ± 124 kb (mean \pm SE), $n = 7$). One lineage (M2) suffered an abnormally large deletion on the left chromosome arm, and this strain was no longer able to develop an aerial mycelium, resulting in a bald phenotype (fig. S1). However, no apparent deletions in known *bld* genes could be

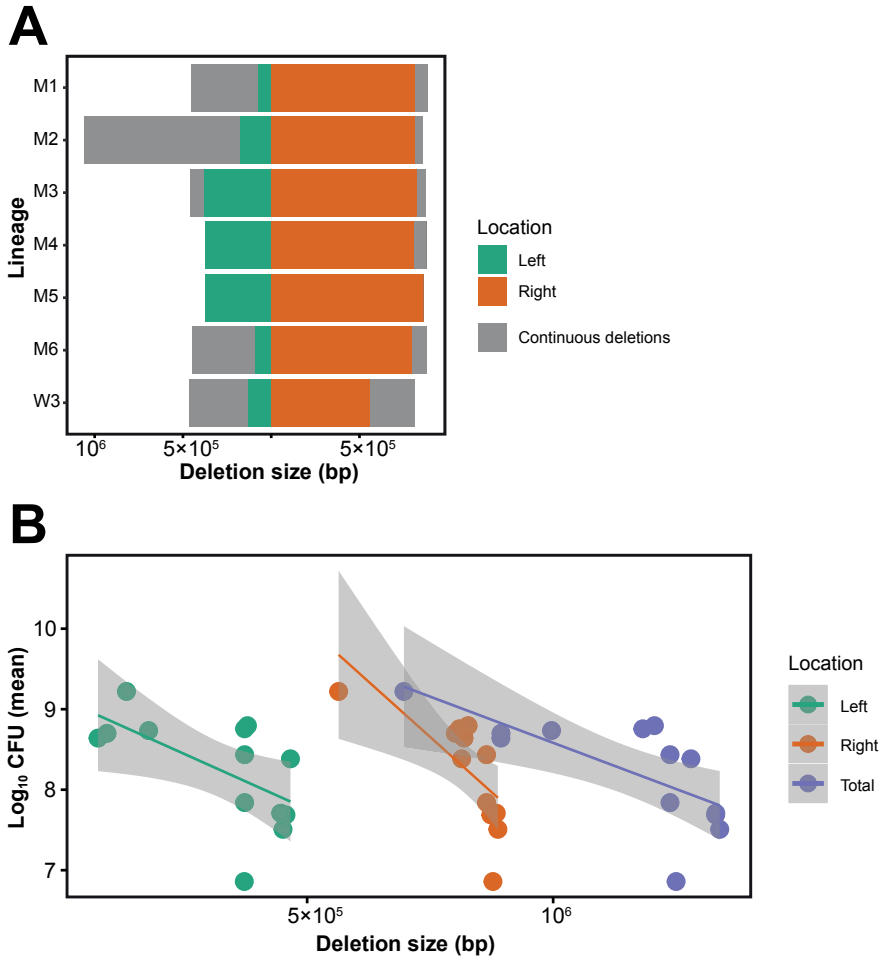


Fig. 4. Genomic deletions and their effects on strain fitness. (A) Initial and final deletion sizes on the left and right chromosome arms. **(B)** Significant negative correlation between the size of the chromosome deletions and strain fitness, shown for the left arm, the right arm and the entire genome. Regression lines include the 95% confidence interval.

identified (111), suggesting other causes for this phenotype. Additionally, one lineage (M5) that began with the shortest genome did not gain further deletions, suggesting that further genome loss may not have been possible due to the presence of essential genes near the border of the chromosome ends. Fig. 4B plots the relationship between CFU and the size of genomic deletions on the left arm, right arm or entire chromosome. These results confirm and extend our previous observations. CFU and the deletion size are negatively correlated for the left arm ($F_{1,11} = 6.03$, $r^2 = 0.354$, $P = 0.031$), the right arm ($F_{1,11} = 9.88$, $r^2 = 0.47$, $P = 0.009$) and for the whole chromosome ($F_{1,11} = 10.75$, $r^2 = 0.49$, $P = 0.007$).

Increased base-substitution rates in mutant lineages

To address other sources of mutational variation, in addition to gross chromosome changes, we estimated the base-substitution and indel mutation rates from mutant and WT lineages. Unexpectedly, we found that mutant lineages fixed significantly more mutations than the WT lineages. Overall, mutants fixed 29.5 mutations per lineage (median, IQR 12.25-32.5, $n = 6$) while the WT lineages fixed 5 mutations per lineage (median, IQR 4-6, $n = 5$). To account for differences in the number of transfers of different lineages (due to the impact of W3 that became a mutant after 5th transfer), we calculated a per transfer mutation rate. This analysis showed that the base-substitution rate for mutants was 12.78 per 10^8 nucleotides per transfer (median, IQR 7.62-17.46, $n = 7$) compared to 1.5 per 10^8 nucleotides per transfer (median, IQR 1.28-2.03, $n = 6$) in WT, exhibiting a roughly 10-fold difference (Wilcoxon rank-sum test with continuity correction, $U = 4$, $P = 0.018$) (Fig. 5A). When we partitioned this result into different mutant classes, we observed that mutants acquired synonymous and non-synonymous mutations as well as changes in non-coding regions at a significantly higher rate (Fig. 5B). Further, looking across different transitions and transversions, we found that mutants fixed more mutations in 4 out of 6 mutation classes (Fig. 5C). Four mutant lineages fixed mutations in alleles affecting DNA replication or repair (168, 169), including DNA polymerase III (synonymous), DNA topoisomerase IV (synonymous), DNA polymerase I (non-synonymous) and DNA ligase (non-synonymous) (tables S1 and S2). Although suggestive, at present we cannot confirm that these specific changes are causally associated with increased mutation fixation. These results thus indicate that mutant lineages become mutators, in addition to acquiring large genomic deletions. Both factors likely contribute to their dramatic fitness reductions.

Discussion

Division of labor allows populations of individuals to more efficiently carry out functions that are mutually incompatible (49, 50, 52). In microbes, division of labor can facilitate biofilm formation (121, 124, 173), energy transfer (174), and coordinated metabolism (62, 166), among other behaviors. In some cases, division of labor leads to sub-populations of cells that carry out functions that are lethal to themselves but that benefit the entire colony (175). For example, colicin secretion in *E. coli* requires cell lysis (176), a fate limited to a small fraction of cells with low reproductive value. By this process, the burden of colicin-secretion is disproportionately borne by the cells with the least to lose in terms of their own fitness (177, 178). We recently provided evidence for a similar phenomenon in *Streptomyces*, whereby a sub-fraction of cells within a multicellular colony hyperproduces antibiotics at the expense of their own reproduction, in part due to large and irreversible deletions from their chromosome ends (166). The aim of the present work was to examine the fate of these altruistic cells after their emergence. We found that although *Streptomyces* cells hyper-producing antibiotics do not lyse, like *E. coli* colicin producers, they continue

to accumulate large deletions and also evolve an increased mutation rate across their genome. These effects, which lead to an “effective lethality”, suggest that these cells are equivalent to the sterile worker castes in social insects (123).

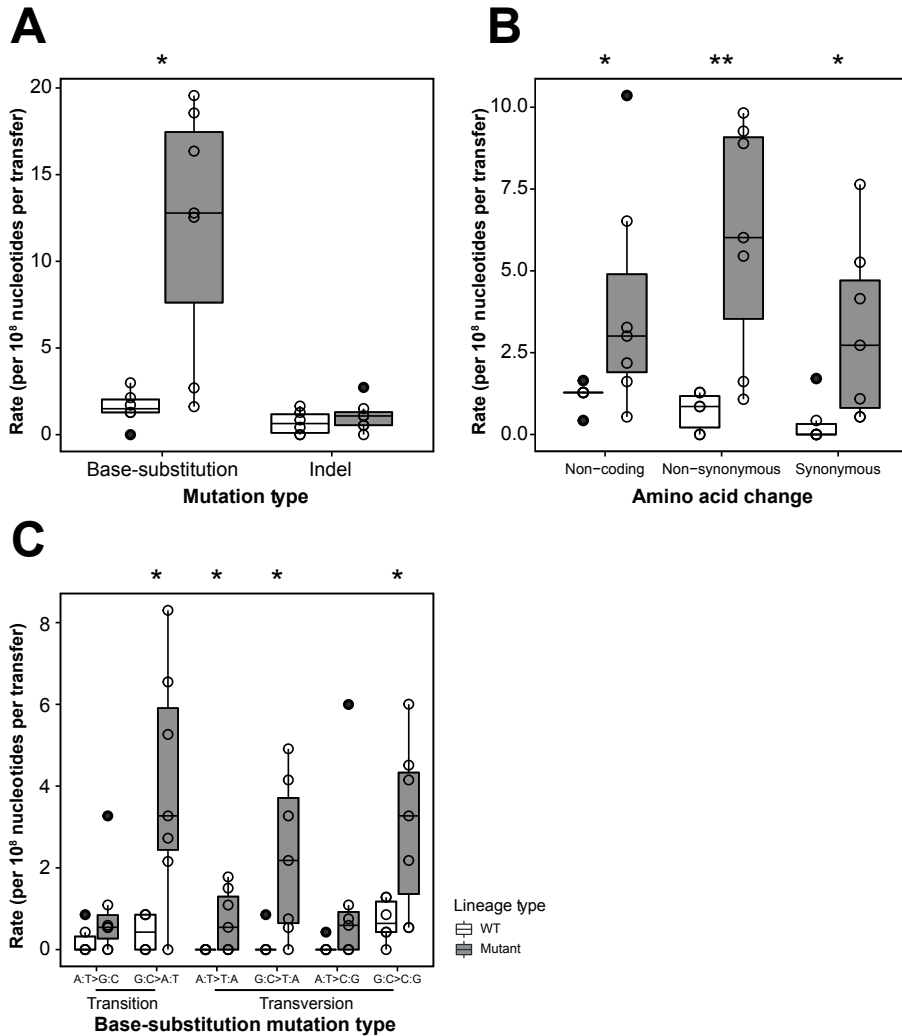


Fig. 5. Mutation rates of WT and mutant lineages. Mutation rates are partitioned according to: **(A)** Base-substitutions and indels; **(B)** the types of amino acid changes; and **(C)** for different classes of transitions or transversions. Levels of significance are indicated as * ($P < 0.05$) and ** ($P < 0.01$) (Wilcoxon rank-sum test).

Our experimental approach was designed to approximate the natural growth and development of *Streptomyces* that disperse via spores, such that each new colony passes through a single-cell bottleneck. This resembled a classic mutation accumulation experimental design, which has been widely used to examine fitness declines in microbes due to the accumulation of deleterious mutations via Muller's ratchet, a process in which deleterious mutations accumulate irreversibly in a population lacking recombination (179, 180). As in mutation accumulation experiments, our mutants lost fitness (42, 167); however, their rate of decline was exceptionally rapid due to mutations of very large effects via genome loss as well as point mutations. Results in Fig. 4B show a significant negative relationship between the total genome size and CFU production, consistent with studies performed in *E. coli* containing manipulated reduced genomes (181). Given the 679-1817 genes that are lost from these populations, it is not possible to know which ones are responsible for the fitness reductions, either alone or in combination. In addition to genome loss, we were surprised that mutant lineages, but not wild-type ones, have an approximately 10-fold increased mutation rate, likely due to mutations in genes for DNA replication and repair (168, 169). Mutations were found in several mutation classes and are higher in both coding and non-coding regions, indicating broad and non-specific mutagenesis. Decreased competitiveness, massively compromised CFU as cells pass through single-spore bottlenecks, and the combined accumulation of large deletions and an increased mutation burden, lead to synergistic declines in fitness that resembles a type of mutational meltdown. First, ecologically deficient mutants develop a higher mutation rate. Second, these lineages rapidly accumulate further deletions, which magnifies their fitness reductions and causes an irreversible decrease in their effective population size, ultimately leading to extinction. Although this process occurs within an organism over a very short time period, this process closely resembles the idea of a classical mutational meltdown, in which a small population going through Muller's ratchet experiences accelerating fitness declines caused by deleterious mutations (182).

Even though mutant lineages are deteriorating at a pace that far exceeds results from other MA experiments, they don't die immediately, as do *E. coli* colicin producers. Why do antibiotic producing strains of *Streptomyces* die via mutational meltdown instead of lysing? One possible cause of this difference may be the intrinsic differences in the activity of antibiotics and colicins. Whereas the latter can act at very low concentrations, e.g. via single-hit kinetics (176), antibiotics may require higher concentrations to provide sufficient protection to large *Streptomyces* colonies. Antibiotics can also bind tightly to abiotic substrates, potentially requiring higher levels of production within colonies (183). These possibilities would necessitate continued survival and growth of producing cells, thereby generating spatially clustered mutant sub-populations within colonies that hyperproduce antibiotics, whereas sufficient toxin quantities could be produced by single *E. coli* cells either dispersed randomly throughout the colony or on the colony edge facing impending threats (177, 178). A related issue that remains unresolved is the origin of

mutant cells within growing colonies. Specifically, it remains unclear if low-level antibiotic production somehow causes subsequent genome decay due to local toxicity, or if stochastically damaged cells subsequently adopt a new fate to hyper-produce antibiotics. At present, we are unable to fully address these issues and they remain important areas for future study.

Altruistic behaviors can be explained by their indirect fitness benefits, whereby individuals offset the loss of their own reproduction by increasing the reproduction of their relatives (184). In multicellular bacteria, like streptomycetes, clonality, and therefore high relatedness, among cells in the colony is ensured by their mode of filamentous growth (51, 59). For this reason, division of labor with extreme specialization can evolve and lead to the elaboration of multiple cell types. Streptomycetes are typically divided into two functional classes of cells: spores and vegetative cells (7, 8). Our work supports the notion that colonies can be further partitioned into at least one more cell type, those producing antibiotics and that accumulate extreme and irreversible genetic damage leading to their demise. We would predict similar diversification among other streptomycetes, as well as the discovery of additional divisions of labor among other multicellular bacteria.

Materials and methods

Bacterial strains and cultural conditions

Strains used in this study all derived from *Streptomyces coelicolor* A3 (2) M145. Strains were maintained and assayed at 30°C on soya flour mannitol media (SFM) containing 20 g mannitol, 20 g agar and 20 g soya flour per liter of water. Spores of *S. coelicolor* were diluted and plated onto an SFM plate. To obtain initial isolates for mutation accumulation, one random WT colony (designated as WT_{ancestor}) was diluted and plated onto SFM agar. One random WT and mutant colony were then picked and replated onto separate SFM plates. Six random colonies were then chosen from each plate and designated as ancestors for subsequent serial passage through single-colony transfer, for a total of 12 lineages (6 WT and 6 mutants). During each transfer, a single colony from each lineage growing closest to a randomly placed spot on the back of the plate was chosen and streaked onto another SFM plate. This procedure was repeated every 3-4 days for 25 transfer cycles (Fig 1A). Transferred lineages were archived by creating a full lawn from the transferred colony, after which spores were harvested after ~ 7 days of growth and sporulation as previously described (149). All stocks were maintained at -20°C.

Competition assay

We estimated the fitness of two mutant (M1 and M5) and one WT lineages (W1) from T0, following the protocol in (166). T0 strains were marked with apramycin resistance and the WT ancestor was marked with hygromycin B resistance, by using integrating

plasmids pSET152 and pIJ82, respectively. After diluting strains to 10^6 CFU ml⁻¹, they were mixed with the reciprocally marked WT ancestor at different initial frequencies. 100 µl of each mixture was plated onto 25 ml SFM agar plates and incubated at 30°C for 5 days. At the same time, each mixture was serially diluted and plated onto SFM agar plates containing either apramycin (50 µg ml⁻¹) or hygromycin B (50 µg ml⁻¹) to obtain precise estimates of initial frequencies. After 5 days, each plate was harvested in H₂O and passed through an 18-gauge syringe plugged with cotton wool to remove mycelial fragments and resuspended in 1 ml 20% glycerol. Each sample was then serially diluted onto plates containing either antibiotic to calculate final frequencies.

Estimating antibiotic resistance

To estimate changes to antibiotic resistance, minimal inhibitory concentration (MIC) was determined for all strains by spot dilution onto large SFM agar plates (150 x 20 mm, Sarstedt, Germany) supplemented with different antibiotic concentrations. Drug concentrations ranged from 2 to 32 µg ml⁻¹ (chloramphenicol, oxytetracycline and ciprofloxacin) and 1 to 16 µg ml⁻¹ (streptomycin). Plates were inoculated using a 96-pin replicator from master 96-well plates containing $\sim 10^7$ spores ml⁻¹. Approximately 1 µl from this stock was applied to each plate; the replicator was flame sterilized between each transfer to ensure that no cells or antibiotics were transferred between assay plates. The plates were incubated for 4 days at 30°C and then imaged and scored for growth. The MIC was determined as the drug concentration where no growth was visible after 4 days ($n = 3$ per strain per drug concentration).

Auxotrophy assay

To test for auxotrophy, strains were grown on minimal media (MM) containing per liter 0.5 g asparagine, 0.5 g K₂HPO₄, 0.2 g MgSO₄·7H₂O, 0.01 g FeSO₄·H₂O and 10 g agar, supplied with either 0.5% mannitol or 0.5% mannitol plus 0.0079% arginine. Bacteria were spotted onto plates using a pin-replicator, as for MIC assays, and grown for 4 days at 30°C. Auxotrophy was detected by comparing growth of colonies on plates with or without supplemented arginine ($n = 3$ per strain).

CFU estimation

We used CFU to estimate the fitness of strains from each lineage. For each strain, 10^5 spores were plated onto SFM as a confluent lawn. After 5 days of growth, spores were harvested by adding 10 ml H₂O to the plates, gently scraping the plate surface to create a spore suspension, and then filtering the liquid through an 18-gauge syringe with cotton wool to remove mycelia. After centrifugation, spore stocks were resuspended in 1 ml 20% glycerol and then serially diluted onto SFM to calculate the total CFU for each strain ($n = 3$ per strain, except $n = 2$ for M1 at T19).

Whole-genome sequencing

Strains were sequenced using two approaches. Long reads sequencing (PacBio, USA) was performed as previously reported (166). Short reads sequencing (BGISEQ-500) was done using the following protocol. DNA was extracted after growth in liquid TSBS : YEME (1:1 v:v) supplemented with 0.5% glycine and 5 mM MgCl_2 . Approximately 10^8 spores were inoculated in 25 ml and incubated at 30°C with a shaking speed of 200 rpm for 12-48 hours. TSBS contains 30 g tryptic soya broth powder and 100 g sucrose per liter and YEME contains 3 g yeast extract, 5 g peptone, 3 g malt extract, 10 g glucose and 340 g sucrose per liter. DNA was extracted using phenol/chloroform (149). Visible cell pellets were washed with 10.3% sucrose solution after centrifugation. Pellets were resuspended in 300 μl GTE buffer, containing 50 mM glucose, 10 mM EDTA, 20 mM Tris-HCl, pH 7.5 and 4 mg ml^{-1} lysozyme and incubated at 37°C for 1 hour. Then 300 μl 2M NaCl was added and gently inverted ten times, followed by the addition of 500 μl phenol/chloroform (bottom layer). After mixing, each tube was centrifuged for 5min and the upper layer was transferred to a new tube. This procedure was repeated at least twice until the intermediate layer was almost invisible. The final transferred upper layer was mixed with a same volume of 2-propanol, and centrifugated for 10 min. Liquid in the supernatant was discarded and pellets were dried at room temperature before being dissolved in 200 μl Milli-Q H_2O . After adding 1 μl RNase, the DNA was resuspended at 37°C for 1 hour. Phenol/chloroform washing and DNA precipitation was repeated once to remove the RNase. After adding phenol/chloroform, the upper layer was transferred to a new tube, and then mixed with 16 μl 3M pH 5.2 NaCH_3COO and 400 μl 96% ethanol. This mixture was cooled at -20°C for 1 hour and centrifuged for 10 min to obtain the DNA pellets. Pellets were washed with pre-cooled 96% ethanol and dried at room temperature. DNA was dissolved in Milli-Q H_2O and sent for commercial sequencing at BGI (Hong Kong).

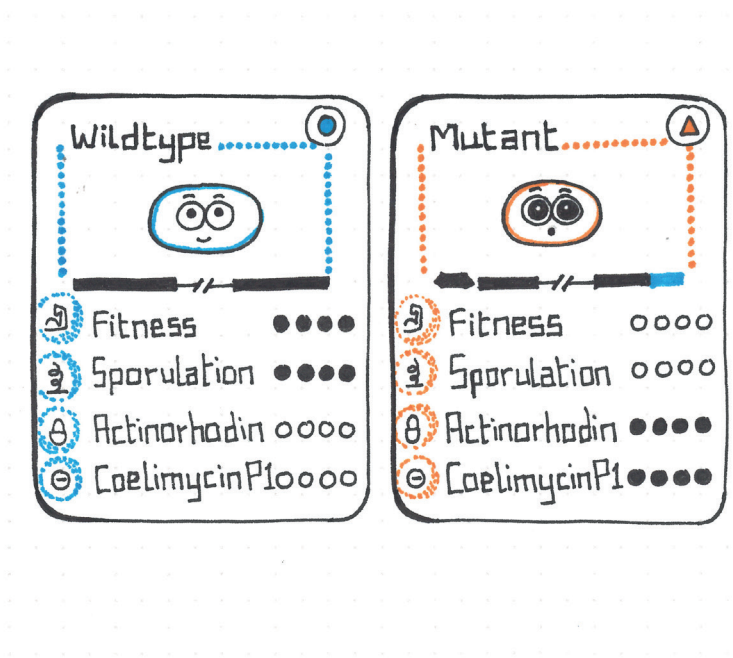
Sequencing processing

The raw data of PacBio sequencing was processed as outlined in Zhang *et al.* (2020) (166) and genome length was evaluated based on these results. The BGISEQ-500 data was handled using CLC Genomics Workbench (QIAGEN, v 8.5.4). Filtered raw reads were first imported and mapped to the reference genome NC_003888.3 (35) through the “NGS core” - “Map to the reference” function. Variants were then called by using “Basic variant detection” function, with the filter parameters set to minimum coverage as 5, minimum count as 2 and minimum frequency as 50%. Variants were identified by comparing lineages to their corresponding parental strain by applying the “Resequencing analysis” - “Compare Variants” - “Compare Sample Variant Tracks” option. By using the annotation information in the GenBank file, final variants were then annotated by applying the “Track tools” - “Annotate with overlap information” option, and amino acid changes were added to the variant track by “Resequencing analysis” - “Functional consequences” - “Amino

acid changes" option. Final results were exported as excel sheets and variants in genes that were not detected in PacBio sequencing were removed before performing further analyses.

Statistical analyses

All statistical analyses were performed in R (v 3.6.2). Welch's t test was used to test the difference of CFU production across the course of the experiment. One-sample Wilcoxon signed-rank test was used to test if the CFU changed after serial transfer while Wilcoxon rank-sum test (Mann-Whitney U test) was used to compare the difference between WT and mutant lineages. All tests are two-sided.



Chapter 5

Proteomic and metabolomic changes driven by spontaneous genomic rearrangements in *Streptomyces coelicolor*

Zheren Zhang, Chao Du, Dennis Claessen, Somayah Elsayed,
Gilles P. van Wezel and Daniel E. Rozen
Institute of Biology, Leiden University, Leiden, the Netherlands

Abstract

Filamentous bacteria from the genus *Streptomyces* are an important source of antibiotics. Previous work has demonstrated that antibiotic production in these bacteria is organized by a division of labor in which a small fraction of cells reduces its own fitness to produce costly antibiotics that benefit the whole colony. However, little is known about the molecular and cellular mechanisms that underlie these phenotypic changes. In this study, we combine proteomics and metabolomics approaches to begin to identify the mechanistic basis of these altruistic traits in mutant strains. We first confirm that mutants have increased antibacterial activity and production and decreased fitness compared to their parental wild-type. Second, we find that proteins from several secondary metabolite biosynthetic gene clusters, including those for actinorhodin, calcium-dependent antibiotic and coelimycin P1, are upregulated in mutants with higher antibacterial activity. Finally, we show that many proteins in pathways that coordinate *Streptomyces* development and sporulation are significantly downregulated in mutants with reduced fitness. These results uncover mechanistic targets driving the trade-off between secondary metabolism and fitness in these multicellular bacteria. They also provide insights into the cellular basis for the division of labor in this species.

Introduction

Streptomycetes are multicellular filamentous soil bacteria with a complex life cycle. Beginning from a germinating spore, bacteria grow by tip extension into the surrounding medium via connected multi-chromosomal compartments known as a vegetative mycelium. When resources are exhausted, the vegetative mycelium undergoes a transition that leads to the formation of aerial structures containing millions of uni-genomic spores (7–9). Concurrently, the colony produces specialized metabolites like antibiotics or antifungal agents (9, 10, 12). Development and antibiotic production have been extensively studied and this work has uncovered many key genes that regulate these phenotypes, including the crucial *bld* and *whi* genes that are involved in aerial growth and sporulation, respectively (8, 111, 185–187), and biosynthetic gene clusters (BGCs) for four well-known antibiotics produced by *Streptomyces coelicolor*, namely actinorhodin, coelimycin P1, calcium dependent antibiotic (CDA) and prodiginines (13, 145). However, one particularly intriguing aspect of development and antibiotic secretion has eluded understanding. Since the 1960s (21), several research groups have recognized that a high frequency of spores from *Streptomyces* colonies have aberrant primary and secondary metabolism, and further that these phenotypes are associated with large deletions at the ends of the *Streptomyces* linear chromosome (22, 25–32). Although the size and frequency of these genome changes have been well characterized, the mechanisms underlying the phenotypic and evolutionary consequences of these deletions remain poorly understood.

We recently sought to address these issues in *S. coelicolor*. We first demonstrated that mutant strains arising as a consequence of genome deletions have dramatically decreased fitness, manifest as a significant reduction in spore numbers, as well as significantly increased and diversified antibiotic production (166). We next showed that this trade-off allows colonies to benefit from a type of division of labor for antibiotic production that maximizes the efficiency of both antibiotic and spore production. In analogy with sterile workers in social insect colonies, mutant cells suffer continued genomic decay and eventual extinction after having produced antibiotics. These results highlighted the evolutionary importance of genomic instability for *S. coelicolor* and potentially other streptomycetes yet left unclear the molecular details underlying the altered phenotypes of these mutant strains.

To address these issues, we used mass spectrometry-based approaches to study proteomic and metabolomic changes in mutant cells. By combining omics data with phenotypic assays, we find that large chromosomal deletions: (i) lead to the upregulation of antibiotic biosynthesis proteins which result in antibiotic overproduction; and (ii) lead to the downregulation of well-known developmental proteins involved in both aerial growth and sporulation, possibly contributing to the dramatically reduced fitness of mutant strains. Our results provide key insights into the mechanisms of the negative phenotypic

correlation between *Streptomyces* development and antibiotic secretion and the division of labor coordinating antibiotic production in this species.

Results

Strains with spontaneous genomic rearrangements show increased antibacterial activity and decreased fitness

We selected five fully sequenced mutant strains from an earlier study (166), each containing different sized genomic rearrangements (Fig. 1A); two of these strains contain large genomic deletions that lead to arginine auxotrophy. We measured colony forming units (CFU) and antibiotic activity on SFM agar by spotting colonies on a cellophane disc, to mirror conditions used for the omics analyses below. Consistent with earlier results from assays carried out on agar without cellophane, these experiments revealed significant increases in antibacterial activity and significant reductions in CFU production (Fig. 1B), with a pronounced negative correlation between these traits (fig. S1. $F_{1,4} = 14.74$, $r^2 = 0.787$, $P = 0.018$).

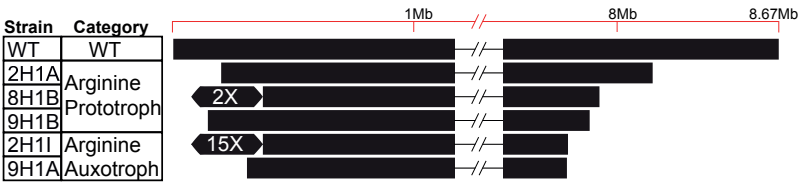
Proteome and metabolome levels vary in different strains

To study the effects of genomic rearrangements on the global expression profiles of proteins and secondary metabolites, we applied liquid chromatography (LC)-MS/MS-based proteomics and metabolomics. Proteomic analyses identified on average 1435 proteins (ranging from 1165 to 1648) in eighteen samples (6 strains \times 3 replicates); replicate samples are highly correlated, confirming the reproducibility of these measurements (fig. S2). Principal component analysis (PCA) of both proteomics and metabolomics results indicate a partitioning into three mutant classes, each distinct from the WT (Fig. 2). These results indicate that the proteomes and secondary metabolomes of these strains have been altered due to genomic rearrangements, consistent with the phenotypic results in Fig. 1.

Proteins affecting antibiotic production in mutant strains

PCA score plots (Fig. 2) show excellent correlations between samples without taking phenotypic results (antibacterial activity and CFU production) into consideration. To identify specific proteins that are associated with antibiotic production, we used a PLS approach (partial least squares/projection to latent structures) which examines the correlation between proteomics profiles and the halo size, indicative of antibiotic production, of each strain. As with the PCA score plot of the proteomics experiments (Fig. 2A), different strains from three classes are distinctly partitioned from each other and from the WT, as shown in the PLS score plot ($R^2 = 0.97$) (Fig. 3A). To assess which proteins contribute to increased antibacterial activity, we used a variance importance in projection

A



B

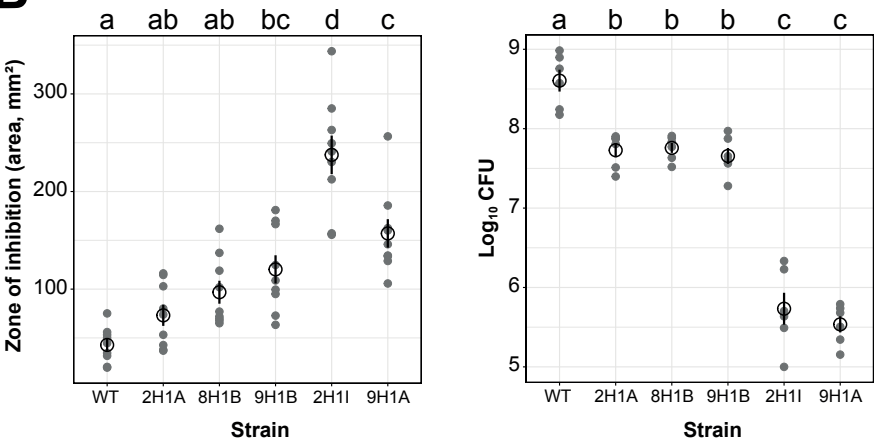


Fig. 1. Overview of the six strains used in this study. Traits shown include (A) genomic organization and the category different strains belong to, (B) antibacterial activity represented by zone of inhibition against *B. subtilis* (left) and fitness represented by CFU production (right). Values are shown as mean \pm SEM. Letters indicate the statistical difference clarified by one-way ANOVA followed by Tukey's tests ($P < 0.05$).

(VIP) plot. High VIP values indicate a larger contribution of that protein to the overall PLS model. Proteins with a VIP>1.4 were ranked by their regression coefficient (table S1 and S2), which reveals that proteins encoded by the BGCs for actinorhodin, coelimycin P1 and CDA, are upregulated in mutant strains and positively correlated with their antibacterial activity (Fig. 3B). Fig. 3C details expression levels of the proteins involved in all four antibiotic biosynthesis pathways compared to the WT strain. These results indicate that, with the exception of prodiginines, most proteins in these BGCs are upregulated in mutants, while none of the proteins in these pathways are downregulated.

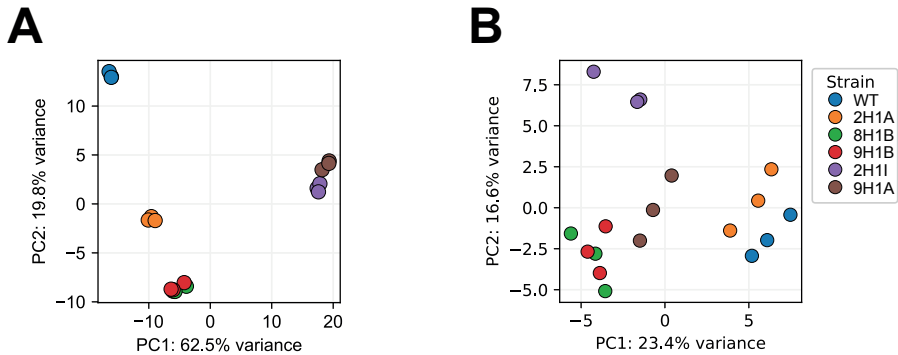


Fig. 2. PCA score plots based on different omics data from six strains. (A) Proteomics (B) Metabolomics.

Because upregulated BGCs in proteomes perfectly predict increased production of their corresponding compounds (141), our proteomics data suggest that mutant strains will produce more antibiotics in terms of quantity and diversity versus the WT. To confirm this prediction, we analyzed metabolomics data to investigate the quantity of the antibiotics indicated above based on their MS information. This revealed that three mutants produced significantly more actinorhodin compared to WT (two-sample t tests, all Bonferroni adjusted $P < 0.05$) while no significant difference in undecylprodigiosin production was observed (Fig. 3D and fig. S3), consistent with the proteomics results (Fig. 3B and C). Although we were unable to identify coelimycin P1 and CDA in our extraction and testing conditions, possibly due to the low yield in our extraction method, further experiments revealed that strains have an increased halo size against *B. subtilis* in calcium-supplemented media. This supports the idea that elevated levels of CDA are present in the mutant strains (fig. S4), consistent with the increased expression of proteins in this biosynthetic pathway. These data demonstrate that the increased killing by mutant colonies is caused by the upregulation of proteins underlying production of several different antibiotics.

Downregulation of developmental proteins are linked to the fitness decline

Following the same PLS approach as above, we next sought to identify proteins whose expression changes correlated with CFU. We first confirmed that strains were partitioned from each other and from the WT ($R^2=0.99$), as shown in Fig. 4A. Next, we ranked proteins with high VIP ($VIP>1.4$) based on their regression coefficients (Fig. 4B; table S3 and S4), which reveals that several proteins essential for development, cell division and sporulation strongly correlate with reduced fitness and are significantly downregulated

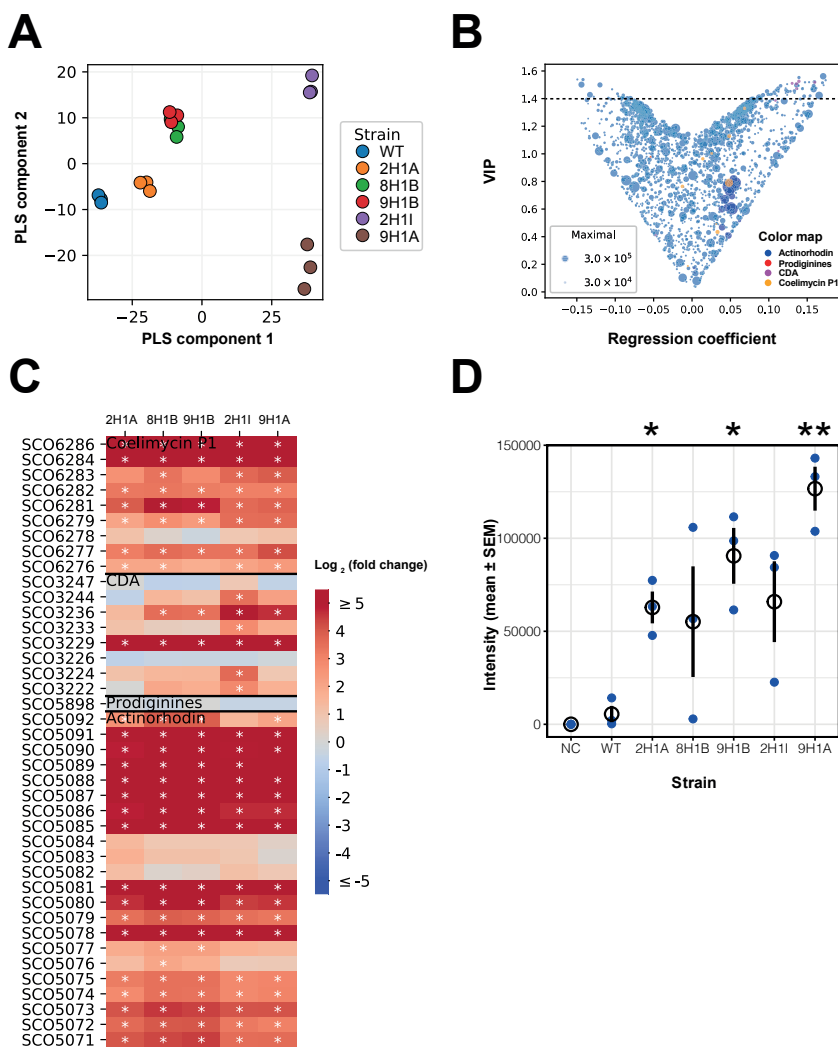


Fig. 3. Antibiotic production increases due to the upregulation of proteins in antibiotic biosynthesis pathways. (A) PLS score plot based on proteomics data. (B) V-plots of VIP and regression coefficient. (C) Log₂ (fold change) of proteins in mutants compared to WT. Asterisks indicate significance according to one-sample *t* tests ($P < 0.05$ and log₂ (fold change) > 1). (D) Actinorhodin production quantified by LC-MS/MS. Asterisks indicate significant differences compared to WT based on two-sample *t* tests with Bonferroni adjusted *P* value (* $P < 0.05$, ** $P < 0.01$).

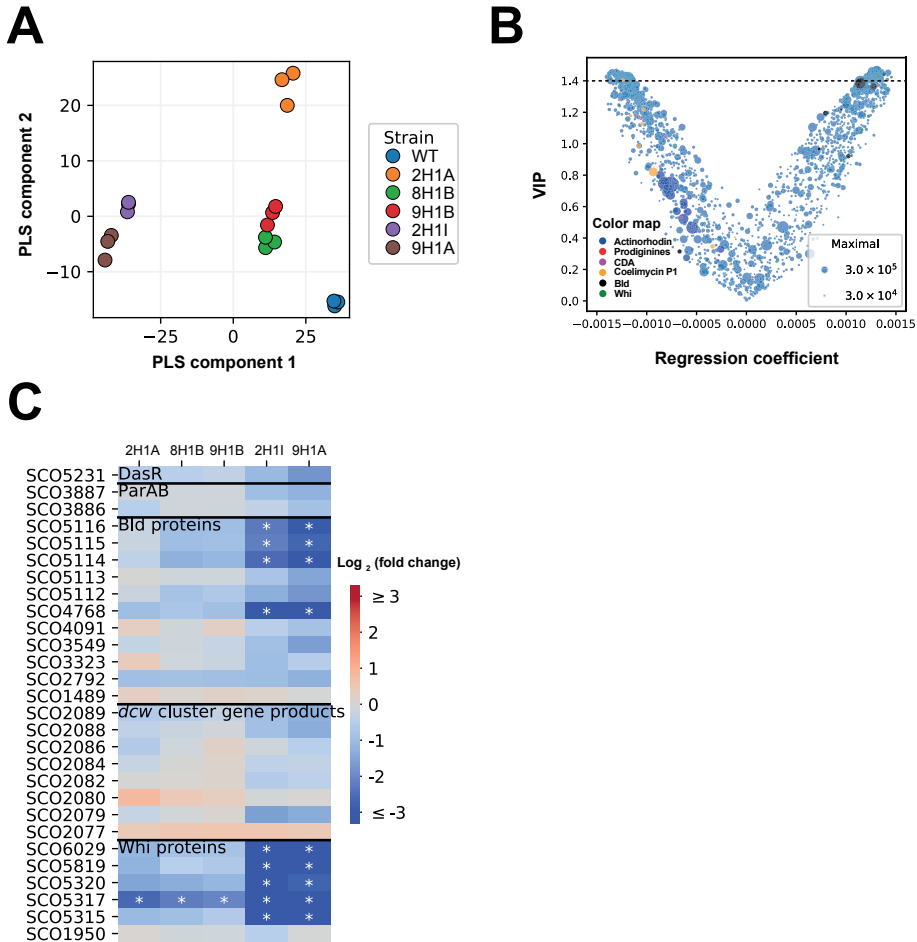


Fig. 4. Decreased fitness correlates to downregulation of developmental proteins. (A) PLS score plot based on proteomics data. (B) V-plots of VIP and regression coefficient. (C) Log₂ (fold change) of proteins in mutants compared to WT. Asterisks indicate the significance according to one-sample *t* tests ($P < 0.05$).

in mutant strains (Fig. 4C). This also reveals a clear negative correlation between CFU and the expression of antibiotic biosynthetic gene clusters, consistent with a trade-off between these functions (Fig. 4B). Key downregulated developmental proteins include gene products of the *bld* genes that regulate the transition to aerial growth, the *dcw* gene cluster that coordinates cell wall formation and cell division, and the *whi* genes that are required for sporulation. Mutations in these pathways have significant negative impacts on *Streptomyces* fitness (8, 111, 188–193), suggesting that the downregulation we observe here is likely causally related to decreased CFU. In addition to these proteins,

we also examined the expression of proteins involved in different developmental stages in *Streptomyces* (9), including ParAB, that regulate DNA condensation and segregation (194–196), Ssg proteins that control cell division (197, 198), DasR that globally regulates development and antibiotic production (109), and proteins that are related to formation of the surface layers that envelope aerial structures including SapB (199–202), chaplins (203, 204) and rodlines (205, 206) (Fig. 4C). We further observed a pronounced reduction in SCO7036 (ArgG) (table S4), as expected given that two strains (2H11 and 9H1A) are arginine auxotrophs, owing to deletions in this region of the genome (172). Interestingly, we find that proteins from the arginine and pyrimidine biosynthesis clusters negatively correlate with fitness (table S4), indicating that changes in primary metabolism can also be a vital factor in influencing the fitness of mutant strains (142). Taken together, these data demonstrate the connection between these developmental proteins and fitness differences of different strains.

Discussion

We previously showed that genomic rearrangements occur frequently in *S. coelicolor* and that these changes reduce fitness while increasing antibacterial activity. This inverse correlation leads to a division of labor within the colony, whereby some cells produce spores while others produce antibiotics, but bear the costs of doing so. In this study, we sought to understand the causes of this trade-off by integrating phenotypic and omics data, based on expressed proteins and metabolites. We have found that the upregulation of proteins in antibiotic biosynthesis clusters directly contributes to enhanced antibacterial activity, which is reflected in the overproduction of antibiotics. Although we only detected actinorhodin and undecylprodigiosin in our extracts, we found significant upregulation of CDA and coelimycin P1 clusters at proteomic level, suggesting that this division of labor involves a combination of antibiotics that can suppress different competing bacteria. This combination of antibiotics is likely to be active against different species by targeting different essential functions in diverse species. Because genomic rearrangements occur spontaneously, leading to a variety of genome sizes that each have different effects, it is possible that these behaviors can also be considered a bet-hedging strategy that *Streptomyces* uses to overcome rapidly fluctuating biotic threats.

This study, and our previous work, indicated that increased production of antibiotics is coupled to a decrease in fitness. More specifically, the number of spores was reduced up to 1000-fold. Morphological development has been studied for decades, and the formation of aerial hyphae and spores depend, amongst others, on the classical *bld* and *whi* genes, respectively (8, 111, 129, 207). Here we find that the levels of BldM and WhiH are reduced in mutants with low fitness. BldM is an atypical response regulator that is crucial for the formation of aerial hyphae (208, 209). Notably, BldM is one of the last proteins that is formed in the developmental *bld* cascade, while BldKE, which is also reduced, is

known as an early stage regulator (201). Taken together, these suggest that genomic rearrangements have global effects on both early and late development stages.

Trade-offs in microbes can be mediated by mutations in genes, often global regulators, that have pleiotropic effects on different traits. For example, mutations in transporters or efflux pumps can simultaneously affect resource uptake and antibiotic import and export (210). It was therefore surprising that in *Streptomyces*, the trade-off between fitness and antibiotic production can be explained by gross, and apparently random, genomic deletions. The linear chromosome of *Streptomyces* consists of a core region containing essential genes that are conserved across species, and two so-called “dispensable” arms that contain a diverse set of genes, both within and across species (34, 35). Our results challenge the assumption that these genomic regions are non-essential. Although their deletions are not lethal, they significantly impact several key phenotypes, including sporulation and the regulation of secondary metabolites. The massive size of these deletions suggests that it will be challenging to identify the causal factors leading to increased antibiotic production and reduced fitness. Do deletions lead to developmental stress that, in turn, causes the overproduction of antibiotics, if both functions are coordinated by general stress responses? Or is it the reverse, that deletions lead to the derepression of antibiotics, and that metabolic constraints imposed by secondary metabolites compromise development? At present this remains unclear. However, in either case, our study proves that proteomics is a powerful tool to identify causal factors that underlie these trade-offs. Similar methods, and their integration with other omics approaches, offer potential to extend studies to a wide range of *Streptomyces* species, in the lab and in nature, to test if proteins tied to trade-offs that arise from deletions are conserved.

Our results will help to identify mechanisms driving the trade-off between antibiotics and fitness. They also lead to questions regarding the mechanisms of division of labor in these bacteria. Deletions appear to arise stochastically, possibly as a by-product of programmed cell death. But they may also arise via a regulated process that is responsive to environmental cues. For example, colonies may increase the proportion of cells containing deletions if there are more competing bacteria nearby, requiring an antibiotic “cocktail”, while this fraction could decline in the absence of competition. Similar adjustments of division of labor are seen in social insects (123). Characterizing the plasticity of division of labor in *Streptomyces* remains an important aim for future work. However, what is already clear is that the irreversibility of these deletions, together with their large and progressively negative impacts, implies that this division of labor is established independently in each colony.

Genomic deletions occur universally in many streptomycetes with linear chromosomes (20, 33, 134, 136, 170, 211). Some authors have suggested that linear chromosomes may be more mutable, although this has been disputed (212–214). It may also be that

chromosome linearity creates recombination hotspots at chromosome ends that causes increased variation in these regions. If high variability is coupled to intrinsic instability, this would serve to maximize within colony phenotypic heterogeneity. In the present case, and perhaps in all *Streptomyces*, the result is a division of labor that is favored by a strong functional trade-off between secondary metabolism and development that is evident phenotypically and in terms of protein and metabolite expression.

Materials and methods

Bacterial strains and culturing conditions

Strains used in this chapter are from previous study and are stored in 20% glycerol at -80°C . During culturing, all strains were diluted to 10^7 CFU ml^{-1} . We then plated $1\mu\text{l}$ onto the SFM agar covered with a piece of sterile cellophane. SFM agar contains 20 g mannitol, 20 g agar and 20 g soya flour per liter of water. Bacteria were cultivated at 30°C .

CFU estimation

Colonies grown on cellophane were harvested after 5 days by aliquoting 5 ml Milli-Q water onto the cellophane surface followed by gently scraping all the spores. The 5 ml water was then filtered through a cotton-plugged syringe to remove mycelial fragments. CFU were estimated by plating serial dilutions.

Antibacterial activity assay

Overlay soft agar was prepared by adding $300\mu\text{l}$ freshly grown *B. subtilis* ($\text{OD}_{600}=0.4-0.6$) to 5 ml soft LB media containing 0.7% agar, 1% tryptone, 0.5% yeast extract and 1% NaCl. For testing the effects of calcium ions in antibacterial activity, 20 mM calcium nitrate was added to the soft agar (215). Each plate was overlaid with 5 ml soft agar on top and incubated at 30°C overnight. Pictures were taken and the sizes of the zone of inhibition were measured using ImageJ.

Extraction of the proteome

At the time of protein extraction, all mycelia were scraped from cellophane disc and put into 2 ml Eppendorf tubes containing metal beads. Tubes were snap frozen in liquid nitrogen and the proteins were extracted and processed as described before (166). Briefly, frozen mycelium was disrupted using TissueLyser II (QIAGEN, Germany) and then dissolved in disrupting buffer (4% SDS, 0.06 M DTT, 100 mM Tris-HCl pH 7.6, 50 mM EDTA). Cell debris was then removed by centrifugation, and proteins were precipitated using chloroform-methanol method (151). Protein pellets were then dissolved in RapiGest SF surfactant (Waters), reduced using DTT, and treated with iodoacetamide. Trypsin (recombinant, proteomics grade, Roche) was then added to digest the proteins. RapiGest SF surfactant

was then degraded by acidification. Resulted peptide solution was then desalted using STAGE-Tips as described by Rappsilber *et al.* (216). LC-MS/MS measurement was performed using nanoACQUITY UPLC system (Waters) connected in line with Synapt G2-Si HDMS mass spectrometer (Waters) using an UDMS^E method set up as described previously (154, 166).

Quantification of proteomics

Identification and quantification of the proteins was done as described previously (166). Briefly, raw data from all samples were first analysed using the vendor software ProteinLynx Global SERVER (PLGS) version 3.0.3. Default protein identification workflow with an additional variable modification, acetyl in N-terminal, was used. Reference protein database was downloaded from GenBank with the accession number NC_003888.3. The resulted dataset was imported to ISOQuant version 1.8 for label-free quantification (154). TOP3 quantification was filtered to remove identifications meet these two criteria: 1. identified in lower than 70% of samples of each strain and 2. sum of TOP3 value less than 1×10^5 . Cleaned quantification data was further subjected to DESeq2 package (version 1.22.2) (217) for variance stabilizing transformation (vst) and PCA was conducted using the normalized data.

Extraction of metabolites

The agar with mycelia was cut into small pieces and extracted with ethyl acetate (or methanol) by soaking in the solvent overnight at room temperature. The extracts were washed twice with 30 ml of water and then dried in a fume hood at room temperature for 24 h until further analyses.

Liquid chromatography tandem-mass spectrometry (LC-MS/MS)

LC-MS/MS acquisition was performed using Shimadzu Nexera X2 UHPLC system, coupled to Shimadzu 9030 QTOF mass spectrometer, equipped with a standard ESI source unit, in which a calibrant delivery system (CDS) is installed. The dry extracts were dissolved in 90% methanol to a final concentration of 1 mg ml^{-1} , and $2 \mu\text{L}$ were injected into a Waters ACQUITY HSS C18 column ($1.8 \mu\text{m}$, 100 \AA , $2.1 \times 100 \text{ mm}$). The column was maintained at 30°C , and run at a flow rate of 0.5 ml min^{-1} , using 0.1% formic acid in H_2O as solvent A, and 0.1% formic acid in acetonitrile as solvent B. A gradient was employed for chromatographic separation starting at 5% B for 1 min, then 5 – 85% B for 9 min, 85 – 100% B for 1 min, and finally held at 100% B for 4 min. The column was re-equilibrated to 5% B for 3 min before the next run was started. The LC flow was switched to the waste the first 0.5 min, then to the MS for 13.5 min, then back to the waste to the end of the run.

All the samples were analyzed in positive (negative) polarity, using data dependent

acquisition mode. In this regard, full scan MS spectra (m/z 100 – 2000, scan rate 20 Hz) were followed by three data dependent MS/MS spectra (m/z 100 – 2000, scan rate 20 Hz) for the three most intense ions per scan. The ions were selected when they reach an intensity threshold of 1000, isolated at the tuning file Q1 resolution, fragmented using collision induced dissociation (CID) with collision energy ramp (CE 20 – 50 eV), and excluded for 0.05 s (one MS scan) before being re-selected for fragmentation.

Multivariate and statistical analyses

Multivariate analyses (PCA and PLS) were done by using scikit-learn (version 0.22) package in Python (version 3.76) following the instruction on the website. Partial least squares/projection to latent structures (PLS) regression is applied to investigate proteins relevant to a corresponding phenotypic traits (antibacterial activity or fitness).

All other statistical analyses were performed in R (v 3.6.2). Shapiro-Wilk test was performed to confirm the normal distribution of data in the same group and Bartlett's test was performed to assess the equality of variances between groups. ANOVA was performed followed by a Tukey's honestly significant difference (HSD) post hoc test. Two-sample Student's t test or Welch's t test was performed to compare the difference between groups.

Proteome data availability

The proteomics data have been deposited to the ProteomeXchange Consortium via the PRIDE partner repository with the dataset identifier PXD014413 and 10.6019/PXD014413 (160, 161).

Chapter 6

General discussion

Genomic instability in streptomycetes has been recognized for decades and has puzzled scientists since its discovery. Initial studies mainly focused on explaining the phenotypic traits it influences (17, 20, 134–136, 170, 218, 219), its rate in different species (17, 20, 134–136, 218), the reagents that affect it (17, 24, 133, 135, 218) and the patterns of chromosomal rearrangements (20, 33, 134–136, 170, 211, 219–221). Despite this, little research has been done to understand the ecological and evolutionary function of genomic instability in *Streptomyces*. In this thesis, I examined the role of genomic instability by interpreting it as a division of labor, in which the population redirects the cost of antibiotics to a minor proportion of cells through terminal genomic rearrangements, thus maintaining the overall fitness of the colony while maintaining high levels of antibiotic production. Furthermore, I investigated the fate of these altruistic mutant cells after their emergence and find that there is a process analogous to a mutational melt-down occurring through the accumulation of both point mutations and large genomic deletions. This leads to a rapid reduction of fitness in mutants and provides the potential to flexibly adjust caste ratios in reaction to environmental changes. To understand the molecular mechanisms that cause the trade-off between fitness and antibiotic production, I used a proteomics approach to identify both global and specific changes in protein abundance underlying the altered fitness and antibiotic secretion in response to genomic rearrangements (Fig. 1).

Division of labor in *Streptomyces*

Like in human society (222), division of labor (DoL) is important for the coordination of complex biological systems. In microorganisms, DoL allows specialized tasks to be carried out more efficiently by collaboration and coordination between different cell types (49, 50). For example, *Bacillus subtilis* promotes migration through the labor divided between surfactin-producing and matrix-producing cells. Some cells produce surfactin to reduce friction, which allows matrix-producing cells to form Van Gogh Bundles to migrate (121). During infection, pathogenic yeast, *Cryptococcus gattii* divides a subpopulation of cells to produce tubular mitochondria in response to host reactive oxygen species. This subpopulation can protect the rest of the cells in macrophages in helping them to proliferate intracellularly (223). These examples from species in various taxa suggest that DoL is a vital strategy in the evolution of microorganisms, which may have been instrumental in the evolution of multicellular life.

Multicellularity in *Streptomyces* has been considered as a canonical example of DoL given that these bacteria form germ cells (aerial mycelia and spores) and somatic cells (vegetative mycelia) (51, 59). Dispersed spores germinate and form vegetative mycelia that forage for nutrients to support growth. Later on, when nutrients are depleted, aerial mycelia will form and produce chains of spores that eventually give rise to another cycle of life (7, 8). During this transition, secondary metabolites including antibiotics are produced by

vegetative mycelia for the benefit of the whole colony (10). In addition to this example of DoL, our results in **Chapter 3** highlight a new type of DoL for antibiotic production. In our scenario of DoL, a proportion of cells in a colony undergoes genomic rearrangements that terminally differentiate into a “sterile caste” specializing in diverse antibiotic production at the cost of fitness. Overall, the colony benefits from the sacrifice of this proportion of “sterilized” cells and gains advantages in competition with other bacterial species. This is comparable to classical DoL between sterile helpers and reproductive castes in social insects (123). Because mutant helpers in *Streptomyces* are derived from the WT through genomic rearrangements, the genetic information in mutants is also present in WT, meaning the fitness interests between these two types of cells are well aligned. Following Hamilton’s rule (224–226), this high relatedness would allow the maintenance of altruistic traits in mutants, thus leading to the DoL in antibiotic production.

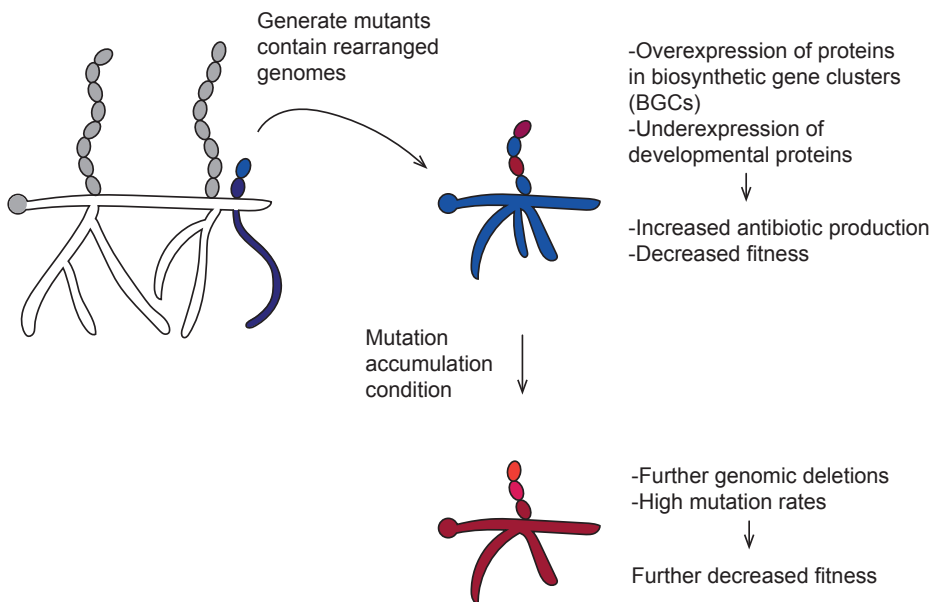


Fig. 1. Schematic summary of this thesis. *Streptomyces* generates mutants containing genomic rearrangements at a high frequency. Mutants produce increased antibiotics at a cost of reduced fitness due to the expression changes in relevant proteins. Under the mutation accumulation condition where natural selection is minimized, mutant cells will continuously accumulate genomic deletions leading to further decreased fitness. Gray colored spores and hyphae contain the intact wild-type genome. Blue and red colored spores and hyphae contain the genome with various degrees of rearrangements.

Phenotypic variation, as a prerequisite for DoL, can be achieved at both genetic and nongenetic levels (227). Among many DoL examples in a single species, nongenetic variation is frequently used as a mechanism to create phenotypic variation (50). However genetic variation including changes in DNA sequences and epigenetic inheritance can also happen in a population derived from isogenic parents (58, 228, 229). In known microbial DoL examples, it appears that most genetic changes in DNA sequences are attributable to point mutations. It is however not common to observe phenotypic variation generated by massive genomic rearrangements as in *Streptomyces*. Our finding is specifically compelling from this perspective, because it has been argued that phenotypic variation caused by genetic changes would not be favored in most conditions due to a high chance of being invaded by cheaters caused by reduced relatedness. I believe the DoL shown in **Chapter 3** is favored because of two relevant reasons. Firstly, the mutant genomes are highly related to the wild-type genome to support kin selection. Secondly, because the filamentous nature of *Streptomyces* makes cells physically connected to each other, it also makes invasion of cheaters difficult to occur. Evidence of DoL in filamentous cyanobacteria and cable bacteria where cells are also physically connected suggests this might play an important role in maintaining a stable DoL (62, 174). Further studies in testing whether DoL is more widespread in physically connected bacteria will help to understand the role of the second factor.

Another interesting aspect of this type of DoL concerns whether the genomic rearrangements are a cause or a consequence of the emergence of altruistic helpers. I hypothesize that the emergence of mutant cells within the mycelium is a stochastic process: during colony development, some cells are prone to genomic damage, leading to mutants that consequently produce antibiotics rather than reproduce. Similar outcomes are observed in some green algae, such as *Volvox carteri* in which cell sizes correlate with the tasks they perform for the colony: cells larger than 8 μm specialize at reproduction and growth while smaller cells specialize at locomotion, constructing a classical germ-soma DoL (230, 231). These smaller somatic cells, interestingly, undergo programmed death which is comparable to altruistic mutants in *Streptomyces* (232, 233). Studies have shown that larger germ cells and smaller somatic cells are more efficient at performing their local tasks (234), respectively, supporting the idea that fitness return in various cell types is a key factor in determining the tasks they perform. However, cell differentiation seems to be regulated and programmed in volvocine algae. Future studies on elaborating our hypothesis about *Streptomyces* DoL will benefit from comparing it to research in *Volvox*. Many follow-up questions can be asked: is this type of DoL genomically encoded? Is it an evolutionarily stable strategy? Can conditions alter the ratio between altruistic mutant helpers and WT reproducers as in some other species? These require more research in the future and are fundamentally important for both the *Streptomyces* and microbial evolution fields.

I have demonstrated that producing antibiotics is a costly activity that dramatically trades off with fitness, meaning that cooperative cell types are likely favored to exist. An extreme example of this type of mutually incompatible tasks would be nitrogen fixation and photosynthesis in some cyanobacteria (99). Our findings help to understand the ecological functions of antibiotics produced by *Streptomyces*, which possibly explain why cryptic antibiotics, that are predicted in genome but not produced in lab conditions, exist in many *Streptomyces* species (145, 235). From an application perspective, knowing that producing antibiotics is costly also raises a new idea about how to find new antibiotics from “old” *Streptomyces*. Future studies focusing on testing whether similar DoL are present in other *Streptomyces* would be helpful to prove if DoL in antibiotic production mediated by genomic rearrangements is a common rule that can be applied in many *Streptomyces*. And if so, then it could possibility lead to novel solutions to elicit new antibiotics.

Mutational meltdown due to massive genomic deletions

From a mechanistic perspective, it is impressive to observe that overproduction of antibiotics is directly linked to genomic rearrangements, specifically large deletions located at the ends of the genome. Older studies have focused on elaborating the pattern of genomic changes rather than focusing on their impacts on cells. In **Chapter 4**, I studied how large genomic deletions influence the evolution of these sterile mutants and what their fate will be over time. In our experimental set-up, we simulated the spore-to-spore transfer which maximizes genetic drift while natural selection is minimized. This is very similar to a mutation accumulation experiment which also allows us to estimate the mutation rates of different lineages.

In our experimental condition, cells were transferred through single cell bottlenecks, leading to a small population size. Considering that *Streptomyces* propagate asexually, this allows us to see the effect of Muller’s ratchet, a process in which deleterious mutations accumulate irreversibly in a population lacking recombination (179, 180). This will further lead to mutation accumulation in all lineages. We observed the meltdown in mutant lineages but not WT ones over a period of 25 transfers. First, mutants had a higher base-substitution mutation rate and smaller effective population size, explaining why a mutational meltdown (182) is likely to happen more rapidly in mutants compared to WT lineages. Second, lineages with terminal deletions quickly accumulate further deletions which in turn decrease the fitness and thus reduce the effective population size. These two effects together cause mutants in *S. coelicolor* to undergo an irreversible and accelerating mutational meltdown (Fig. 2). This fits the idea of a classical mutational meltdown, in which a small population going through Muller’s ratchet experience accelerating fitness declines caused by deleterious mutations (182).

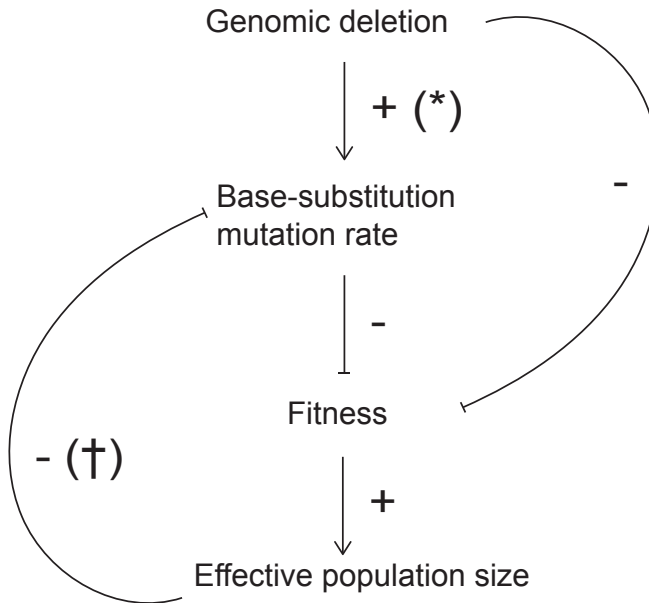


Fig. 2. Mutational meltdown in *Streptomyces coelicolor*. Genomic deletions result in a higher base-substitution mutation rate and lower fitness. The latter subsequently leads to a smaller effective population size. According to Drake's rule (*) (236) and drift-barrier hypothesis (†) (237–239) respectively, these genomic deletions and the smaller effective population size will lead to a higher base-substitution mutation rate. Taken together, these summarize a mutational meltdown in *S. coelicolor*.

Proteomic level changes due to genomic rearrangements

Chapter 5 demonstrates that genomic rearrangements increase the expression of proteins from antibiotic biosynthetic gene clusters (BGCs) and decrease the expression of many developmental proteins, which is consistent with the trade-off we observed in our studies. The fact that different sized genomic rearrangements result in similar proteomic changes in these proteins is intriguing, because it brings up new questions about how large genomic rearrangements affect protein expression. Future studies on finding the quantitative connections between omics data by using mutants with strictly controlled levels of genomic rearrangements will be important in elaborating the genetic network underlying phenotypic changes to spore and antibiotic production. This may be challenging because classical molecular studies in explaining gene networks requires precise knock-out strains. However, as we have observed that mutants with diverse genomic rearrangements universally behave similarly, studies using omics approaches can provide a good beginning in providing directions for further detailed studies.

Genomic instability and adaptation

Genomic instability exists in a wide range of *Streptomyces* species. For the first time, this thesis explains what the evolutionary function of genomic instability is by linking it to a DoL. However this does not exclude the possibility that genomic instability can play other roles in the evolution of *Streptomyces*. For instance, some filamentous actinomycetes have the ability to extrude specialized cells in hyperosmotic conditions that frequently harbor rearranged chromosomes, suggesting genomic instability might be a way of rapidly adapting to certain stressful environments (240). Another study where *Streptomyces clavuligerus* was evolved by competing it serially against methicillin-resistant *Staphylococcus aureus* resulted in strains overproducing the antibiotic holomycin, caused by deletion of a large megaplasmid (241). These studies suggest that genomic instability is an important strategy for *Streptomyces* to adapt to changing environments. Experimental evolution will be a powerful approach to test relevant hypotheses. For example, we can set up a condition where *Streptomyces* competes with another bacterium and test frequencies of evolving lineages harboring genomic rearrangements. Reciprocally, we can test whether a *Streptomyces* strain with a higher level of genomic instability will evolve to produce antibiotics more rapidly. Similar studies have been done in testing functions of bacterial mutators in gaining antibiotic resistance, in which mutators readily become antibiotic resistant while selecting resistant strains also result in mutators. Comparing genomic rearrangements to point mutations will be important, because both of them are double edged swords for bacteria themselves due to the deleterious effects of many mutations. Identifying the advantages of these two types of mutations will help us to understand their evolutionary importance.

As discoveries in modern science requires interdisciplinary knowledge, fundamental research in microbiology requires a comprehensive understanding in both evolutionary and molecular biology. I have used a breadth of techniques to study fundamental evolutionary questions in this thesis. Overall, this research will benefit both evolutionary biologists and molecular microbiologists with the blossoming prospect of the discovery of new antimicrobials that are so urgently needed.

Nederlandse samenvatting

Hoewel bacteriën niet met het blote oog waarneembaar zijn, vormen ze het grootste en meest diverse domein op aarde (1, 2). Binnen deze diversiteit nemen de streptomyceten een speciale plaats in. Door streptomyceten geproduceerde metabolieten vormen het merendeel van de antibiotica en antischimmelmiddelen die in de kliniek worden gebruikt en dit heeft er voor gezorgd dat het maatschappelijk belang van deze bacteriën niet kan worden onderschat (12, 13). Een belangrijke uitdaging voor de exploitatie van deze organismen is echter het feit dat ze een enorme genomische instabiliteit vertonen, een eigenschap die kan leiden tot de verandering van functies die relevant zijn voor hun economische waarde, met name de productie van antibiotica (17–20). Meercellige organismen kenmerken zich door hun vermogen om taken te verdelen tussen de cellen waaruit ze bestaan. Deze taakverdeling kan worden gedefinieerd als de situatie waarin individuele cellen binnen een lichaam, of subpopulaties binnen samenlevingen, complementaire taken uitvoeren om het functioneren van het organisme of de kolonie te verbeteren (49–52). Het beschrijven van dergelijke taakverdelingen bestaat idealiter uit het identificeren van de omvang en oorzaken van reeds bestaande fenotypische variatie en samenwerkingen, en het maken van kwantitatieve schattingen van de adaptieve voordelen die hieraan zijn verbonden (50). Het meten van deze eigenschappen is relatief makkelijk in microben en dit heeft in de afgelopen jaren geleid tot een significante toename van de literatuur over microbiële taakverdelingen. In **Hoofdstuk 2** bespreken we een deel van deze literatuur, ten eerste om een beter inzicht te krijgen in de oorzaken en gevolgen van microbiële taakverdelingen, en ten tweede om onze latere beschrijving van taakverdelingen binnen streptomyceten-kolonies beter in een kader te kunnen plaatsen. Eerst beschrijven we de taakverdeling tussen somatische cellen en geslachtscellen en beargumenteren we hoe een vergelijkbare taakverdeling van toepassing is bij *Myxococcus* en *Dictostylium*. We gaan hierbij ook in op de parallellen tussen de productie van sporen bij microben en de kastenverhoudingen bij sociale insecten, en hoe deze verdelingen via kin-selectie bescherming bieden tegen uitbuiting en conflict. Vervolgens beschrijven we hoe cel-differentiatie in andere meercellige bacteriën soms volgens vaste patronen verloopt, zoals bij streptomyceten en cyanobacteriën. Dit wordt gevolgd door een bespreking van theoretisch mogelijke taakverdelingen bij streptomyceten en hoe dergelijke verdelingen eerder onderzocht zijn in andere bacteriesoorten.

Hyperpigmentatie wordt regelmatig waargenomen in sommige kolonies van *Streptomyces coelicolor* die worden gegenereerd als gevolg van genomische instabiliteit. Omdat de bekende antibiotica die *S. coelicolor* produceert ook gepigmenteerd zijn, onderzochten we de hypothese dat genomische instabiliteit ten grondslag ligt aan een taakverdeling met betrekking tot de productie van antibiotica. Door gebruik te maken van diverse technieken uit de microbiële evolutie en verschillende omics benaderingen, biedt **Hoofdstuk 3** een

nieuw inzicht in hoe terminale differentiatie van het genoom de productie van antibiotica beïnvloedt in *S. coelicolor*. We laten zien dat mutanten ontstaan, met een frequentie van ongeveer 1%, die zich minder goed voortplanten, maar die wel een grotere diversiteit en kwantiteit aan antibiotica produceren. Deze veranderingen zijn geassocieerd met genoomdeleties en laten daarmee een duidelijke afweging tussen antibioticaproductie en voortplanting zien. Door competitie-experimenten uit te voeren met mengsels van mutanten en wild-type cellen, laten we vervolgens zien dat deze taakverdeling leidt tot een verhoogde reproductie op het niveau van de kolonie.

Omdat de mutanten zich relatief minder succesvol voortplanten dan de wild-type cellen, worden ze snel door competitie binnen de kolonie weggeconcentreerd. In **Hoofdstuk 4** breiden we onze studie uit met een analyse van de afstammingslijnen van deze mutanten om hun genetische lot in kaart te brengen. De resultaten laten zien dat mutanten met initiële genoom-deleties in latere generaties nog meer deleties ondergaan, aan zowel de linker- als de rechterzijde van het lineaire chromosoom, en dat deze secundaire deleties gepaard gaan met een aanzienlijke verlaging van de sporenproductie. Daarnaast hebben de mutanten regelmatig een verhoogde mutatiefrequentie, wat zorgt voor een snellere accumulatie van schadelijke mutaties. Deze resultaten suggereren dat mutanten in *S. coelicolor* parallellen vertonen met de steriele kasten bij sociale insecten. Vanwege diverse en voortdurende genomische schade worden ze gemakkelijk weggeconcentreerd tijdens de groei van de kolonie en moeten ze daarom voortdurend opnieuw worden gegenereerd tijdens de kolonie-ontwikkeling. Deze gegevens voegen een nieuwe dimensie toe aan het idee van mutationele ineenstorting, omdat forse genomische deleties samen met de opkomst van verhoogde mutatiefrequenties er via een verlaagde sporen productie voor zorgen dat de mutanten doorgaans snel uitsterven.

In **Hoofdstuk 5** bestuderen we de effecten van genomische reorganisaties in *S. coelicolor*, met behulp van op massaspectrometrie gebaseerde proteomics en metabolomics. We tonen aan dat verhoogde antibacteriële activiteit in de mutanten daadwerkelijk wordt veroorzaakt door overproductie van antibiotica. We nemen een toename waar van meerdere eiwitten die deel uitmaken van biosynthetische genclusters voor antibiotica. Daarnaast worden verschillende belangrijke ontwikkelingseiwitten in mindere mate aangemaakt in de mutanten, wat mogelijk samenhangt met de verlaagde reproductie. Dit hoofdstuk geeft gedetailleerde moleculaire informatie over hoe de afweging tussen antibioticaproductie en voortplanting wordt gestuurd door genomische differentiatie, en helpt ons daarmee om de taakverdeling in *S. coelicolor* kolonies beter te begrijpen.

Tot slot biedt **Hoofdstuk 6** een bespreking van de resultaten uit de voortgaande hoofdstukken, en ook perspectieven voor het verder bestuderen van genomische instabiliteit in streptomyceten en andere meercellige bacteriën.

References

1. F. D. Ciccarelli, T. Doerks, C. J. Creevey, B. Snel, P. Bork, Toward automatic reconstruction of a highly resolved tree of life. *Science*. **311**, 1283–1287 (2006).
2. L. A. Hug, B. J. Baker, K. Anantharaman, C. T. Brown, A. J. Probst, C. J. Castelle, C. N. Butterfield, A. W. HERNSDORF, Y. Amano, K. Ise, Y. Suzuki, N. Dudek, D. A. Relman, K. M. Finstad, R. Amundson, B. C. Thomas, J. F. Banfield, A new view of the tree of life. *Nat. Microbiol.* **1**, 16048 (2016).
3. K. D. Young, The selective value of bacterial shape. *Microbiol. Mol. Biol. Rev.* **70**, 660–703 (2006).
4. D. T. Kysela, A. M. Randich, P. D. Caccamo, Y. V. Brun, Diversity takes shape: understanding the mechanistic and adaptive basis of bacterial morphology. *PLoS Biol.* **14**, e1002565 (2016).
5. T. Cross, Aquatic actinomycetes: a critical survey of the occurrence, growth and role of actinomycetes in aquatic habitats. *J. Appl. Bacteriol.* **50**, 397–423 (1981).
6. M. Goodfellow, S. T. Williams, Ecology of actinomycetes. *Annu. Rev. Microbiol.* **37**, 189–216 (1983).
7. K. F. Chater, R. Losick, in *Bacteria as multicellular organisms* (Oxford University Press, New York, 1997), pp. 149–182.
8. K. Flärdh, M. J. Buttner, *Streptomyces* morphogenetics: dissecting differentiation in a filamentous bacterium. *Nat. Rev. Microbiol.* **7**, 36–49 (2009).
9. E. A. Barka, P. Vatsa, L. Sanchez, N. Gaveau-Vaillant, C. Jacquard, H.-P. Klenk, C. Clément, Y. Ouhdouch, G. P. van Wezel, Taxonomy, physiology, and natural products of Actinobacteria. *Microbiol. Mol. Biol. Rev.* **80**, 1–43 (2016).
10. D. A. Hopwood, *Streptomyces in nature and medicine: the antibiotic makers* (Oxford University Press, New York, 2007).
11. K. F. Chater, S. Biró, K. J. Lee, T. Palmer, H. Schrempf, The complex extracellular biology of *Streptomyces*. *FEMS Microbiol. Rev.* **34**, 171–198 (2010).
12. J. Bérdy, Bioactive microbial metabolites. *J. Antibiot. (Tokyo)*. **58**, 1–26 (2005).
13. H. U. Van Der Heul, B. L. Bilyk, K. J. McDowall, R. F. Seipke, G. P. Van Wezel, Regulation of antibiotic production in Actinobacteria: new perspectives from the post-genomic era. *Nat. Prod. Rep.* **35**, 575–604 (2018).

14. S. A. Waksman, Streptomycin: background, isolation, properties, and utilization. *Science*. **118**, 259–266 (1953).
15. M. Debono, M. Barnhart, C. B. Carrell, J. A. Hoffmann, J. L. Occolowitz, B. J. Abbott, D. S. Fukuda, R. L. Hamill, K. Biemann, W. C. Herlihy, A21978C, a complex of new acidic peptide antibiotics: isolation, chemistry, and mass spectral structure elucidation. *J. Antibiot. (Tokyo)*. **40**, 761–777 (1987).
16. S. Westhoff, S. B. Otto, A. Swinkels, B. Bode, G. P. Wezel, D. E. Rozen, Spatial structure increases the benefits of antibiotic production in *Streptomyces*. *Evolution*. **74**, 179–187 (2020).
17. M. Matsubara-Nakano, Y. Kataoka, H. Ogawara, Unstable mutation of β -lactamase production in *Streptomyces lavendulae*. *Antimicrob. Agents Chemother.* **17**, 124–128 (1980).
18. T. Miyoshi, M. Iseki, T. Konomi, H. Imanaka, Biosynthesis of bicyclomycin. I. Appearance of aerial mycelia negative strains (am-). *J. Antibiot. (Tokyo)*. **33**, 480–487 (1980).
19. M. Roth, D. Noack, Genetic stability of differentiated functions in *Streptomyces hygroscopicus* in relation to conditions of continuous culture. *J. Gen. Microbiol.* **128**, 107–114 (1982).
20. B. Gravius, T. Bezmalinovic, D. Hranueli, J. Cullum, Genetic instability and strain degeneration in *Streptomyces rimosus*. *Appl. Environ. Microbiol.* **59**, 2220–2228 (1993).
21. K. F. Gregory, J. C. Huang, Tyrosinase inheritance in *Streptomyces scabies*. I. Genetic recombination. *J. Bacteriol.* **87**, 1281–1286 (1964).
22. J. Cullum, J. Altenbuchner, F. Flett, W. Piendl, DNA amplification and genetic instability in *Streptomyces*. *Biotechnol. Genet. Eng. Rev.* **4**, 59–78 (1986).
23. K. F. Gregory, J. C. Huang, Tyrosinase inheritance in *Streptomyces scabies*. II. Induction of tyrosinase deficiency by acridine dyes. *J. Bacteriol.* **87**, 1287–1294 (1964).
24. J.-N. Volff, D. Vandewiele, J.-M. Simonet, B. Decaris, Ultraviolet light, mitomycin C and nitrous acid induce genetic instability in *Streptomyces ambofaciens* ATCC23877. *Mutat. Res. Mol. Mech. Mutagen.* **287**, 141–156 (1993).
25. P. Leblond, P. Demuyter, J. M. Simonet, B. Decaris, Genetic instability and hypervariability in *Streptomyces ambofaciens*: towards an understanding of a

References

- mechanism of genome plasticity. *Mol. Microbiol.* **4**, 707–714 (1990).
26. A. Birch, A. Hausler, R. Hutter, Genome rearrangement and genetic instability in *Streptomyces* spp. *J. Bacteriol.* **172**, 4138–4142 (1990).
27. P. Leblond, B. Decaris, New insights into the genetic instability of *Streptomyces*. *FEMS Microbiol. Lett.* **123**, 225–232 (1994).
28. P. Leblond, B. Decaris, Chromosome geometry and intraspecific genetic polymorphism in Gram-positive bacteria revealed by pulsed-field gel electrophoresis. *Electrophoresis.* **19**, 582–588 (1998).
29. J.-N. Volff, J. Altenbuchner, Genetic instability of the *Streptomyces* chromosome. **27**, 239–246 (1998).
30. A. Dary, P. Martin, T. Wenner, P. Leblond, B. Decaris, Evolution of the linear chromosomal DNA in *Streptomyces*: is genomic variability developmentally modulated? *Res. Microbiol.* **150**, 439–445 (1999).
31. A. Dary, P. Martin, T. Wenner, B. Decaris, P. Leblond, DNA rearrangements at the extremities of the *Streptomyces ambofaciens* linear chromosome: evidence for developmental control. *Biochimie.* **82**, 29–34 (2000).
32. C. W. Chen, C. H. Huang, H. H. Lee, H. H. Tsai, R. Kirby, Once the circle has been broken: dynamics and evolution of *Streptomyces* chromosomes. *Trends Genet.* **18**, 522–529 (2002).
33. S. E. Fishman, C. L. Hershberger, Amplified DNA in *Streptomyces fradiae*. *J. Bacteriol.* **155**, 459–466 (1983).
34. Y. Lin, H. M. Kieser, D. A. Hopwood, C. W. Chen, The chromosomal DNA of *Streptomyces lividans* 66 is linear. *Mol. Microbiol.* **10**, 923–933 (1993).
35. S. D. Bentley, K. F. Chater, A.-M. Cerdeno-Tárraga, G. L. Challis, N. R. Thomson, K. D. James, D. E. Harris, M. A. Quail, H. Kieser, D. Harper, A. Bateman, S. Brown, G. Chandra, C. W. Chen, M. Collins, A. Cronin, A. Fraser, A. Goble, J. Hidalgo, T. Hornsby, S. Howarth, C.-H. Huang, T. Kieser, L. Larke, L. Murphy, K. Oliver, S. O’Neil, E. Rabinowitsch, M.-A. Rajandream, K. Rutherford, S. Rutter, K. Seeger, D. Saunders, S. Sharp, R. Squares, S. Squares, K. Taylor, T. Warren, A. Wietzorrek, J. Woodward, B. G. Barrell, J. Parkhill, D. A. Hopwood, Complete genome sequence of the model actinomycete *Streptomyces coelicolor* A3(2). *Nature.* **417**, 141–147 (2002).
36. D. A. Hopwood, Soil to genomics: the *Streptomyces* chromosome. *Annu. Rev. Genet.* **40**, 1–23 (2006).

37. H. Zhu, J. Swierstra, C. Wu, G. Girard, Y. H. Choi, W. van Wamel, S. K. Sandiford, G. P. van Wezel, Eliciting antibiotics active against the ESKAPE pathogens in a collection of actinomycetes isolated from mountain soils. *Microbiology*. **160**, 1714–1726 (2014).
38. S. M. Rosenberg, Evolving responsively: adaptive mutation. *Nat. Rev. Genet.* **2**, 504–515 (2001).
39. J. A. G. M. de Visser, The fate of microbial mutators. *Microbiology*. **148**, 1247–1252 (2002).
40. I. Martincorena, A. S. N. Seshasayee, N. M. Luscombe, Evidence of non-random mutation rates suggests an evolutionary risk management strategy. *Nature*. **485**, 95–98 (2012).
41. M. Kimura, On the evolutionary adjustment of spontaneous mutation rates. *Genet. Res.* **9**, 23–34 (1967).
42. T. T. Kibota, M. Lynch, Estimate of the genomic mutation rate deleterious to overall fitness in *E. coli*. *Nature*. **381**, 694–696 (1996).
43. M. Lynch, M. S. Ackerman, J.-F. Gout, H. Long, W. Sung, W. K. Thomas, P. L. Foster, Genetic drift, selection and the evolution of the mutation rate. *Nat. Rev. Genet.* **17**, 704–714 (2016).
44. F. Taddei, M. Radman, J. Maynard-Smith, B. Toupance, P. H. Gouyon, B. Godelle, Role of mutator alleles in adaptive evolution. *Nature*. **387**, 700–702 (1997).
45. A. Giraud, I. Matic, O. Tenaillon, A. Clara, M. Radman, M. Fons, F. Taddei, Costs and benefits of high mutation rates: adaptive evolution of bacteria in the mouse gut. *Science*. **291**, 2606–2608 (2001).
46. A. Oliver, A. Mena, Bacterial hypermutation in cystic fibrosis, not only for antibiotic resistance. *Clin. Microbiol. Infect.* **16**, 798–808 (2010).
47. I. Matic, B. Picard, Highly variable mutation rates in commensal and pathogenic *Escherichia coli*. *Science*. **277**, 1833–1834 (1997).
48. J. W. Drake, B. Charlesworth, D. Charlesworth, J. F. Crow, Rates of spontaneous mutation. *Genetics*. **148**, 1667–1686 (1998).
49. J. van Gestel, H. Vlamakis, R. Kolter, Division of labor in biofilms: the ecology of cell differentiation. *Microbiol. Spectr.* **3**, MB-0002-2014 (2015).

References

50. S. A. West, G. A. Cooper, Division of labour in microorganisms: an evolutionary perspective. *Nat. Rev. Microbiol.* **14**, 716–723 (2016).
51. Z. Zhang, D. Claessen, D. E. Rozen, Understanding microbial divisions of labor. *Front. Microbiol.* **7**, 2070 (2016).
52. S. Giri, S. Waschina, C. Kaleta, C. Kost, Defining division of labor in microbial communities. *J. Mol. Biol.* **431**, 4712–4731 (2019).
53. C. R. Smith, A. L. Toth, A. V. Suarez, G. E. Robinson, Genetic and genomic analyses of the division of labour in insect societies. *Nat. Rev. Genet.* **9**, 735–748 (2008).
54. E. O. Wilson, Caste and division of labor in leaf-cutter ants (Hymenoptera: Formicidae: *Atta*). *Behav. Ecol. Sociobiol.* **7**, 143–156 (1980).
55. J.-W. Veening, W. K. Smits, O. P. Kuipers, Bistability, epigenetics, and bet-hedging in bacteria. *Annu. Rev. Microbiol.* **62**, 193–210 (2008).
56. G. J. Velicer, M. Vos, Sociobiology of the myxobacteria. *Annu. Rev. Microbiol.* **63**, 599–623 (2009).
57. V. Rossetti, H. C. Bagheri, Advantages of the division of labour for the long-term population dynamics of cyanobacteria at different latitudes. *Proc. R. Soc. B Biol. Sci.* **279**, 3457–3466 (2012).
58. W. Kim, S. B. Levy, K. R. Foster, Rapid radiation in bacteria leads to a division of labour. *Nat. Commun.* **7**, 10508 (2016).
59. D. Claessen, D. E. Rozen, O. P. Kuipers, L. Søgaard-Andersen, G. P. Van Wezel, Bacterial solutions to multicellularity: a tale of biofilms, filaments and fruiting bodies. *Nat. Rev. Microbiol.* **12**, 115–124 (2014).
60. L. J. Shimkets, Social and developmental biology of the myxobacteria. *Microbiol. Rev.* **54**, 473–501 (1990).
61. J. E. Strassmann, O. M. Gilbert, D. C. Queller, Kin discrimination and cooperation in microbes. *Annu. Rev. Microbiol.* **65**, 349–367 (2011).
62. A. Herrero, J. Stavans, E. Flores, The multicellular nature of filamentous heterocyst-forming cyanobacteria. *FEMS Microbiol. Rev.* **40**, 831–854 (2016).
63. S. Borgeaud, L. C. Metzger, T. Scrignari, M. Blokesch, The type VI secretion system of *Vibrio cholerae* fosters horizontal gene transfer. *Science*. **347**, 63–67 (2015).

64. N. M. Oliveira, R. Niehus, K. R. Foster, Evolutionary limits to cooperation in microbial communities. *Proc. Natl. Acad. Sci. U. S. A.* **111**, 17941–17946 (2014).
65. S. A. West, A. S. Griffin, A. Gardner, S. P. Diggle, Social evolution theory for microorganisms. *Nat. Rev. Microbiol.* **4**, 597–607 (2006).
66. S. A. West, S. P. Diggle, A. Buckling, A. Gardner, A. S. Griffin, The social lives of microbes. *Annu. Rev. Ecol. Evol. Syst.* **38**, 53–77 (2007).
67. A. D. Morgan, R. C. MacLean, K. L. Hillesland, G. J. Velicer, Comparative analysis of *Myxococcus* predation on soil bacteria. *Appl. Environ. Microbiol.* **76**, 6920–6927 (2010).
68. Y. Xiao, X. Wei, R. Ebricht, D. Wall, Antibiotic production by myxobacteria plays a role in predation. *J. Bacteriol.* **193**, 4626–4633 (2011).
69. J. Muñoz-Dorado, F. J. Marcos-Torres, E. García-Bravo, A. Moraleda-Muñoz, J. Pérez, Myxobacteria: moving, killing, feeding, and surviving together. *Front. Microbiol.* **7**, 781 (2016).
70. K. Lewis, Programmed death in bacteria. *Microbiol. Mol. Biol. Rev.* **64**, 503–514 (2000).
71. S. Bhat, T. O. Boynton, D. Pham, L. J. Shimkets, Fatty acids from membrane lipids become incorporated into lipid bodies during *Myxococcus xanthus* differentiation. *PLoS One*. **9**, e99622 (2014).
72. S. Bhat, T. Ahrendt, C. Dauth, H. B. Bode, L. J. Shimkets, Two lipid signals guide fruiting body development of *Myxococcus xanthus*. *MBio*. **5**, e00939-13 (2014).
73. L. Passera, E. Roncin, B. Kaufmann, L. Keller, Increased soldier production in ant colonies exposed to intraspecific competition. *Nature*. **379**, 630–631 (1996).
74. J. A. Harvey, L. S. Corley, M. R. Strand, Competition induces adaptive shifts in caste ratios of a polyembryonic wasp. *Nature*. **406**, 183–186 (2000).
75. S. A. Kraemer, G. J. Velicer, Endemic social diversity within natural kin groups of a cooperative bacterium. *Proc. Natl. Acad. Sci. U. S. A.* **108**, 10823–10830 (2011).
76. G. J. Velicer, L. Kroos, R. E. Lenski, Developmental cheating in the social bacterium *Myxococcus xanthus*. *Nature*. **404**, 598–601 (2000).
77. F. Fiegna, G. J. Velicer, Exploitative and hierarchical antagonism in a cooperative bacterium. *PLoS Biol.* **3**, e370 (2005).

References

78. M. Vos, G. J. Velicer, Social conflict in centimeter- and global-scale populations of the bacterium *Myxococcus xanthus*. *Curr. Biol.* **19**, 1763–1767 (2009).
79. S. A. Kraemer, G. J. Velicer, Social complementation and growth advantages promote socially defective bacterial isolates. *Proc. R. Soc. B Biol. Sci.* **281**, 20140036 (2014).
80. G. J. Velicer, R. E. Lenski, L. Kroos, Rescue of social motility lost during evolution of *Myxococcus xanthus* in an asocial environment. *J. Bacteriol.* **184**, 2719–2727 (2002).
81. S. A. Kraemer, M. A. Toups, G. J. Velicer, Natural variation in developmental life-history traits of the bacterium *Myxococcus xanthus*. *FEMS Microbiol. Ecol.* **73**, 226–233 (2010).
82. O. Rendueles, P. C. Zee, I. Dinkelacker, M. Amherd, S. Wielgoss, G. J. Velicer, Rapid and widespread de novo evolution of kin discrimination. *Proc. Natl. Acad. Sci.* **112**, 9076–9081 (2015).
83. D. Wall, Kin recognition in bacteria. *Annu. Rev. Microbiol.* **70**, 143–160 (2016).
84. S. I. Li, M. D. Purugganan, The cooperative amoeba: *Dictyostelium* as a model for social evolution. *Trends Genet.* **27**, 48–54 (2011).
85. J. E. Strassmann, D. C. Queller, How social evolution theory impacts our understanding of development in the social amoeba *Dictyostelium*. *Dev. Growth Differ.* **53**, 597–607 (2011).
86. N. J. Buttery, D. E. Rozen, J. B. Wolf, C. R. L. Thompson, Quantification of social behavior in *D. discoideum* reveals complex fixed and facultative strategies. *Curr. Biol.* **19**, 1373–1377 (2009).
87. A. Fortunato, D. C. Queller, J. E. Strassmann, A linear dominance hierarchy among clones in chimeras of the social amoeba *Dictyostelium discoideum*. *J. Evol. Biol.* **16**, 438–445 (2003).
88. J. E. Strassmann, Y. Zhu, D. C. Queller, Altruism and social cheating in the social amoeba *Dictyostelium discoideum*. *Nature.* **408**, 965–967 (2000).
89. J. B. Wolf, J. A. Howie, K. Parkinson, N. Gruenheit, D. Melo, D. Rozen, C. R. L. Thompson, Fitness trade-offs result in the illusion of social success. *Curr. Biol.* **25**, 1086–1090 (2015).
90. R. Martínez-García, C. E. Tarnita, Lack of ecological and life history context can

- create the illusion of social interactions in *Dictyostelium discoideum*. *PLoS Comput. Biol.* **12**, e1005246 (2016).
91. C. E. Tarnita, A. Washburne, R. Martinez-Garcia, A. E. Sgro, S. A. Levin, Fitness tradeoffs between spores and nonaggregating cells can explain the coexistence of diverse genotypes in cellular slime molds. *Proc. Natl. Acad. Sci. U. S. A.* **112**, 2776–2781 (2015).
 92. J. E. Strassmann, Kin discrimination in *Dictyostelium* social amoebae. *J. Eukaryot. Microbiol.* **63**, 378–383 (2016).
 93. N. J. Buttery, C. N. Jack, B. Adu-Oppong, K. T. Snyder, C. R. L. Thompson, D. C. Queller, J. E. Strassmann, Structured growth and genetic drift raise relatedness in the social amoeba *Dictyostelium discoideum*. *Biol. Lett.* **8**, 794–797 (2012).
 94. J. Smith, J. E. Strassmann, D. C. Queller, Fine-scale spatial ecology drives kin selection relatedness among cooperating amoebae. *Evolution*. **70**, 848–859 (2016).
 95. H.-I. Ho, S. Hirose, A. Kuspa, G. Shaulsky, Kin recognition protects cooperators against cheaters. *Curr. Biol.* **23**, 1590–1595 (2013).
 96. O. M. Gilbert, K. R. Foster, N. J. Mehdiabadi, J. E. Strassmann, D. C. Queller, High relatedness maintains multicellular cooperation in a social amoeba by controlling cheater mutants. *Proc. Natl. Acad. Sci. U. S. A.* **104**, 8913–8917 (2007).
 97. O. M. Gilbert, D. C. Queller, J. E. Strassmann, Discovery of a large clonal patch of a social amoeba: implications for social evolution. *Mol. Ecol.* **18**, 1273–1281 (2009).
 98. R. M. Fisher, C. K. Cornwallis, S. A. West, Group formation, relatedness, and the evolution of multicellularity. *Curr. Biol.* **23**, 1120–1125 (2013).
 99. E. Flores, A. Herrero, Compartmentalized function through cell differentiation in filamentous cyanobacteria. *Nat. Rev. Microbiol.* **8**, 39–50 (2010).
 100. V. Rossetti, B. E. Schirrmeister, M. V. Bernasconi, H. C. Bagheri, The evolutionary path to terminal differentiation and division of labor in cyanobacteria. *J. Theor. Biol.* **262**, 23–34 (2010).
 101. J. C. Meeks, J. Elhai, Regulation of cellular differentiation in filamentous cyanobacteria in free-living and plant-associated symbiotic growth states. *Microbiol. Mol. Biol. Rev.* **66**, 94–121 (2002).
 102. D. G. Adams, P. S. Duggan, Heterocyst and akinete differentiation in cyanobacteria. *New Phytol.* **144**, 3–33 (1999).

References

103. A. Manteca, U. Mäder, B. A. Connolly, J. Sanchez, A proteomic analysis of *Streptomyces coelicolor* programmed cell death. *Proteomics*. **6**, 6008–6022 (2006).
104. P. Yagüe, M. T. Lopez-Garcia, B. Rioseras, J. Sanchez, A. Manteca, New insights on the development of *Streptomyces* and their relationships with secondary metabolite production. *Curr. trends Microbiol.* **8**, 65–73 (2012).
105. A. M. Nedelcu, W. W. Driscoll, P. M. Durand, M. D. Herron, A. Rashidi, On the paradigm of altruistic suicide in the unicellular world. *Evolution*. **65**, 3–20 (2011).
106. D. H. Braendle, W. Szybalski, Genetic interaction among streptomycetes: heterokaryosis and synkaryosis. *Proc. Natl. Acad. Sci.* **43**, 947–955 (1957).
107. D. H. Braendle, W. Szybalski, Heterokaryotic compatibility, metabolic cooperation, and genic recombination in *Streptomyces*. *Ann. N. Y. Acad. Sci.* **81**, 824–851 (1959).
108. S. Rigali, H. Nothaft, E. E. E. Noens, M. Schlicht, S. Colson, M. Müller, B. Joris, H. K. Koerten, D. A. Hopwood, F. Titgemeyer, G. P. Van Wezel, The sugar phosphotransferase system of *Streptomyces coelicolor* is regulated by the GntR-family regulator DasR and links N-acetylglucosamine metabolism to the control of development. *Mol. Microbiol.* **61**, 1237–1251 (2006).
109. S. Rigali, F. Titgemeyer, S. Barends, S. Mulder, A. W. Thomae, D. A. Hopwood, G. P. van Wezel, Feast or famine: the global regulator DasR links nutrient stress to antibiotic production by *Streptomyces*. *EMBO Rep.* **9**, 670–675 (2008).
110. E. Tenconi, M. Urem, M. A. Świątek-Połatyńska, F. Titgemeyer, Y. A. Muller, G. P. van Wezel, S. Rigali, Multiple allosteric effectors control the affinity of DasR for its target sites. *Biochem. Biophys. Res. Commun.* **464**, 324–329 (2015).
111. D. Claessen, W. de Jong, L. Dijkhuizen, H. A. B. Wösten, Regulation of *Streptomyces* development: reach for the sky! *Trends Microbiol.* **14**, 313–319 (2006).
112. R. E. Michod, The group covariance effect and fitness trade-offs during evolutionary transitions in individuality. *Proc. Natl. Acad. Sci. U. S. A.* **103**, 9113–9117 (2006).
113. R. J. Bleichrodt, G. J. van Veluw, B. Recter, J. I. Maruyama, K. Kitamoto, H. A. B. Wösten, Hyphal heterogeneity in *Aspergillus oryzae* is the result of dynamic closure of septa by Woronin bodies. *Mol. Microbiol.* **86**, 1334–1344 (2012).
114. A. M. Levin, R. P. de Vries, A. Conesa, C. de Bekker, M. Talon, H. H. Menke, N. N. M. E. van Peij, H. A. B. Wösten, Spatial differentiation in the vegetative mycelium of *Aspergillus niger*. *Eukaryot. Cell.* **6**, 2311–2322 (2007).

115. A. Vinck, M. Terlouw, W. R. Pestman, E. P. Martens, A. F. Ram, C. A. M. J. J. Van Den Hondel, H. A. B. Wösten, Hyphal differentiation in the exploring mycelium of *Aspergillus niger*. *Mol. Microbiol.* **58**, 693–699 (2005).
116. A. Vinck, C. De Bekker, A. Ossin, R. A. Ohm, R. P. De Vries, H. A. B. Wösten, Heterogenic expression of genes encoding secreted proteins at the periphery of *Aspergillus niger* colonies. *Environ. Microbiol.* **13**, 216–225 (2011).
117. R. J. Bleichrodt, A. Vinck, N. D. Read, H. A. B. Wösten, Selective transport between heterogeneous hyphal compartments via the plasma membrane lining septal walls of *Aspergillus niger*. *Fungal Genet. Biol.* **82**, 193–200 (2015).
118. H. A. B. Wösten, G. J. van Veluw, C. de Bekker, P. Krijgsheld, Heterogeneity in the mycelium: implications for the use of fungi as cell factories. *Biotechnol. Lett.* **35**, 1155–1164 (2013).
119. K. Celler, R. I. Koning, J. Willemse, A. J. Koster, G. P. Van Wezel, Cross-membranes orchestrate compartmentalization and morphogenesis in *Streptomyces*. *Nat. Commun.* **7**, 11836 (2016).
120. P. Yagüe, J. Willemse, R. I. Koning, B. Rioseras, M. T. López-García, N. Gonzalez-Quíñonez, C. Lopez-Iglesias, P. V. Shliaha, A. Rogowska-Wrzesinska, A. J. Koster, O. N. Jensen, G. P. Van Wezel, Á. Manteca, Subcompartmentalization by cross-membranes during early growth of *Streptomyces* hyphae. *Nat. Commun.* **7**, 12467 (2016).
121. J. van Gestel, H. Vlamakis, R. Kolter, From cell differentiation to cell collectives: *Bacillus subtilis* uses division of labor to migrate. *PLoS Biol.* **13**, e1002141 (2015).
122. W. Kim, F. Racimo, J. Schluter, S. B. Levy, K. R. Foster, Importance of positioning for microbial evolution. *Proc. Natl. Acad. Sci. U. S. A.* **111**, E1639–1647 (2014).
123. G. E. Robinson, Regulation of division of labor in insect societies. *Annu. Rev. Entomol.* **37**, 637–665 (1992).
124. A. Dragoš, H. Kieseewalter, M. Martin, C.-Y. Hsu, R. Hartmann, T. Wechsler, C. Eriksen, S. Brix, K. Drescher, N. Stanley-Wall, R. Kümmerli, Á. T. Kovács, Division of labor during biofilm matrix production. *Curr. Biol.* **28**, 1903–1913 (2018).
125. A. Dragoš, M. Martin, C. F. Garcia, L. Kricks, P. Pausch, T. Heimerl, B. Bálint, G. Maróti, G. Bange, D. López, O. Lieleg, Á. T. Kovács, Collapse of genetic division of labour and evolution of autonomy in pellicle biofilms. *Nat. Microbiol.* **3**, 1451–1460 (2018).

References

126. C. E. Tarnita, The ecology and evolution of social behavior in microbes. *J. Exp. Biol.* **220**, 18–24 (2017).
127. K. T. Schiessl, A. Ross-Gillespie, D. M. Cornforth, M. Weigert, C. Bigosch, S. P. Brown, M. Ackermann, R. Kümmerli, Individual- versus group-optimality in the production of secreted bacterial compounds. *Evolution*. **73**, 675–688 (2019).
128. M. I. Abrudan, F. Smakman, A. J. Grimbergen, S. Westhoff, E. L. Miller, G. P. van Wezel, D. E. Rozen, Socially mediated induction and suppression of antibiosis during bacterial coexistence. *Proc. Natl. Acad. Sci. U. S. A.* **112**, 11054–11059 (2015).
129. J. R. McCormick, K. Flärdh, Signals and regulators that govern *Streptomyces* development. *FEMS Microbiol. Rev.* **36**, 206–231 (2012).
130. J. Sun, G. H. Kelemen, J. M. Fernández-Abalos, M. J. Bibb, Green fluorescent protein as a reporter for spatial and temporal gene expression in *Streptomyces coelicolor* A3(2). *Microbiology*. **145**, 2221–2227 (1999).
131. G. H. Kelemen, P. H. Viollier, J. Tenor, L. Marri, M. J. Buttner, C. J. Thompson, A connection between stress and development in the multicellular prokaryote *Streptomyces coelicolor* A3(2). *Mol. Microbiol.* **40**, 804–814 (2001).
132. R. F. Freeman, M. J. Bibb, D. A. Hopwood, Chloramphenicol acetyltransferase independent chloramphenicol resistance in *Streptomyces coelicolor* A3(2). *J. Gen. Microbiol.* **98**, 453–465 (1977).
133. V. E. Coyne, K. Usdin, R. Kirby, The effect of inhibitors of DNA repair on the genetic instability of *Streptomyces cattleya*. *J. Gen. Microbiol.* **130**, 887–892 (1984).
134. J. Altenbuchner, J. Cullum, DNA amplification and an unstable arginine gene in *Streptomyces lividans* 66. *MGG Mol. Gen. Genet.* **195**, 134–138 (1984).
135. P. Dyson, H. Schrempf, Genetic instability and DNA amplification in *Streptomyces lividans* 66. *J. Bacteriol.* **169**, 4796–4803 (1987).
136. P. Leblond, P. Demuyter, L. Moutier, M. Laakel, B. Decaris, J. Simonet, Hypervariability, a new phenomenon of genetic instability, related to DNA amplification in *Streptomyces ambofaciens*. *J. Bacteriol.* **171**, 419–423 (1989).
137. H. Krügel, P. Krubasik, K. Weber, H. P. Saluz, G. Sandmann, Functional analysis of genes from *Streptomyces griseus* involved in the synthesis of isorenieratene, a carotenoid with aromatic end groups, revealed a novel type of carotenoid desaturase. *Biochim. Biophys. Acta - Mol. Cell Biol. Lipids.* **1439**, 57–64 (1999).

138. H. Takano, S. Obitsu, T. Beppu, K. Ueda, Light-induced carotenogenesis in *Streptomyces coelicolor* A3(2): identification of an extracytoplasmic function sigma factor that directs photodependent transcription of the carotenoid biosynthesis gene cluster. *J. Bacteriol.* **187**, 1825–1832 (2005).
139. H. K. Kim, Y. H. Choi, R. Verpoorte, NMR-based metabolomic analysis of plants. *Nat. Protoc.* **5**, 536–549 (2010).
140. C. Wu, C. Du, J. Gubbens, Y. H. Choi, G. P. Van Wezel, Metabolomics-driven discovery of a prenylated isatin antibiotic produced by *Streptomyces* species MBT28. *J. Nat. Prod.* **78**, 2355–2363 (2015).
141. J. Gubbens, H. Zhu, G. Girard, L. Song, B. I. Florea, P. Aston, K. Ichinose, D. V. Filippov, Y. H. Choi, H. S. Overkleeft, G. L. Challis, G. P. Van Wezel, Natural product proteomining, a quantitative proteomics platform, allows rapid discovery of biosynthetic gene clusters for different classes of natural products. *Chem. Biol.* **21**, 707–718 (2014).
142. R. Pérez-Redondo, A. Rodríguez-García, A. Botas, I. Santamarta, J. F. Martín, P. Liras, ArgR of *Streptomyces coelicolor* is a versatile regulator. *PLoS One.* **7**, e32697 (2012).
143. M. Komatsu, T. Uchiyama, S. Omura, D. E. Cane, H. Ikeda, Genome-minimized *Streptomyces* host for the heterologous expression of secondary metabolism. *Proc. Natl. Acad. Sci.* **107**, 2646–2651 (2010).
144. G. L. Challis, D. A. Hopwood, Synergy and contingency as driving forces for the evolution of multiple secondary metabolite production by *Streptomyces* species. *Proc. Natl. Acad. Sci. U. S. A.* **100**, 14555–14561 (2003).
145. A. Craney, S. Ahmed, J. Nodwell, Towards a new science of secondary metabolism. *J. Antibiot. (Tokyo)*. **66**, 387–400 (2013).
146. A. van der Meij, S. F. Worsley, M. I. Hutchings, G. P. van Wezel, Chemical ecology of antibiotic production by actinomycetes. *FEMS Microbiol. Rev.* **41**, 392–416 (2017).
147. M. F. Traxler, J. D. Watrous, T. Alexandrov, P. C. Dorrestein, R. Kolter, Interspecies interactions stimulate diversification of the *Streptomyces coelicolor* secreted metabolome. *MBio.* **4**, e00459-13 (2013).
148. E. M. Widenbrant, C. M. Kao, Introduction of the foreign transposon Tn4560 in *Streptomyces coelicolor* leads to genetic instability near the native insertion sequence IS1649. *J. Bacteriol.* **189**, 9108–9116 (2007).
149. Kieser T, Bibb MJ, Buttner MJ, Chater KF, D. A. Hopwood, *Practical Streptomyces*

References

- genetics* (John Innes Foundation, Norwich, UK, 2000).
150. C. T. Rueden, J. Schindelin, M. C. Hiner, B. E. DeZonia, A. E. Walter, E. T. Arena, K. W. Eliceiri, ImageJ2: ImageJ for the next generation of scientific image data. *BMC Bioinformatics*. **18**, 529 (2017).
 151. D. Wessel, U. I. Flügge, A method for the quantitative recovery of protein in dilute solution in the presence of detergents and lipids. *Anal. Biochem.* **138**, 141–143 (1984).
 152. E. J. van Rooden, B. I. Florea, H. Deng, M. P. Baggelaar, A. C. M. van Esbroeck, J. Zhou, H. S. Overkleeft, M. van der Stelt, Mapping in vivo target interaction profiles of covalent inhibitors using chemical proteomics with label-free quantification. *Nat. Protoc.* **13**, 752–767 (2018).
 153. J. Rappsilber, Y. Ishihama, M. Mann, Stop and go extraction tips for matrix-assisted laser desorption/ionization, nanoelectrospray, and LC/MS sample pretreatment in proteomics. *Anal. Chem.* **75**, 663–670 (2003).
 154. U. Distler, J. Kuharev, P. Navarro, Y. Levin, H. Schild, S. Tenzer, Drift time-specific collision energies enable deep-coverage data-independent acquisition proteomics. *Nat. Methods*. **11**, 167–170 (2014).
 155. M. J. Chaisson, G. Tesler, Mapping single molecule sequencing reads using basic local alignment with successive refinement (BLASR): application and theory. *BMC Bioinformatics*. **13**, 238 (2012).
 156. H. Li, B. Handsaker, A. Wysoker, T. Fennell, J. Ruan, N. Homer, G. Marth, G. Abecasis, R. Durbin, 1000 Genome Project Data Processing Subgroup, The Sequence Alignment/Map format and SAMtools. *Bioinformatics*. **25**, 2078–2079 (2009).
 157. J. T. et al Robinson, H. Thorvaldsdóttir, W. Winckler, M. Guttman, E. S. Lander, G. Getz, J. P. Mesirov, Integrative genomics viewer. *Nat. Biotechnol.* **29**, 24–26 (2011).
 158. H. Thorvaldsdóttir, J. T. Robinson, J. P. Mesirov, Integrative Genomics Viewer (IGV): high-performance genomics data visualization and exploration. *Brief. Bioinform.* **14**, 178–192 (2013).
 159. R. E. Lenski, M. R. Rose, S. C. Simpson, S. C. Tadler, Long-term experimental evolution in *Escherichia coli*. I. Adaptation and divergence during 2,000 generations. *Am. Nat.* **138**, 1315–1341 (1991).
 160. E. W. Deutsch, A. Csordas, Z. Sun, A. Jarnuczak, Y. Perez-Riverol, T. Ternent, D. S. Campbell, M. Bernal-Llinares, S. Okuda, S. Kawano, R. L. Moritz, J. J. Carver, M.

- Wang, Y. Ishihama, N. Bandeira, H. Hermjakob, J. A. Vizcaíno, The ProteomeXchange consortium in 2017: supporting the cultural change in proteomics public data deposition. *Nucleic Acids Res.* **45**, D1100–D1106 (2017).
161. Y. Perez-Riverol, A. Csordas, J. Bai, M. Bernal-Llinares, S. Hewapathirana, D. J. Kundu, A. Inuganti, J. Griss, G. Mayer, M. Eisenacher, E. Pérez, J. Uszkoreit, J. Pfeuffer, T. Sachsenberg, Ş. Yilmaz, S. Tiwary, J. Cox, E. Audain, M. Walzer, A. F. Jarnuczak, T. Ternent, A. Brazma, J. A. Vizcaíno, The PRIDE database and related tools and resources in 2019: improving support for quantification data. *Nucleic Acids Res.* **47**, D442–D450 (2019).
 162. D. C. Queller, Relatedness and the fraternal major transitions. *Philos. Trans. R. Soc. B Biol. Sci.* **355**, 1647–1655 (2000).
 163. G. A. Cooper, S. A. West, Division of labour and the evolution of extreme specialization. *Nat. Ecol. Evol.* **2**, 1161–1167 (2018).
 164. J. J. Kuzdzal-Fick, S. A. Fox, J. E. Strassmann, D. C. Queller, High relatedness is necessary and sufficient to maintain multicellularity in *Dictyostelium*. *Science*. **334**, 1548–1551 (2011).
 165. D. C. Queller, J. E. Strassmann, Kin selection and social insects: social insects provide the most surprising predictions and satisfying tests of kin selection. *Bioscience*. **48**, 165–175 (1998).
 166. Z. Zhang, C. Du, F. de Barsy, M. Liem, A. Liakopoulos, G. P. van Wezel, Y. H. Choi, D. Claessen, D. E. Rozen, Antibiotic production in *Streptomyces* is organized by a division of labor through terminal genomic differentiation. *Sci. Adv.* **6**, eaay5781 (2020).
 167. D. I. Andersson, D. Hughes, Muller's ratchet decreases fitness of a DNA-based microbe. *Proc. Natl. Acad. Sci. U. S. A.* **93**, 906–907 (1996).
 168. J. P. Horst, T. hui Wu, M. G. Marinus, *Escherichia coli* mutator genes. *Trends Microbiol.* **7**, 29–36 (1999).
 169. V. F. Liu, D. Bhaumik, T. S.-F. Wang, Mutator phenotype induced by aberrant replication. *Mol. Cell. Biol.* **19**, 1126–1135 (1999).
 170. F. Flett, J. Cullum, DNA deletions in spontaneous chloramphenicol-sensitive mutants of *Streptomyces coelicolor* A3(2) and *Streptomyces lividans* 66. *MGG Mol. Gen. Genet.* **207**, 499–502 (1987).
 171. J. J. Vecchione, B. Alexander, J. K. Sello, Two distinct major facilitator superfamily

References

- drug efflux pumps mediate chloramphenicol resistance in *Streptomyces coelicolor*. *Antimicrob. Agents Chemother.* **53**, 4673–4677 (2009).
172. F. Flett, J. Platt, J. Cullum, DNA rearrangements associated with instability of an arginine gene in *Streptomyces coelicolor* A3(2). *J. Basic Microbiol.* **27**, 3–10 (1987).
173. D. G. Davies, M. R. Parsek, J. P. Pearson, B. H. Iglewski, J. W. Costerton, E. P. Greenberg, The involvement of cell-to-cell signals in the development of a bacterial biofilm. *Science*. **280**, 295–298 (1998).
174. N. M. J. Geerlings, C. Karman, S. Trashin, K. S. As, M. V. M. Kienhuis, S. Hidalgo-Martinez, D. Vasquez-Cardenas, H. T. S. Boschker, K. de Wael, J. J. Middelburg, L. Polerecky, F. J. R. Meysman, Division of labor and growth during electrical cooperation in multicellular cable bacteria. *Proc. Natl. Acad. Sci. U. S. A.* **117**, 5478–5485 (2020).
175. B. von Bronk, S. A. Schaffer, A. Götz, M. Opitz, Effects of stochasticity and division of labor in toxin production on two-strain bacterial competition in *Escherichia coli*. *PLoS Biol.* **15**, e2001457 (2017).
176. E. Cascales, S. K. Buchanan, D. Duche, C. Kleanthous, R. Lloubes, K. Postle, M. Riley, S. Slatin, D. Cavard, Colicin biology. *Microbiol. Mol. Biol. Rev.* **71**, 158–229 (2007).
177. D. A. I. Mavridou, D. Gonzalez, W. Kim, S. A. West, K. R. Foster, Bacteria use collective behavior to generate diverse combat strategies. *Curr. Biol.* **28**, 345–355 (2018).
178. E. T. Granato, K. R. Foster, The evolution of mass cell suicide in bacterial warfare. *Curr. Biol.* **30**, 2836–2843 (2020).
179. H. J. Muller, The relation of recombination to mutational advance. *Mutat. Res. - Fundam. Mol. Mech. Mutagen.* **1**, 2–9 (1964).
180. J. Felsenstein, The evolution advantage of recombination. *Genetics*. **78**, 737–756 (1974).
181. M. Kurokawa, S. Seno, H. Matsuda, B. W. Ying, Correlation between genome reduction and bacterial growth. *DNA Res.* **23**, 517–525 (2016).
182. W. Gabriel, M. Lynch, R. Burger, Muller's ratchet and mutational meltdowns. *Evolution*. **47**, 1744–1757 (1993).
183. M. Cycoń, A. Mroziak, Z. Piotrowska-Seget, Antibiotics in the soil environment—degradation and their impact on microbial activity and diversity. *Front. Microbiol.* **10**, 338 (2019).

184. S. A. West, A. S. Griffin, A. Gardner, Evolutionary explanations for cooperation. *Curr. Biol.* **17**, R661–R672 (2007).
185. M. J. Merrick, A morphological and genetic mapping study of bald colony mutants of *Streptomyces coelicolor*. *J. Gen. Microbiol.* **96**, 299–315 (1976).
186. D. A. Hopwood, H. Wildermuth, H. M. Palmer, Mutants of *Streptomyces coelicolor* defective in sporulation. *J. Gen. Microbiol.* **61**, 397–408 (1970).
187. K. F. Chater, A morphological and genetic mapping study of white colony mutants of *Streptomyces coelicolor*. *J. Gen. Microbiol.* **72**, 9–28 (1972).
188. J. R. McCormick, E. P. Su, A. Driks, R. Losick, Growth and viability of *Streptomyces coelicolor* mutant for the cell division gene *ftsZ*. *Mol. Microbiol.* **14**, 243–254 (1994).
189. J. R. McCormick, R. Losick, Cell division gene *ftsQ* is required for efficient sporulation but not growth and viability in *Streptomyces coelicolor* A3(2). *J. Bacteriol.* **178**, 5295–5301 (1996).
190. K. Flärdh, Essential role of DivIVA in polar growth and morphogenesis in *Streptomyces coelicolor* A3(2). *Mol. Microbiol.* **49**, 1523–1536 (2003).
191. J. A. Bennett, R. M. Aimino, J. R. McCormick, *Streptomyces coelicolor* genes *ftsL* and *divIC* play a role in cell division but are dispensable for colony formation. *J. Bacteriol.* **189**, 8982–8992 (2007).
192. L. Zhang, J. Willemse, D. Claessen, G. P. van Wezel, SepG coordinates sporulation-specific cell division and nucleoid organization in *Streptomyces coelicolor*. *Open Biol.* **6**, 150164 (2016).
193. L. Zhang, J. Willemse, P. A. Hoskisson, G. P. van Wezel, Sporulation-specific cell division defects in *ylmE* mutants of *Streptomyces coelicolor* are rescued by additional deletion of *ylmD*. *Sci. Rep.* **8**, 7328 (2018).
194. H. J. Kim, M. J. Calcutt, F. J. Schmidt, K. F. Chater, Partitioning of the linear chromosome during sporulation of *Streptomyces coelicolor* A3(2) involves an *oriC*-linked *parAB* locus. *J. Bacteriol.* **182**, 1313–1320 (2000).
195. D. Jakimowicz, B. Gust, J. Zakrzewska-Czerwinska, K. F. Chater, Developmental-stage-specific assembly of ParB complexes in *Streptomyces coelicolor* hyphae. *J. Bacteriol.* **187**, 3572–3580 (2005).
196. D. Jakimowicz, P. Żydek, A. Kois, J. Zakrzewska-Czerwińska, K. F. Chater, Alignment of multiple chromosomes along helical ParA scaffolding in sporulating *Streptomyces*

References

- hyphae. *Mol. Microbiol.* **65**, 625–641 (2007).
197. B. A. Traag, G. P. van Wezel, The SsgA-like proteins in actinomycetes: small proteins up to a big task. *Antonie van Leeuwenhoek, Int. J. Gen. Mol. Microbiol.* **94**, 85–97 (2008).
198. B. J. F. Keijser, E. E. E. Noens, B. Kraal, H. K. Koerten, G. P. Van Wezel, The *Streptomyces coelicolor* *ssgB* gene is required for early stages of sporulation. *FEMS Microbiol. Lett.* **225**, 59–67 (2003).
199. J. Willey, R. Santamaria, J. Guijarro, M. Geistlich, R. Losick, Extracellular complementation of a developmental mutation implicates a small sporulation protein in aerial mycelium formation by *S. coelicolor*. *Cell*, **65**, 641–650 (1991).
200. T. J. O'Connor, P. Kanellis, J. R. Nodwell, The *ramC* gene is required for morphogenesis in *Streptomyces coelicolor* and expressed in a cell type-specific manner under the direct control of RamR. *Mol. Microbiol.* **45**, 45–57 (2002).
201. K. T. Nguyen, J. M. Willey, L. D. Nguyen, L. T. Nguyen, P. H. Viollier, C. J. Thompson, A central regulator of morphological differentiation in the multicellular bacterium *Streptomyces coelicolor*. *Mol. Microbiol.* **46**, 1223–1238 (2002).
202. S. Kodani, M. E. Hudson, M. C. Durrant, M. J. Buttner, J. R. Nodwell, J. M. Willey, The SapB morphogen is a lantibiotic-like peptide derived from the product of the developmental gene *ramS* in *Streptomyces coelicolor*. *Proc. Natl. Acad. Sci. U. S. A.* **101**, 11448–11453 (2004).
203. D. Claessen, R. Rink, W. De Jong, J. Siebring, P. De Vreugd, F. G. H. Boersma, L. Dijkhuizen, H. A. B. Wösten, A novel class of secreted hydrophobic proteins is involved in aerial hyphae formation in *Streptomyces coelicolor* by forming amyloid-like fibrils. *Genes Dev.* **17**, 1714–1726 (2003).
204. M. A. Elliot, N. Karoonuthaisiri, J. Huang, M. J. Bibb, S. N. Cohen, C. M. Kao, M. J. Buttner, The chaplins: a family of hydrophobic cell-surface proteins involved in aerial mycelium formation in *Streptomyces coelicolor*. *Genes Dev.* **17**, 1727–1740 (2003).
205. D. Claessen, H. A. B. Wösten, G. Van Keulen, O. G. Faber, A. M. C. R. Alves, W. G. Meijer, L. Dijkhuizen, Two novel homologous proteins of *Streptomyces coelicolor* and *Streptomyces lividans* are involved in the formation of the rodlet layer and mediate attachment to a hydrophobic surface. *Mol. Microbiol.* **44**, 1483–1492 (2002).

206. W. Yang, J. Willemse, E. B. Sawyer, F. Lou, W. Gong, H. Zhang, S. L. Gras, D. Claessen, S. Perrett, The propensity of the bacterial rodlin protein RdlB to form amyloid fibrils determines its function in *Streptomyces coelicolor*. *Sci. Rep.* **7**, 42867 (2017).
207. G. H. Kelemen, M. J. Buttner, Initiation of aerial mycelium formation in *Streptomyces*. *Curr. Opin. Microbiol.* **1**, 656–662 (1998).
208. V. Molle, M. J. Buttner, Different alleles of the response regulator gene *bldM* arrest *Streptomyces coelicolor* development at distinct stages. *Mol. Microbiol.* **36**, 1265–1278 (2000).
209. M. M. Al-Bassam, M. J. Bibb, M. J. Bush, G. Chandra, M. J. Buttner, Response regulator heterodimer formation controls a key stage in *Streptomyces* development. *PLoS Genet.* **10**, e1004554 (2014).
210. K. Phan, T. Ferenci, The fitness costs and trade-off shapes associated with the exclusion of nine antibiotics by OmpF porin channels. *ISME J.* **11**, 1472–1482 (2017).
211. A. Birch, A. Hausler, C. Ruttener, R. Hutter, Chromosomal deletion and rearrangement in *Streptomyces glaucescens*. *J. Bacteriol.* **173**, 3531–3538 (1991).
212. J.-N. Volff, P. Viell, J. Altenbuchner, Artificial circularization of the chromosome with concomitant deletion of its terminal inverted repeats enhances genetic instability and genome rearrangement in *Streptomyces lividans*. *MGG Mol. Gen. Genet.* **253**, 753–760 (1997).
213. G. Fischer, B. Decaris, P. Leblond, Occurrence of deletions, associated with genetic instability in *Streptomyces ambofaciens*, is independent of the linearity of the chromosomal DNA. *J. Bacteriol.* **179**, 4553–4558 (1997).
214. Y. Lin, C. W. Chen, Instability of artificially circularized chromosomes of *Streptomyces lividans*. *Mol. Microbiol.* **26**, 709–719 (1997).
215. J. H. Lakey, E. J. A. Lea, B. A. M. Rudd, H. M. Wright, D. A. Hopwood, A new channel-forming antibiotic from *Streptomyces coelicolor* A3(2) which requires calcium for its activity. *J. Gen. Microbiol.* **129**, 3565–3573 (1983).
216. J. Rappsilber, M. Mann, Y. Ishihama, Protocol for micro-purification, enrichment, pre-fractionation and storage of peptides for proteomics using StageTips. *Nat. Protoc.* **2**, 1896–1906 (2007).
217. M. I. Love, W. Huber, S. Anders, Moderated estimation of fold change and dispersion for RNA-seq data with DESeq2. *Genome Biol.* **15**, 550 (2014).

References

218. R. Cramer, T. Kieser, H. Ono, J. Sanchez, R. Hütter, Chromosomal instability in *Streptomyces glaucescens*: mapping of streptomycin-sensitive mutants. *J. Gen. Microbiol.* **129**, 519–527 (1983).
219. H. Schrempf, Deletion and amplification of DNA sequences in melanin-negative variants of *Streptomyces reticuli*. *MGG Mol. Gen. Genet.* **189**, 501–505 (1983).
220. M. Betzler, P. Dyson, H. Schrempf, Relationship of an unstable *argG* gene to a 5.7-kilobase amplifiable DNA sequence in *Streptomyces lividans* 66. *J. Bacteriol.* **169**, 4804–4810 (1987).
221. P. Leblond, P. Demuyter, J. M. Simonet, B. Decaris, Genetic instability and associated genome plasticity in *Streptomyces ambofaciens*: Pulsed-field gel electrophoresis evidence for large DNA alterations in a limited genomic region. *J. Bacteriol.* **173**, 4229–4233 (1991).
222. A. Smith, *An Inquiry into the Nature and Causes of the Wealth of Nations* (W. Strahan and T. Cadell, London, 1776).
223. K. Voelz, S. A. Johnston, L. M. Smith, R. A. Hall, A. Idnurm, R. C. May, “Division of labour” in response to host oxidative burst drives a fatal *Cryptococcus gattii* outbreak. *Nat. Commun.* **5**, 5194 (2014).
224. W. D. Hamilton, The evolution of altruistic behavior. *Am. Nat.* **97**, 354–356 (1963).
225. W. D. Hamilton, The genetical evolution of social behaviour. I. *J. Theor. Biol.* **7**, 1–16 (1964).
226. W. D. Hamilton, The genetical evolution of social behaviour. II. *J. Theor. Biol.* **7**, 17–52 (1964).
227. C. J. Davidson, M. G. Surette, Individuality in bacteria. *Annu. Rev. Genet.* **42**, 253–268 (2008).
228. J.-W. Veening, E. J. Stewart, T. W. Berngruber, F. Taddei, O. P. Kuipers, L. W. Hamoen, Bet-hedging and epigenetic inheritance in bacterial cell development. *Proc. Natl. Acad. Sci. U. S. A.* **105**, 4393–4398 (2008).
229. A. Solopova, J. Van Gestel, F. J. Weissing, H. Bachmann, B. Teusink, J. Kok, O. P. Kuipers, Bet-hedging during bacterial diauxic shift. *Proc. Natl. Acad. Sci. U. S. A.* **111**, 7427–7432 (2014).
230. M. M. Kirk, A. Ransick, S. E. McRae, D. L. Kirk, The relationship between cell size and cell fate in *Volvox carteri*. *J. Cell Biol.* **123**, 191–208 (1993).

231. D. L. Kirk, Asymmetric division, cell size and germ-soma specification in *Volvox*. *Semin. Dev. Biol.* **6**, 369–379 (1995).
232. J. C. Pommerville, G. D. Kochert, Changes in somatic cell structure during senescence of *Volvox carteri*. *Eur. J. Cell Biol.* **24**, 236–243 (1981).
233. J. Pommerville, G. Kochert, Effects of senescence on somatic cell physiology in the green alga *Volvox carteri*. *Exp. Cell Res.* **140**, 39–45 (1982).
234. C. A. Solari, J. O. Kessler, R. E. Michod, A hydrodynamics approach to the evolution of multicellularity: flagellar motility and germ-soma differentiation in volvocalean green algae. *Am. Nat.* **167**, 537–554 (2006).
235. Á. Manteca, P. Yagüe, in *Antimicrobials, antibiotic resistance, antibiofilm strategies and activity methods*, S. Kirmusaoğlu, Ed. (IntechOpen, London, 2019), pp. 1–21.
236. J. W. Drake, A constant rate of spontaneous mutation in DNA-based microbes. *Proc Natl Acad Sci USA.* **88**, 7160–7164 (1991).
237. M. Lynch, Evolution of the mutation rate. *Trends Genet.* **26**, 345–352 (2010).
238. M. Lynch, The lower bound to the evolution of mutation rates. *Genome Biol. Evol.* **3**, 1107–1118 (2011).
239. W. Sung, M. S. Ackerman, S. F. Miller, T. G. Doak, M. Lynch, Drift-barrier hypothesis and mutation-rate evolution. *Proc. Natl. Acad. Sci. U. S. A.* **109**, 18488–18492 (2012).
240. K. Ramijan, E. Ultee, J. Willemse, Z. Zhang, J. A. J. Wondergem, A. van der Meij, D. Heinrich, A. Briegel, G. P. van Wezel, D. Claessen, Stress-induced formation of cell wall-deficient cells in filamentous actinomycetes. *Nat. Commun.* **9**, 5164 (2018).
241. P. Charusanti, N. L. Fong, H. Nagarajan, A. R. Pereira, H. J. Li, E. A. Abate, Y. Su, W. H. Gerwick, B. O. Palsson, Exploiting adaptive laboratory evolution of *Streptomyces clavuligerus* for antibiotic discovery and overproduction. *PLoS One.* **7**, e33727 (2012).
242. B. Stecher, R. Robbiani, A. W. Walker, A. M. Westendorf, M. Barthel, M. Kremer, S. Chaffron, A. J. Macpherson, J. Buer, J. Parkhill, G. Dougan, C. Von Mering, W. D. Hardt, *Salmonella enterica* serovar Typhimurium exploits inflammation to compete with the intestinal microbiota. *PLoS Biol.* **5**, e244 (2007).
243. M. Arnoldini, I. A. Vizcarra, R. Peña-Miller, N. Stocker, M. Diard, V. Vogel, R. E. Beardmore, W. D. Hardt, M. Ackermann, Bistable expression of virulence genes in *salmonella* leads to the formation of an antibiotic-tolerant subpopulation. *PLoS*

References

- Biol.* **12**, e1001928 (2014).
244. M. Klausen, A. Aaes-Jørgensen, S. Molin, T. Tolker-Nielsen, Involvement of bacterial migration in the development of complex multicellular structures in *Pseudomonas aeruginosa* biofilms. *Mol. Microbiol.* **50**, 61–68 (2003).
245. K. Sauer, A. K. Camper, G. D. Ehrlich, J. W. Costerton, D. G. Davies, *Pseudomonas aeruginosa* displays multiple phenotypes during development as a biofilm. *J. Bacteriol.* **184**, 1140–1154 (2002).
246. W. J. Bennett, *An Overview of the Genus Aspergillus* (Caister Academic Press, U.K., 2010).
247. P. Krijgheld, R. Bleichrodt, G. J. van Veluw, F. Wang, W. H. Müller, J. Dijksterhuis, H. A. B. Wösten, Development in *Aspergillus*. *Stud. Mycol.* **74**, 1–29 (2013).

Appendix I

Supplementary materials for Chapter 2

Table S1. A selection of studies examining microbial divisions of labor across different model systems. Prokaryotic examples are shown above while eukaryotic examples are shown below in gray.

* Check the section of References in this book

Species	Colony-level benefits	Cooperative cell types	Interactions between cells	References*	Evidence: Benefits of division of labor
<i>Bacillus subtilis</i>	Flagellum-independent migration on solid surfaces	Surfactin-producing cells Matrix-producing cells	Surfactin-producing cells lubricate cells and substrate to allow matrix-producing cells to form van Gogh bundles for colony expansion	(121)	Experimentally confirmed
<i>Pseudomonas fluorescens</i>	Mobility and population size	D-cells (Dry) M-cells (Mucoid)	D-cells push M-cells during colony spreading while M-cells produce a mucoid polymer to reduce resistance to movement	(58)	Experimentally confirmed
<i>Anabaena</i> spp.	Growth under depletion of usable nitrogen	Vegetative cells Heterocysts	Heterocysts fix nitrogen while vegetative cells fix carbon. These products are shared.	(62, 99)	Experimentally confirmed in certain conditions.

<i>Salmonella typhimurium</i>	Cooperative virulence/Antibiotic-tolerance	Virulent cells Avirulent cells	Host colonization/antibiotic tolerance	(242, 243)	Experimentally confirmed
<i>Myxococcus xanthus</i>	Reproduction/ Dispersal	Spore cells Peripheral rod cells Lysed cells	Stalk cells are assumed to undergo PCD, thereby potentially facilitating dispersal and/or spore survival.	(56, 60)	Widely cited as a clear division of labour, but colony-level benefits remain to be quantified. Possible dispersal benefits.
<i>Pseudomonas aeruginosa</i>	Biofilm/Microcolony structure	Motile cells Non-motile cells	Non-motile cells form a stalk, while motile cells migrate to the top of the microcolony where they form a mushroom-like cap. Non-motile cells produce quorum-sensing signals, siderophores, surfactants and polysaccharides to support motile cells.	(49, 244)	Colony-level benefits of phenotypic heterogeneity remain uncertain. Increased individual nutrient access.
<i>Pseudomonas aeruginosa</i>	Dispersal/Virulence/ Iron acquisition	Dispersing cells Lysed cells	Localized cell lysis and siderophore production facilitates microcolony formation and cell dispersal.	(245)	Colony-level benefits remain to be clarified. Possible dispersal benefits.
<i>Streptomyces</i> spp.	Nutrient acquisition /Dispersal	Vegetative hyphae Aerial hyphae Spores	Vegetative hyphae grow into the substrate and secrete enzymes to break down inorganic nutrients. Under nutrient depletion, these hyphae produce antibiotics and undergo PCD that are believed to provide nutrients for the subsequent growth of aerial hyphae, which differentiate into spore chains.	(9, 59)	Colony-level benefits remain to be clarified. Mechanisms of PCD unclear.

<i>Aspergillus</i> spp.	Nutrient acquisition /Dispersal	Vegetative hyphae Aerial hyphae Conidia	Vegetative hyphae absorb nutrients from the environment and grow into the air as aerial hyphae which sporulate as conidia for dispersal.	(246, 247)	Colony-level benefits remain to be quantified.
<i>Cryptococcus gattii</i>	Pathogenicity/ Virulence	Tubular mitochondrial morphology Non-tubular mitochondrial morphology	A sub-population of cells undergoes mitochondrial tubularisation which enhances the proliferation of remaining cells within macrophages.	(223)	Mechanisms confirmed, but the population benefits of increased virulence are uncertain.
<i>Dictyostelium discoideum</i>	Reproduction/ Dispersal	Stalk cells Spore cells	Stalk cells undergo PCD and elevate spores above the substrate.	(92)	Widely cited as a clear division of labour, but colony-level benefits remain to be confirmed. Possible dispersal benefits.

Appendix II

Supplementary materials for Chapter 3

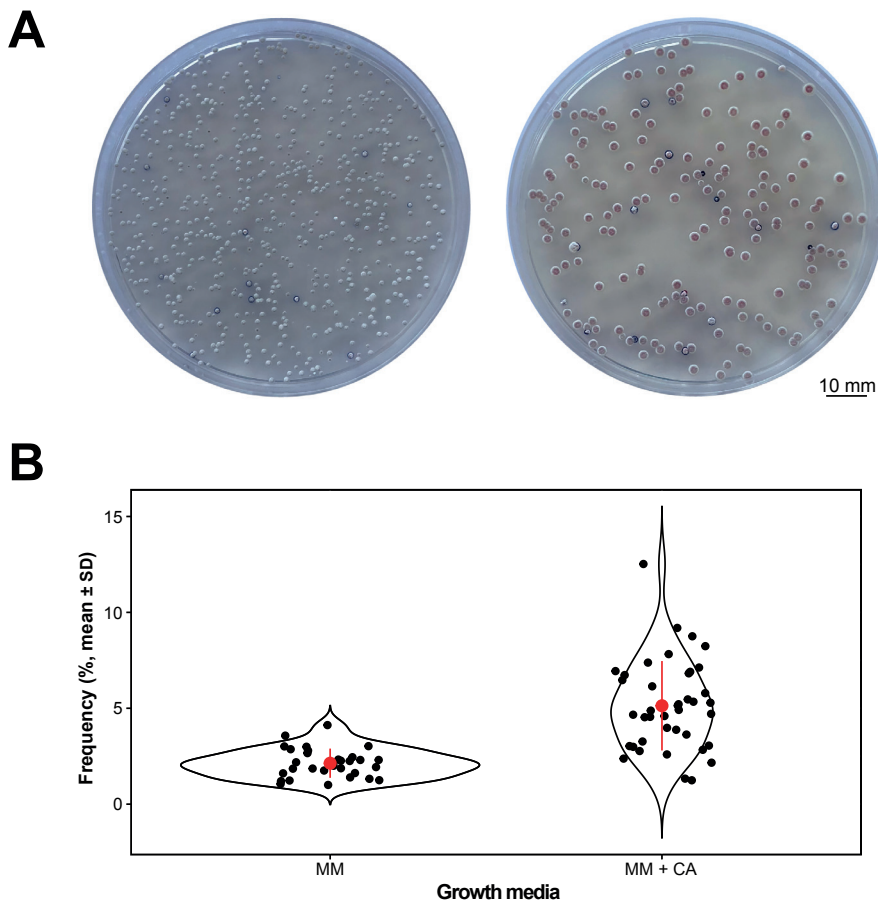


Fig. S1. Mutant frequencies in different media. Phenotypes (**A**) and mutation frequencies (**B**) of colonies grown on minimal media (MM) or minimal media supplemented with casamino acids (MM + CA). (**A**) Examples of mutant and wild-type colonies growing on minimal media (MM) (Left) or minimal media supplemented with casamino acids (MM + CA) (Right). (**B**) The frequency of mutants emerging from WT colonies on both media types.

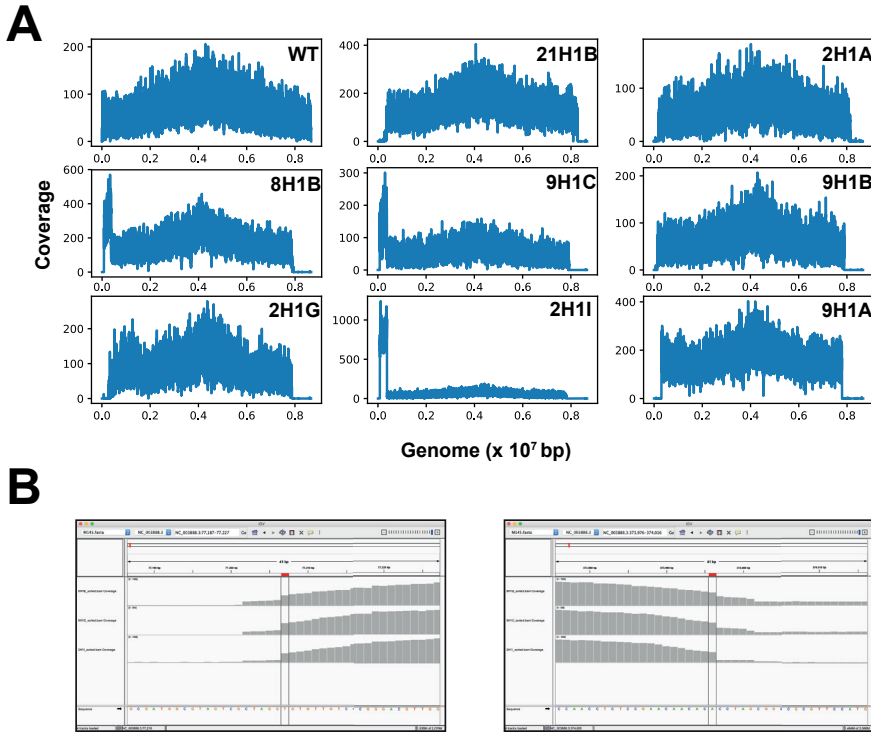


Fig. S2. PacBio sequencing results of nine selected strains. (A) PacBio reads mapped to the *S. coelicolor* M145 reference genome indicating coverage and highlighting breakpoints for genome deletions, where coverage declines to 0, as well as the size of the conserved amplified regions on the left chromosomal arms of strains 8H1B, 9H1C and 2H1I. (B) IGV snapshots of the left and right borders of amplified regions of strains 8H1B, 9H1C and 2H1I.

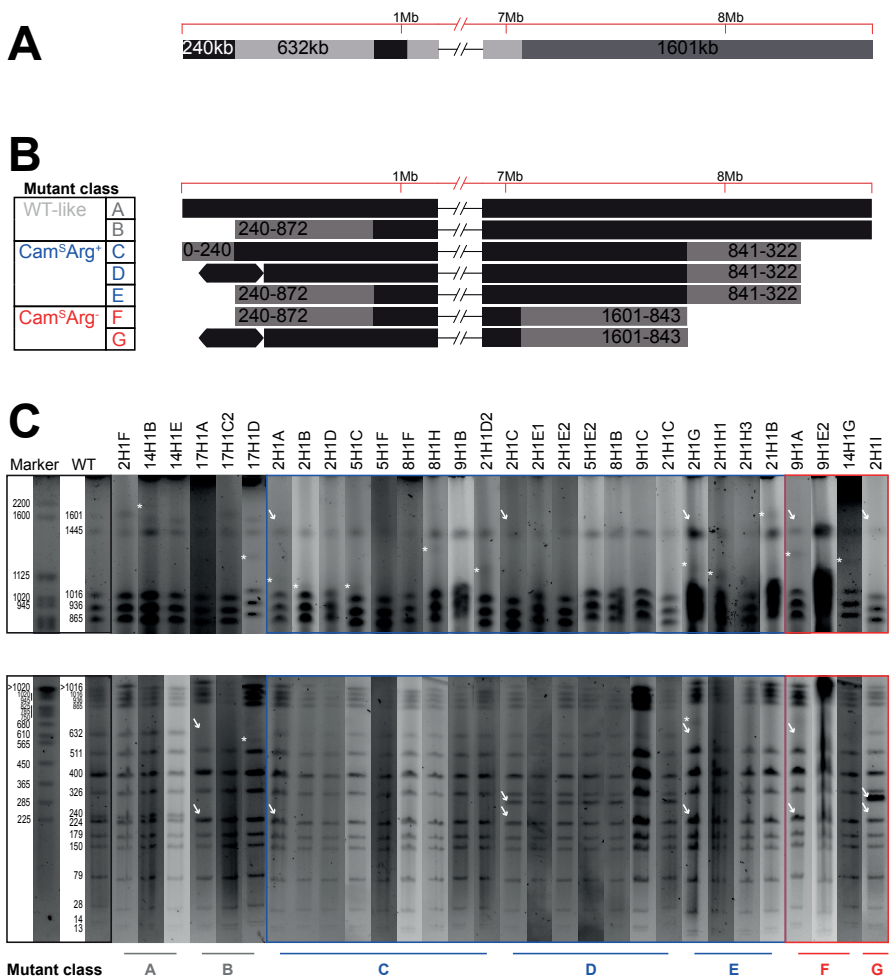
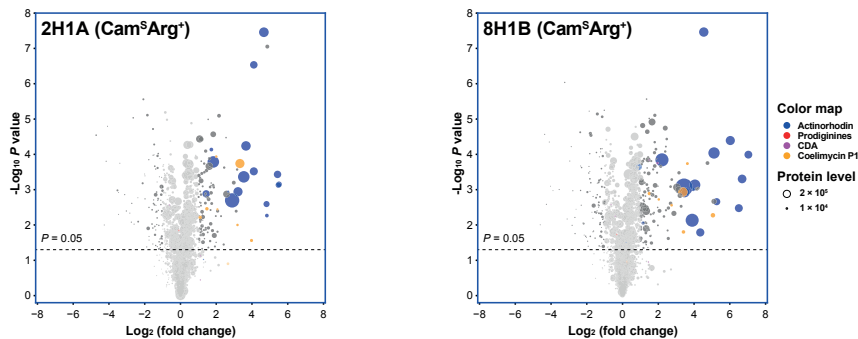


Fig. S3. PFGE results of all sampled strains. (A) The schematic of changes to *S. coelicolor* fragments in mutant isolates after *Ase* I digestion. Two bands (240 kb and 632 kb) and one 1601 kb band can be affected on the left and right arms, respectively. (B) Schematic adjusted from Fig. 2B with more detailed mutant classes, designated A-G. (C) PFGE results of 30 sampled strains. Two running conditions are used to visualize larger (top panel) or smaller (bottom panel) fragments. (Detailed running conditions are given in the Materials and methods). White arrows indicate missing or newly appearing of the bands for different mutant class. Asterisks indicate the new bands that can be used to estimate precise genome length.

A



B

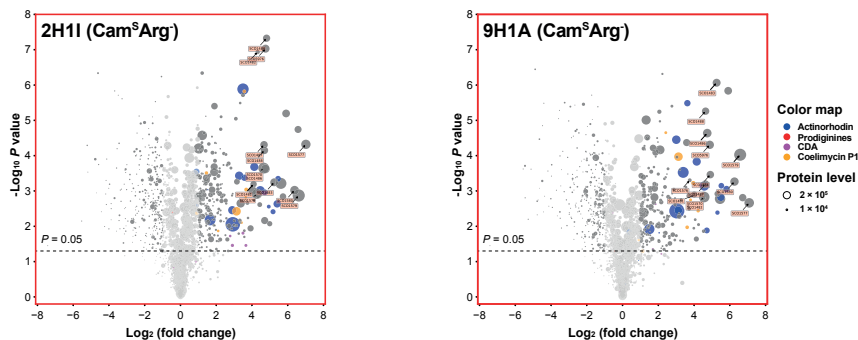


Fig. S4. Volcano plots of proteomics from four mutant strains. Volcano plots of proteomics from two Cam^SArg⁺ strains (**A**) and two Cam^SArg⁻ strains with annotated genes from arginine and pyrimidine biosynthesis pathways (**B**).

A

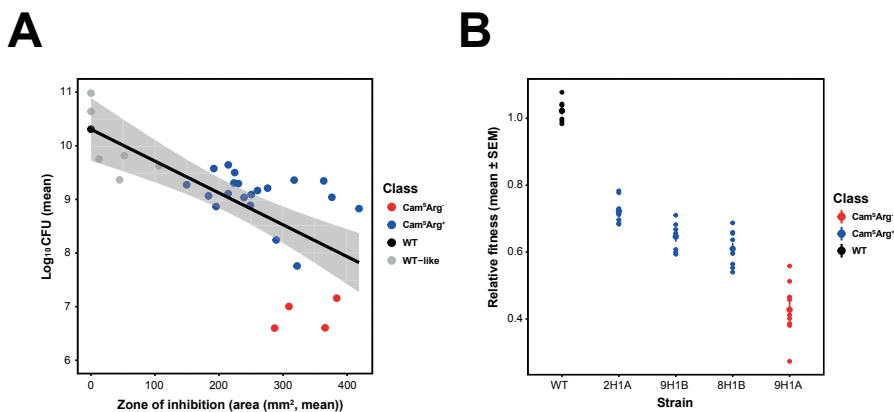


Fig. S5. Trade-off between fitness and antibiotic production. Trade-off between fitness (CFU) and antibiotic production (**A**) and relative fitness of selected strains (**B**). (**A**) The trade-off between antibiotic production and reproductive capacity, partitioned by different mutant classes. (**B**) Relative fitness of four selected strains. Detailed methods are given in the Materials and methods.

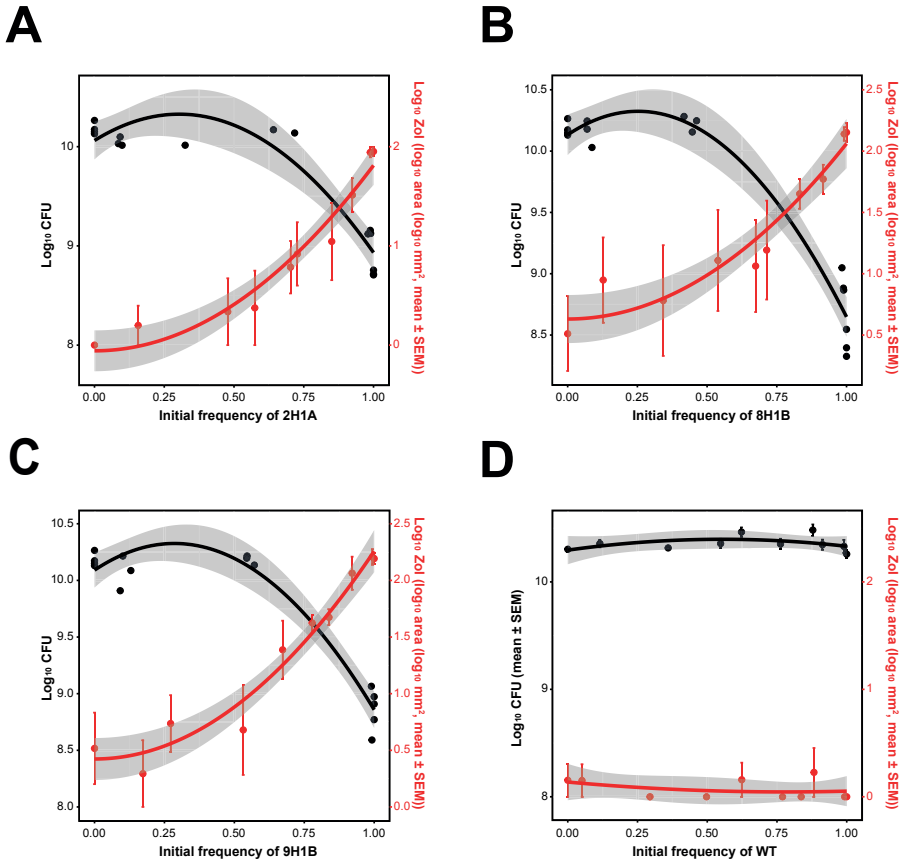


Fig. S6. Extended evidence for division of labor during co-culture of the WT and three mutant strains at different starting frequencies. Increasing frequencies of mutants cause increased antibiotic production (red) for **(A)** 2H1A ($F_{1,8} = 170.3$, $r^2 = 0.955$, $P < 0.001$), **(B)** 8H1B ($F_{1,8} = 105.3$, $r^2 = 0.929$, $P < 0.001$) and **(C)** 9H1B ($F_{1,8} = 201.1$, $r^2 = 0.962$, $P < 0.001$) but not **(D)** WT ($F_{2,7} = 0.576$, $r^2 = 0.141$, $P = 0.587$). Increasing frequencies of mutants only negatively impact colony fitness at frequencies $> 50\%$ (black) for **(A)** 2H1A ($F_{2,13} = 59.44$, $r^2 = 0.901$, $P < 0.001$), **(B)** 8H1B ($F_{2,13} = 131.7$, $r^2 = 0.953$, $P < 0.001$) and **(C)** 9H1B ($F_{2,12} = 101.7$, $r^2 = 0.944$, $P < 0.001$) but not **(D)** WT ($F_{2,7} = 1.076$, $r^2 = 0.235$, $P = 0.391$). Quadratic regression lines include the 95% CI.

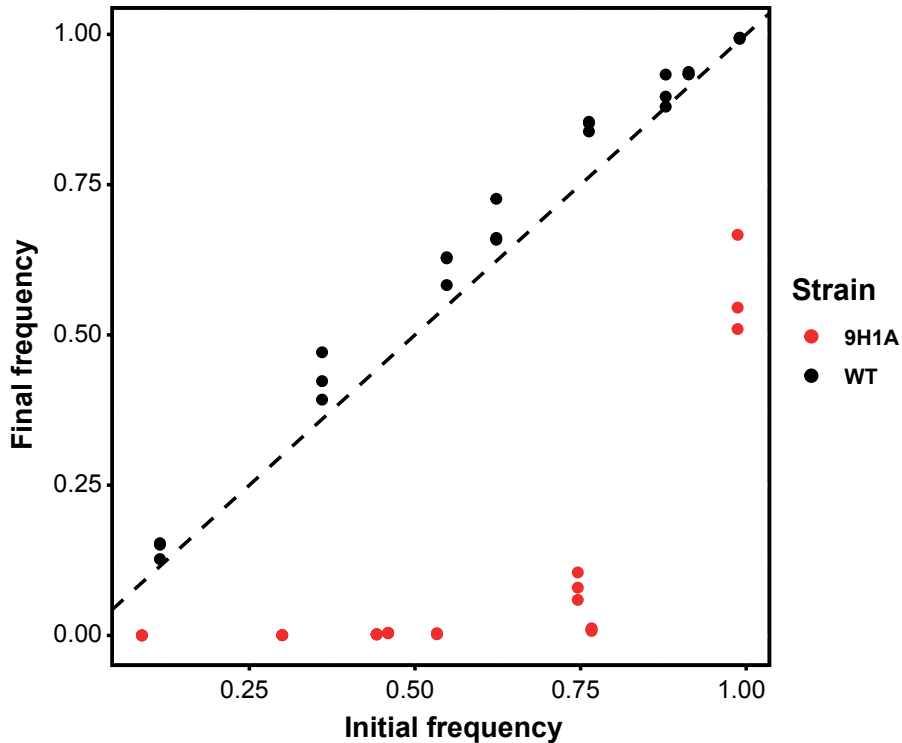


Fig. S7. Competition assays between WT and mutant strain 9H1A at different starting frequencies. Initial and final frequencies of strains during pairwise competition assays between 9H1A (red) and the wild-type or between two differentially marked wild-type strains (black). The dashed line indicates that initial and final frequencies are equal, while values below the line indicate that the competing strain has declined during the competition assay. While the differentially marked wild-type strains have equal fitness, the mutant strain has dramatically reduced fitness at every starting frequency.

Table S1. Filtered proteomics data.

This table presents the data of detected proteins from four antibiotic biosynthetic gene clusters, including CDA (SCO3210-3249), actinorhodin (SCO5071-5092), prodiginines (SCO5877-5898) and coelimycin P1 (SCO6265, 6273-6288). The data of all significantly changed proteins compared to wild type (\log_2 fold change ≥ 1 or ≤ -1 , P value < 0.05) is available online (DOI: 10.1126/sciadv.aay5781).

Protein ID	Mean TOP3 quantification of three replicates						Log ₂ fold change compared to WT						-Log ₁₀ P value					
	WT	2H1A	9H1A	9H1B	8H1B	2H1I	9H1A	2H1A	9H1A	9H1B	8H1B	2H1I	9H1A	2H1A	9H1B	8H1B	2H1I	9H1A
SCO3222	5238	5386	18335	20320	39237	16984		0.040	1.807	1.956	2.905	1.697		0.043	2.168	3.752	1.459	1.354
SCO3224	2595	5617	7283	7083	32793	4916		1.114	1.489	1.449	3.660	0.922		0.444	3.001	0.951	1.459	2.444
SCO3226	11007	7196	8398	8292	8445	10046		-0.613	-0.390	-0.409	-0.382	-0.132		2.569	2.186	2.246	0.826	0.148
SCO3233	3590	7805	5131	5462	24663	12915		1.120	0.515	0.605	2.780	1.847		1.124	0.527	0.739	1.725	2.627
SCO3244	3010	2039	6691	8480	33941	13551		-0.562	1.153	1.494	3.495	2.171		1.344	1.463	3.840	1.806	1.220
SCO3247	8360	8755	5526	5373	15169	5741		0.067	-0.597	-0.638	0.860	-0.542		0.345	2.318	2.579	1.001	2.379
SCO5071	12725	21814	285335	259024	151877	157058		4.101	4.487	4.347	3.577	3.626		6.534	4.448	1.789	3.375	5.486
SCO5072	27430	347484	459418	453737	267041	238684		3.663	4.066	4.048	3.283	3.121		4.239	5.927	3.135	3.433	2.450
SCO5073	14613	250918	319566	340819	255534	259116		4.102	4.451	4.544	4.128	4.148		3.519	4.654	7.463	3.682	3.832
SCO5074	107232	794355	1154078	1162503	814518	878843		2.889	3.428	3.438	2.925	3.035		2.696	2.932	3.070	2.056	2.435
SCO5075	34881	324428	380959	387924	259833	280376		3.217	3.449	3.475	2.897	3.007		2.942	3.227	2.925	2.457	4.451
SCO5077	143690	513528	669521	662288	453526	406203		1.837	2.220	2.205	1.658	1.499		3.786	3.706	3.844	2.180	1.921
SCO5078	4930	212343	288395	321532	209375	223069		5.429	5.870	6.027	5.408	5.500		3.433	3.442	4.392	2.635	2.822
SCO5079	44032	512344	624487	654573	497369	462411		3.540	3.826	3.894	3.498	3.393		3.363	2.667	2.134	5.885	3.527
SCO5080	14247	361477	488741	494139	314194	338898		4.665	5.100	5.116	4.463	4.572		7.458	3.844	4.039	3.011	3.141

SCO5082	2545	6211	3425	2921	5858	4736	1.287	0.429	0.199	1.203	0.896	1.023	2.638	1.507	1.729	1.033
SCO5083	15813	52380	35585	34969	30664	17691	1.728	1.170	1.145	0.955	0.162	4.136	3.231	2.054	2.589	0.352
SCO5084	77413	209543	145087	145515	144054	100427	1.437	0.906	0.911	0.896	0.375	2.882	3.716	3.645	3.547	1.839
SCO5086	5081	142855	194851	195722	132974	133178	4.813	5.261	5.268	4.710	4.712	2.593	4.015	2.660	2.961	1.883
SCO5087	2689	119967	220260	244142	97361	123937	5.479	6.356	6.504	5.178	5.525	3.131	3.984	2.477	2.413	3.148
SCO5088	2821	128458	266321	290656	124184	158883	5.509	6.561	6.687	5.460	5.816	3.149	5.241	3.304	3.347	3.055
SCO5090	1810	51595	227659	237813	55551	71713	4.833	6.974	7.037	4.939	5.308	2.267	3.244	3.992	2.558	2.387
SCO5092	2432	15492	36268	37739	6984	10060	2.671	3.898	3.956	1.522	2.048	2.944	3.037	3.003	3.038	1.816
SCO5898	10329	9660	10899	8235	7579	7539	-0.097	0.078	-0.327	-0.447	-0.454	1.845	0.371	1.731	2.394	1.295
SCO6265	15638	43561	47953	44168	42820	29433	1.478	1.617	1.498	1.453	0.912	2.459	3.404	2.890	3.511	1.614
SCO6276	5769	23084	20376	23495	24895	30836	2.001	1.821	2.026	2.110	2.418	3.937	3.490	2.724	1.868	4.651
SCO6277	2526	23034	27136	31194	26924	47382	3.189	3.426	3.627	3.414	4.230	2.001	3.568	3.738	2.104	2.442
SCO6278	21579	46320	17870	25945	40549	47058	1.102	-0.272	0.266	0.910	1.125	2.215	0.677	0.954	2.366	1.297
SCO6279	4059	17013	21748	27153	48321	49689	2.067	2.422	2.742	3.574	3.614	2.442	3.300	2.560	5.821	1.972
SCO6281	2318	36403	65025	77063	29072	32348	3.973	4.810	5.055	3.649	3.803	1.562	3.058	2.275	2.819	2.748
SCO6282	32474	325323	299293	336899	285156	283698	3.325	3.204	3.375	3.134	3.127	3.740	3.833	2.933	2.425	3.971
SCO6283	4421	27889	32751	46914	56561	68722	2.657	2.889	3.408	3.677	3.958	0.902	1.101	1.803	3.039	3.223

Table S2. The ^1H NMR signals ranked by X and Y weights (w^* and c) for PLS component 1. The association with the zone of inhibition (Zol) on *B. subtilis* suggests their contribution to increased killing. cvSE represents corss-validation standard error.

			Continued			Continued		
Signal (ppm)	w^*c [1]	cvSE	Signal (ppm)	w^*c [1]	cvSE	Signal (ppm)	w^*c [1]	cvSE
2.56	0.123	0.022	7.72	0.064	0.026	3.84	0.001	0.034
2.80	0.115	0.031	5.20	0.064	0.027	9.84	-0.002	0.024
1.56	0.110	0.021	4.00	0.064	0.035	4.76	-0.002	0.015
7.20	0.109	0.019	7.52	0.063	0.017	9.80	-0.002	0.036
7.40	0.106	0.009	6.04	0.063	0.028	8.92	-0.003	0.046
2.84	0.105	0.013	1.84	0.062	0.033	0.40	-0.004	0.030
Zol	0.105	0.031	6.52	0.062	0.020	0.48	-0.004	0.032
7.28	0.105	0.015	1.72	0.062	0.029	9.16	-0.004	0.045
7.12	0.103	0.010	6.48	0.061	0.021	8.88	-0.004	0.046
7.24	0.103	0.019	6.08	0.061	0.034	0.52	-0.005	0.033
8.00	0.101	0.017	1.96	0.060	0.034	0.44	-0.006	0.032
7.88	0.099	0.018	7.92	0.059	0.026	5.88	-0.006	0.039
3.20	0.097	0.017	5.04	0.058	0.019	6.44	-0.007	0.031
2.60	0.095	0.018	5.80	0.058	0.018	0.36	-0.007	0.030
7.00	0.095	0.017	5.68	0.056	0.015	0.32	-0.007	0.028
3.16	0.095	0.024	0.96	0.055	0.033	0.28	-0.007	0.027
7.56	0.094	0.011	5.84	0.055	0.017	0.20	-0.007	0.025
5.48	0.093	0.024	4.20	0.055	0.023	0.24	-0.007	0.025
7.68	0.092	0.011	1.24	0.051	0.024	0.64	-0.008	0.029
7.36	0.089	0.013	8.76	0.050	0.031	4.08	-0.009	0.033
2.64	0.089	0.020	3.40	0.050	0.045	4.56	-0.010	0.026
7.32	0.088	0.022	4.60	0.050	0.024	9.28	-0.010	0.038
6.96	0.088	0.042	3.48	0.049	0.022	5.64	-0.010	0.023
6.76	0.088	0.026	2.12	0.049	0.022	9.20	-0.011	0.041
7.44	0.087	0.029	1.48	0.049	0.015	9.04	-0.011	0.039
7.60	0.086	0.018	8.12	0.049	0.012	8.96	-0.012	0.044
6.80	0.086	0.021	4.04	0.048	0.044	9.36	-0.013	0.043
6.64	0.086	0.023	7.16	0.047	0.017	9.96	-0.013	0.032

8.08	0.085	0.014	9.12	0.047	0.026	8.20	-0.014	0.035
2.52	0.085	0.023	6.88	0.047	0.034	9.72	-0.016	0.033
6.60	0.085	0.017	1.04	0.046	0.034	0.76	-0.017	0.025
2.68	0.084	0.025	0.80	0.045	0.028	0.56	-0.018	0.033
1.92	0.084	0.020	1.00	0.044	0.031	10.00	-0.018	0.017
5.44	0.083	0.016	4.32	0.044	0.018	9.68	-0.019	0.028
3.60	0.083	0.026	5.56	0.043	0.024	9.44	-0.020	0.034
1.40	0.083	0.045	3.44	0.041	0.037	9.32	-0.020	0.036
2.48	0.083	0.021	3.24	0.041	0.024	9.40	-0.022	0.034
6.72	0.083	0.025	8.44	0.041	0.038	9.48	-0.024	0.036
2.44	0.082	0.024	4.64	0.039	0.030	7.84	-0.025	0.038
3.12	0.082	0.027	2.24	0.039	0.045	9.60	-0.030	0.032
2.76	0.082	0.023	4.68	0.038	0.034	3.52	-0.032	0.037
2.88	0.082	0.026	3.76	0.037	0.040	5.24	-0.033	0.034
2.92	0.082	0.025	4.72	0.036	0.030	9.64	-0.034	0.035
2.72	0.082	0.024	8.56	0.036	0.032	9.56	-0.038	0.035
2.40	0.081	0.025	6.92	0.035	0.037	1.52	-0.042	0.041
2.96	0.081	0.024	3.28	0.035	0.023	1.64	-0.042	0.027
7.48	0.081	0.017	1.44	0.034	0.026	0.60	-0.044	0.036
1.80	0.080	0.018	3.96	0.033	0.023	0.68	-0.048	0.038
6.68	0.080	0.022	3.88	0.033	0.029	8.24	-0.049	0.022
5.52	0.080	0.025	5.00	0.031	0.047	2.28	-0.055	0.034
7.08	0.079	0.018	2.20	0.031	0.028	1.36	-0.060	0.027
3.08	0.078	0.027	9.76	0.030	0.033	4.16	-0.062	0.037
6.32	0.077	0.024	0.72	0.030	0.025	3.80	-0.063	0.029
7.04	0.076	0.017	3.72	0.024	0.031	8.28	-0.063	0.028
6.40	0.076	0.019	3.36	0.024	0.026	1.12	-0.066	0.020
7.64	0.076	0.021	8.60	0.024	0.045	8.68	-0.068	0.027
3.04	0.076	0.029	3.92	0.024	0.025	8.64	-0.071	0.021
6.20	0.075	0.028	1.28	0.022	0.047	5.28	-0.074	0.036
3.00	0.074	0.026	1.08	0.021	0.027	4.36	-0.075	0.037
6.24	0.074	0.019	8.52	0.020	0.031	2.08	-0.080	0.033
4.24	0.074	0.026	7.80	0.019	0.026	2.32	-0.085	0.035
5.72	0.074	0.024	4.40	0.018	0.037	3.64	-0.088	0.026

8.04	0.074	0.013	0.84	0.017	0.029	1.20	-0.090	0.021
8.40	0.074	0.018	7.96	0.017	0.046	8.36	-0.093	0.022
6.16	0.072	0.030	9.24	0.017	0.031	2.04	-0.097	0.026
6.12	0.072	0.032	4.52	0.016	0.017	5.16	-0.098	0.035
6.56	0.072	0.021	9.92	0.015	0.018	8.32	-0.100	0.020
6.28	0.071	0.027	3.56	0.014	0.039	8.16	-0.102	0.035
4.28	0.071	0.024	5.60	0.011	0.048	5.12	-0.103	0.034
1.76	0.070	0.030	1.68	0.009	0.027	5.96	-0.104	0.018
4.44	0.070	0.018	8.80	0.009	0.046	9.08	-0.105	0.016
6.36	0.070	0.031	8.48	0.008	0.046	1.60	-0.107	0.027
7.76	0.069	0.014	5.92	0.008	0.020	2.36	-0.108	0.031
6.84	0.069	0.023	4.48	0.006	0.025	1.16	-0.110	0.031
2.16	0.068	0.017	8.84	0.006	0.048	5.32	-0.111	0.029
6.00	0.068	0.016	2.00	0.005	0.033	4.12	-0.119	0.037
8.72	0.067	0.023	3.68	0.005	0.036	5.36	-0.120	0.022
5.40	0.066	0.026	9.52	0.005	0.042	5.08	-0.123	0.028
1.88	0.065	0.021	9.88	0.003	0.026	1.32	-0.125	0.015
5.76	0.065	0.015	9.00	0.002	0.041	0.88	-0.127	0.021
0.92	0.065	0.039	Continue on the right					
Continue on the right								

Table S3. Mutant strains used in this study. This table shows mutant strains that were used in different experiments in this study.

Strain	Experiment							
	CFU production	Antibiotic production	¹ H NMR profiling	PFGE	Pacbio sequencing	Proteomics	Antibiotic production (against soil isolates)	Fitness estimates (competition assay)
2H1A	Yes	Yes	Yes	Yes	Yes	Yes	Yes	Yes
8H1B	Yes	Yes	Yes	Yes	Yes	Yes	Yes	Yes
9H1B	Yes	Yes	Yes	Yes	Yes	Yes	Yes	Yes
9H1A	Yes	Yes	Yes	Yes	Yes	Yes	Yes	Yes
2H1I	Yes	Yes	Yes	Yes	Yes	Yes		
9H1C	Yes	Yes	Yes	Yes	Yes			
2H1G	Yes	Yes	Yes	Yes	Yes			
21H1B	Yes	Yes	Yes	Yes	Yes			
2H1F	Yes	Yes	Yes	Yes				
14H1B	Yes	Yes	Yes	Yes				
14H1E	Yes	Yes	Yes	Yes				
17H1A	Yes	Yes	Yes	Yes				
17H1C2	Yes	Yes	Yes	Yes				
17H1D	Yes	Yes	Yes	Yes				
2H1B	Yes	Yes	Yes	Yes				
2H1D	Yes	Yes	Yes	Yes				
5H1C	Yes	Yes	Yes	Yes				
5H1F	Yes	Yes	Yes	Yes				

8H1F	Yes	Yes	Yes	Yes
8H1H	Yes	Yes	Yes	Yes
21H1D2	Yes	Yes	Yes	Yes
2H1C	Yes	Yes	Yes	Yes
2H1E1	Yes	Yes	Yes	Yes
2H1E2	Yes	Yes	Yes	Yes
5H1E2	Yes	Yes	Yes	Yes
21H1C	Yes	Yes	Yes	Yes
2H1H1	Yes	Yes	Yes	Yes
2H1H3	Yes	Yes	Yes	Yes
9H1E2	Yes	Yes	Yes	Yes
14H1G	Yes	Yes	Yes	Yes

Appendix III

Supplementary materials for Chapter 4

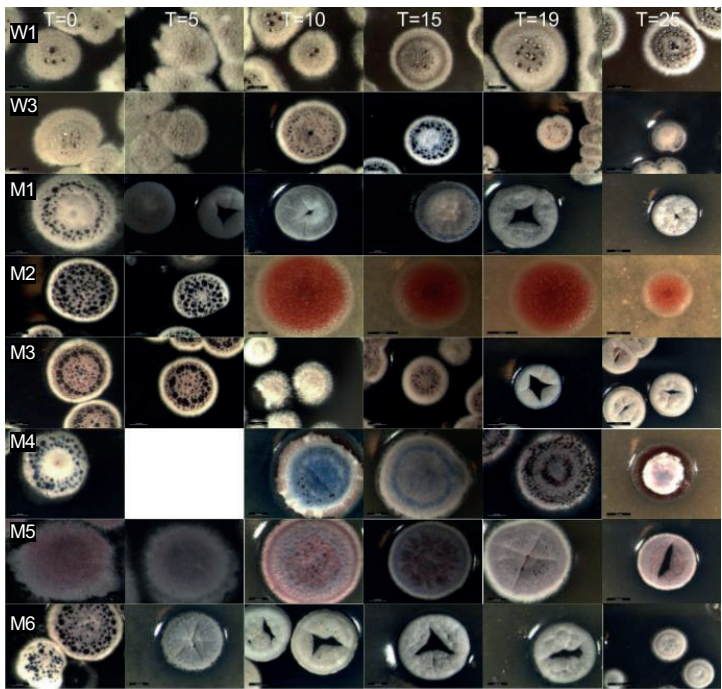


Fig. S1. Morphology of sampled strains. Morphogenesis, including aerial growth, sporulation and pigmentation, varies among and within lineages.

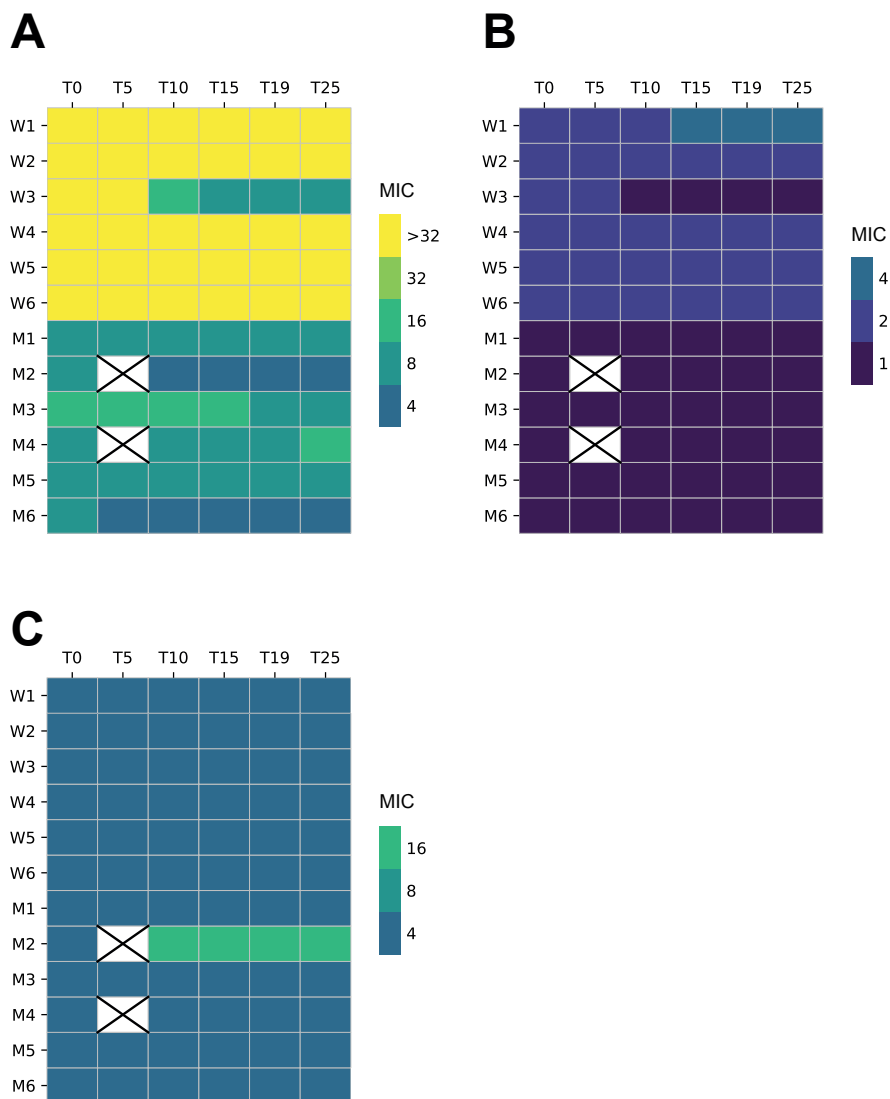


Fig. S2. Antibiotic resistance of sampled strains. MIC of (A) oxytetracycline (B) streptomycin or (C) ciprofloxacin. Unit is shown as $\mu\text{g ml}^{-1}$.

A

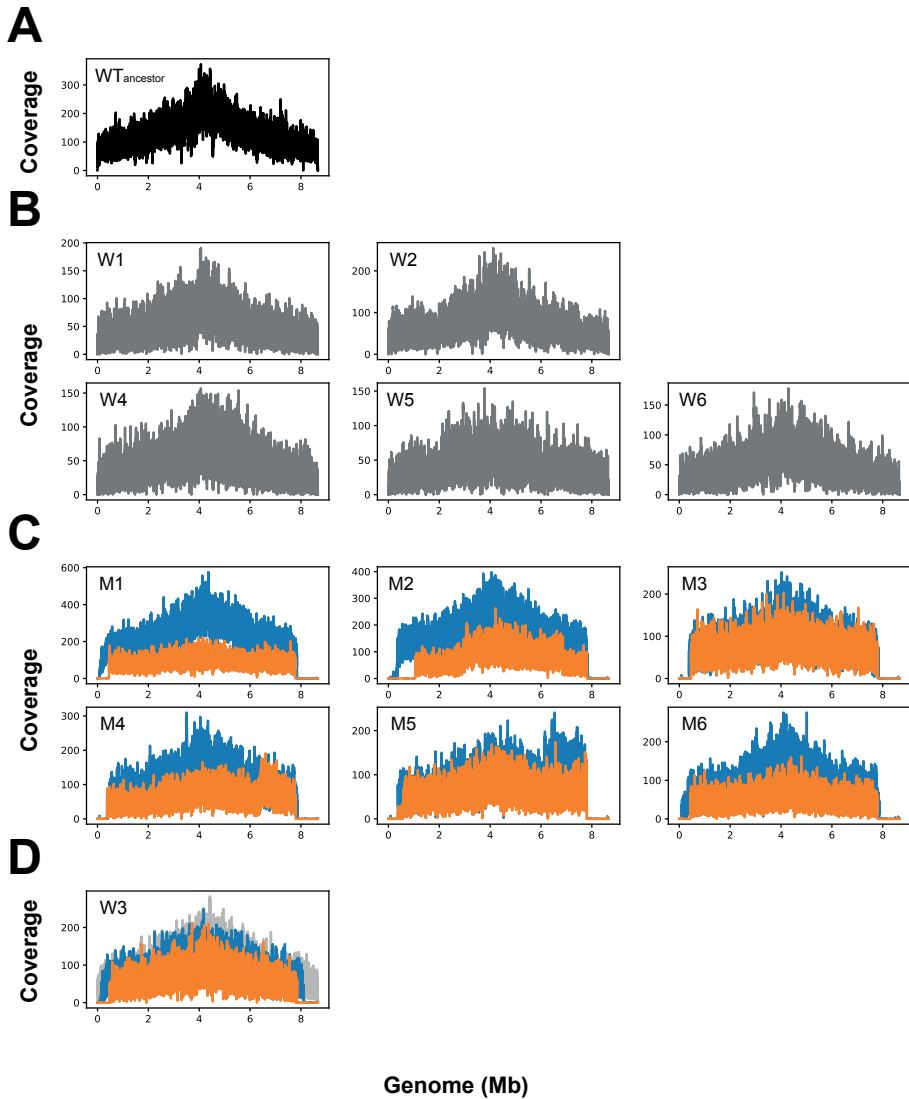


Fig. S3. Pacbio sequencing results of sampled strains. Plots indicate the coverage of reads mapped to the *S. coelicolor* M145 reference genome. **(A)** Ancestor WT. **(B)** T25 strains from WT lineages. **(C)** T0 (blue) and T25 (orange) strains from mutant lineages. **(D)** Strains of lineage W3 at T5 (light gray), T7 (blue) and T25 (orange).

Table S1. Accumulated mutations in wild-type lineages during the experiment.

Lineage	Transfer	Region	Reference	Allele	Amino acid change	Non-synonymous	Mutation type	Gene	Gene product
W1	27	221017	C	G		-	G:C>C:G		
		2208542	G	A	NP_626320.1:p.Ala91Val	Yes	G:C>A:T	SCO2060	integral membrane transport protein
		2349467	A	C	NP_626436.1:p.Glu243Ala	Yes	A:T>C:G	SCO2183	2-oxoacid dehydrogenase subunit E1
		2462887..2462888	GG	-		-	Deletion	<i>mpB</i>	
		4148255	G	C		-	G:C>C:G		
		8355042	C	T	NP_631579.1:p.Ser103Leu	Yes	G:C>A:T	SCO7535	lipoprotein
W2	27	221017	C	G		-	G:C>C:G		
		4744885	C	G	NP_628502.1:p.Asp703Glu	Yes	G:C>C:G	SCO4331	hypothetical protein
		5939426	G	C	NP_629591.1:p.Gly51Ala	Yes	G:C>C:G	SCO5454	two-component system sensor kinase
		6176177^6176178	-	G		-	Insertion		
		7313624	C	-		-	Deletion		
		2458948^2458949	-	C		-	Insertion		
W3	7								
W4	27	221017	C	G		-	G:C>C:G		
		3739268	G	A		-	G:C>A:T		
		7988760	A	G		-	A:T>G:C		
		8613917	C	T		No	G:C>A:T	SCO7788	hypothetical protein

W5	27	373226	G	C	NP_624691.1:p.Ser61Thr	Yes	G:C>C:G	SCO0368	transposase
		1650273	A	G		-	A:T>G:C		
		2458948^2458949	-	C		-	Insertion		
		2462887	G	-		-	Deletion	<i>mpB</i>	
		4938336	C	A	NP_628680.1:p.Arg62Leu	Yes	G:C>T:A	SCO4516	hypothetical protein
		5371295	G	T		No	G:C>T:A	SCO4935	hypothetical protein
		8424413	G	A		No	G:C>A:T	SCO7597	hypothetical protein
		8424416	G	A		No	G:C>A:T	SCO7597	hypothetical protein
		8424506	A	G		No	A:T>G:C	SCO7597	hypothetical protein
		8424513	G	-	NP_631639.1:p.Ala122fs	Yes	Deletion	SCO7597	hypothetical protein
W6	27	221017	C	G		-	G:C>C:G		
		6769943	G	C	NP_630271.1:p.Arg179Pro	Yes	G:C>C:G	SCO6167	proline rich protein membrane protein
		7700826	C	G	NP_631001.1:p.Val185Leu	Yes	G:C>C:G	SCO6935	hypothetical protein

Table S2. Accumulated mutations in mutant lineages during the experiment.

Lineage	Transfer	Region	Reference	Al- lele	Amino acid change	Non-syn- onymous	Mutation type	Gene	Gene product
M1	25	481270	G	A	NP_624779.1:p.Ala87Thr	Yes	G:C>A:T	SCO0459	hypothetical protein
M1	25	712725	C	T		No	G:C>A:T	SCO0673	hypothetical protein
M1	25	1134186	C	T		No	G:C>A:T	SCO1074	hypothetical protein
M1	25	1467045	G	A		No	G:C>A:T	SCO1388	mannose-1-phosphate guanylttransferase
M1	25	1503926	C	T	NP_625691.1:p.Val132Met	Yes	G:C>A:T	SCO1409	hypothetical protein
M1	25	1615858	C	T	NP_733536.1:p.His187Tyr	Yes	G:C>A:T	SCO1511	hypothetical protein
M1	25	1811018	G	T		No	G:C>T:A	SCO1691	TetR family transcriptional regulator
M1	25	1906862	G	T		No	G:C>T:A	<i>ppnK</i>	inorganic polyphosphate/ATP-NAD kinase
M1	25	2119778	G	A	NP_626243.1:p.Val7Ile	Yes	G:C>A:T	SCO1981	hypothetical protein
M1	25	2458948\2458949	-	C		-	Insertion		
M1	25	2489834	C	G	NP_626565.1:p.Gly74Ala	Yes	G:C>C:G	SCO2318	glycosyl transferase
M1	25	2884357	G	C	NP_626888.1:p.Ala92Pro	Yes	G:C>C:G	SCO2652	hypothetical protein
M1	25	2968251	C	A	NP_626956.1:p.Glu646*	Yes	G:C>T:A	SCO2723	ABC transporter ATP-binding protein
M1	25	3345283	C	A		No	G:C>T:A	SCO3052	UDP-glucose 6-dehydrogenase
M1	25	4040725	G	T		No	G:C>T:A	SCO3661	ATP-dependent protease ATP-binding subunit
M1	25	4127767	G	T	NP_733616.1:p.Ala71Asp	Yes	G:C>T:A	SCO3754	ABC transporter
M1	25	4148505	T	C		-	A:T>G:C		
M1	25	4532381	T	C		-	A:T>G:C		

M1	25	4732128	C	G	NP_628492.1:p.Arg849Pro	Yes	G:C>C:G	SCO4321	hypothetical protein
M1	25	5777386	C	T		No	G:C>A:T	SCO5304	sensor-like histidine kinase
M1	25	5840932	C	G		No	G:C>C:G	SCO5371	F0F1 ATP synthase subunit alpha
M1	25	5960922	C	A		-	G:C>T:A		
M1	25	6203952	C	G	NP_629822.1:p.Pro11Ala	Yes	G:C>C:G	SCO5694	1-deoxy-D-xylulose 5-phosphate reductoisomerase
M1	25	6371032	C	A		No	G:C>T:A	SCO5822	DNA topoisomerase IV subunit B
M1	25	6629123	G	C	NP_630149.1:p.Ala170Gly	Yes	G:C>C:G	SCO6038	hypothetical protein
M1	25	6960345	G	C	NP_630397.1:p.Thr489Ser	Yes	G:C>C:G	SCO6300	hydrolase
M1	25	6972333	G	C	NP_630409.1:p.Pro115Ala	Yes	G:C>C:G	SCO6312	transcriptional regulator
M1	25	7009564	G	-	NP_630440.1:p.Ala444fs	Yes	Deletion	SCO6348	hypothetical protein
M1	25	7009566	C	T	NP_630440.1:p.Val443Ile	Yes	G:C>A:T	SCO6348	hypothetical protein
M1	25	7101047	G	T		No	G:C>T:A	SCO6428	hypothetical protein
M1	25	7271648	G	A		No	G:C>A:T	SCO6568	ABC transporter
M1	25	7547616	G	C	NP_630861.1:p.Val132Leu	Yes	G:C>C:G	SCO6789	fatty oxidation protein
M1	25	7559869	G	A		No	G:C>A:T	<i>tdh</i>	L-threonine 3-dehydrogenase
M1	25	7566905	G	C	NP_630878.1:p.Ala148Gly	Yes	G:C>C:G	SCO6806	phage integrase
M1	25	7766466	C	G		No	G:C>C:G	SCO6995	protease
M1	25	7776421	G	A	NP_631068.1:p.Ser251Phe	Yes	G:C>A:T	SCO7003	hypothetical protein
M2	25	1088640	C	A		No	G:C>T:A	SCO1031	ABC transporter
M2	25	1126417	G	A		-	G:C>A:T		
M2	25	1166168	G	C	NP_625402.1:p.Glu85Gln	Yes	G:C>C:G	SCO1109	oxidoreductase
M2	25	1404674	C	T		-	G:C>A:T		

M2	25	1432260	G	A		-	G:C>A:T			bifunctional ornithine acetyltransferase/N-acetylglutamate synthase
M2	25	1690052	C	A	NP_733539.1:p.Ala129Ser	Yes	G:C>T:A	<i>argJ</i>		
M2	25	1719518	G	T		-	G:C>T:A			
M2	25	1807393	C	T		-	G:C>A:T			
M2	25	1926842	C	T	NP_626068.1:p.Val225Ile	Yes	G:C>A:T	SCO1798		ABC transporter ATP-binding protein
M2	25	2542975	G	A		-	G:C>A:T			
M2	25	2613098	C	A		-	G:C>T:A			
M2	25	2758023	C	T	NP_626796.1:p.Gly147Glu	Yes	G:C>A:T	SCO2558		hypothetical protein
M2	25	2864030	G	A	NP_626871.1:p.Val777Met	Yes	G:C>A:T	SCO2635		aminopeptidase
M2	25	2908625	G	C	NP_626907.1:p.Gly87Ala	Yes	G:C>C:G	SCO2672		hypothetical protein
M2	25	2990314	A	T		-	A:T>T:A			
M2	25	2993995	G	C		No	G:C>C:G	SCO2747		bifunctional carbohydrate binding and transport protein
M2	25	3282758	G	C		-	G:C>C:G			
M2	25	3583178	G	A		No	G:C>A:T	SCO3232		CDA peptide synthetase III
M2	25	3585292	C	T		No	G:C>A:T	SCO3234		phosphotransferase
M2	25	3796098	G	T	NP_733604.1:p.Ala456Ser	Yes	G:C>T:A	SCO3434		DNA polymerase I
M2	25	4313821	T	G		-	A:T>C:G			
M2	25	4486909	G	A		No	G:C>A:T	SCO4092		ATP-dependent helicase
M2	25	4617566	A	G	NP_628383.1:p.Val98Ala	Yes	A:T>G:C	SCO4208		integral membrane transport protein
M2	25	4811070	C	T	NP_628563.1:p.His79Tyr	Yes	G:C>A:T	SCO4394		iron repressor
M2	25	5532591	C	T	NP_629239.1:p.Thr48Ile	Yes	G:C>A:T	SCO5089		actinorhodin polyketide synthase

M2	25	577556	G	A		No	G:C>A:T	SCO5302	integral membrane cell-cycle protein
M2	25	6037691	C	G	NP_629674.1:p.Arg355Pro	Yes	G:C>C:G	SCO5540	hypothetical protein
M2	25	7129427	A	T		-	A:T>T:A		
M2	25	7298296	C	G		No	G:C>C:G	SCO6587	dehydrogenase
M2	25	7406743	G	C	NP_630741.1:p.Ser303Arg	Yes	G:C>C:G	SCO6666	hypothetical protein
M2	25	7634733	C	A	NP_630934.1:p.Gly316Cys	Yes	G:C>T:A	SCO6864	hypothetical protein
M2	25	7645276	T	A	NP_630946.1:p.Lys44Met	Yes	A:T>T:A	SCO6876	hypothetical protein
M2	25	7807060	G	T	NP_631085.1:p.Gly14Trp	Yes	G:C>T:A	SCO7021	hypothetical protein
M3	25	1072216..1072217	GA	TC	NP_625312.1:p.Ser110Asp	Yes	G:C>T:A	SCO1016	hypothetical protein
M3	25						A:T>C:G		
M3	25	1252185	C	T	NP_625474.1:p.Arg3Cys	Yes	G:C>A:T	SCO1184	hypothetical protein
M3	25	1344799	A	C	NP_625561.1:p.His218Pro	Yes	A:T>C:G	SCO1274	hypothetical protein
M3	25	1592949	A	C		-	A:T>C:G		
M3	25	1719817	T	G		-	A:T>C:G		
M3	25	1765203	A	G		-	A:T>G:C		
M3	25	1878761	T	G		-	A:T>C:G		
M3	25	1878763	A	G		-	A:T>G:C		
M3	25	1878792	T	C		-	A:T>G:C		
M3	25	2112369	C	T	NP_626236.1:p.Gly248Ser	Yes	G:C>A:T	SCO1973	hypothetical protein
M3	25	2686414	G	T	NP_626736.1:p.Pro407Gln	Yes	G:C>T:A	SCO2494	pyruvate phosphate dikinase
M3	25	2947470	A	T		-	A:T>T:A		
M3	25	4148246	A	C		-	A:T>C:G		

M3	25	4148252	A	C		-	A:T>C:G		
M3	25	4377204^4377205	-	G		-	Insertion		
M3	25	4430625	A	C		-	A:T>C:G		
M3	25	4663287	G	T		No	G:C>T:A	SCO4254	hypothetical protein
M3	25	4770844	A	G	NP_628526.1:p.Leu99Pro	Yes	A:T>G:C	SCO4356	hypothetical protein
M3	25	4880312	C	T		-	G:C>A:T		
M3	25	5255390	A	C		-	A:T>C:G		
M3	25	5612258	A	G		-	A:T>G:C		
M3	25	5612260	T	G		-	A:T>C:G		
M3	25	5612263	C	G		-	G:C>C:G		
M3	25	5830280	T	C		-	A:T>G:C		
M3	25	5871569	C	T		No	G:C>A:T	SCO5399	acetyl-CoA acetyltransferase
M3	25	6105201	C	A	NP_629737.1:p.Leu112Ile	Yes	G:C>T:A	SCO5603	hypothetical protein
M3	25	6113723	G	C	NP_629746.1:p.Val724Leu	Yes	G:C>C:G	SCO5612	ATP binding protein
M3	25	6598610	A	C		-	A:T>C:G		
M3	25	6935489	C	T	NP_630376.1:p.Pro328Leu	Yes	G:C>A:T	SCO6278	integral membrane transport protein
M3	25	7633600	C	G	NP_630933.1:p.Ala74Pro	Yes	G:C>C:G	SCO6863	hypothetical protein
M3	25	7777209	G	C		-	G:C>C:G		
M4	25	527567	G	A	NP_624811.1:p.Pro91Leu	Yes	G:C>A:T	SCO0494	iron-siderophore binding lipoprotein
M4	25	533965	C	T		No	G:C>A:T	SCO0501	hypothetical protein
M4	25	738352^738353	-	G		-	Insertion		
M4	25	5056054	C	G	NP_628793.1:p.Thr76Ser	Yes	G:C>C:G	SCO4632	ATP/GTP binding protein

M4	25	5257242	G	A		-	G:C>A:T		
M4	25	6370279^6370280	-	G		-	Insertion		
M4	25	7595845	G	A	NP_630898.1:p.Ala904Val	Yes	G:C>A:T	SCO6827	polyketide synthase
M5	25	2462887	G	-		-	Deletion	<i>mpB</i>	
M5	25	2961862	G	T		No	G:C>T:A	SCO2718	hypothetical protein
M5	25	5203768	T	C	NP_628940.1:p.Asp10Gly	Yes	A:T>G:C	SCO4782	hypothetical protein
M5	25	6769937	G	C	NP_630271.1:p.Arg177Pro	Yes	G:C>C:G	SCO6167	proline rich protein membrane protein
M6	25	454451^454452	-	C		-	Insertion		
M6	25	489245	G	-	NP_624786.1:p.Arg211fs	Yes	Deletion	SCO0467	hypothetical protein
M6	25	606363	G	T	NP_624876.1:p.Arg65Ser	Yes	G:C>T:A	SCO0563	hypothetical protein
M6	25	681473	C	G	NP_624950.1:p.Glu131Gln	Yes	G:C>C:G	SCO0640	hypothetical protein
M6	25	1251111	G	C		No	G:C>C:G	SCO1183	hypothetical protein
M6	25	1562784	C	G	NP_625746.1:p.Cys246Ser	Yes	G:C>C:G	SCO1465	hypothetical protein
M6	25	1670045	G	T	NP_625836.1:p.Leu210Met	Yes	G:C>T:A	SCO1558	ABC transporter permease
M6	25	1765203^1765204	-	G		-	Insertion		
M6	25	1984265	G	A	NP_626119.1:p.Gly82Arg	Yes	G:C>A:T	SCO1851	cob(I)lyrinic acid a,c-diamide adenosyltransferase
M6	25	1988841	A	C	NP_626123.1:p.Thr125Pro	Yes	A:T>C:G	SCO1856	precorrin-6Y C5,15-methyltransferase
M6	25	2295007	G	A	NP_626389.1:p.Gly376Ser	Yes	G:C>A:T	SCO2133	hypothetical protein
M6	25	2646572	A	G		No	A:T>G:C	SCO2460	hypothetical protein
M6	25	3008164	T	A		-	A:T>T:A		
M6	25	4377204^4377205	-	G		-	Insertion		
M6	25	4564696	C	G		No	G:C>C:G	SCO4148	ABC transporter ATP-binding protein

M6	25	4658248	G	T	NP_628424.1:p.Gly450Trp	Yes	G:C>T:A	SCO250	hypothetical protein
M6	25	4880904	C	T	NP_733638.1:p.Gly24Asp	Yes	G:C>A:T	SCO4458	lipoprotein
M6	25	4940282	A	C	NP_628682.1:p.Trp194Gly	Yes	A:T>C:G	SCO4518	hypothetical protein
M6	25	6503843	G	T	NP_630050.1:p.Pro27His	Yes	G:C>T:A	SCO5933	hypothetical protein
M6	25	6597353	A	T	NP_630127.1:p.Glu104Asp	Yes	A:T>T:A	SCO6014	cationic amino acid transporter
M6	25	6826638	C	T		-	G:C>A:T		
M6	25	6994242	G	C		No	G:C>C:G	SCO6334	transcriptional regulator
M6	25	7163598	G	A		-	G:C>A:T		
M6	25	7198042	C	A	NP_630588.1:p.Asp37Glu	Yes	G:C>T:A	SCO6506	gas vesicle protein
M6	25	7237535	G	T	NP_630625.1:p.Glu108*	Yes	G:C>T:A	SCO6544	hypothetical protein
M6	25	7671689	G	A	NP_630976.1:p.Val119Met	Yes	G:C>A:T	SCO6907	DNA ligase
M6	25	7755660	C	G		No	G:C>C:G	SCO6988	oxidoreductase
M6	25	7783012	G	-	NP_631073.1:p.Val118fs	Yes	Deletion	SCO7008	ABC transporter ATP-binding protein
W3	18	466074	A	C	NP_624768.1:p.Ile29Leu	Yes	A:T>C:G	SCO0447	MarR family regulatory protein
W3	18	515777	C	G		No	G:C>C:G	SCO0492	peptide synthetase
W3	18	1467501	T	A		No	A:T>T:A	SCO1388	mannose-1-phosphate guanylttransferase
W3	18	1765203^1765204	-	G		-	Insertion		
W3	18	1792889	G	A	NP_625946.1:p.Arg682Gln	Yes	G:C>A:T	SCO1671	hypothetical protein
W3	18	2077625	G	A		-	G:C>A:T		
W3	18	2139959	G	C	NP_626262.1:p.Tyr255*	Yes	G:C>C:G	SCO2001	hypothetical protein
W3	18	3137890	G	A	NP_627111.1:p.Arg77Gln	Yes	G:C>A:T	SCO2883	cytochrome P450
W3	18	3155674	G	A		No	G:C>A:T	SCO2902	deoxyribonucleotide triphosphate pyrophosphatase

W3	18	3277441	G	C	NP_627227.1:p.Asp760Glu	Yes	G:C>C:G	SCO3005	preprotein translocase subunit SecA
W3	18	3560736	G	C	NP_627443.1:p.Arg-580IPro	Yes	G:C>C:G	SCO3230	CDA peptide synthetase I
W3	18	3910675	G	A		No	G:C>A:T	SCO3541	DNA polymerase III subunit delta'
W3	18	4377204^4377205	-	G		-	Insertion		
W3	18	4700228	C	A	NP_628456.1:p.Gly106TTrp	Yes	G:C>T:A	SCO4284	N-acetylglucosamine-6-phosphate deacetylase
W3	18	5611647	C	T		No	G:C>A:T	SCO5165	hydrolase
W3	18	6052711	C	T		No	G:C>A:T	SCO5553	3-isopropylmalate dehydratase large subunit
W3	18	6613228	C	G		No	G:C>C:G	SCO6026	fatty acid oxidation complex alpha-subunit
W3	18	7224671	C	G	NP_630614.1:p.Gly95Arg	Yes	G:C>C:G	SCO6533	nitrate reductase subunit delta NarJ
W3	18	7799431	A	T		-	A:T>T:A		

Appendix IV

Supplementary materials for Chapter 5

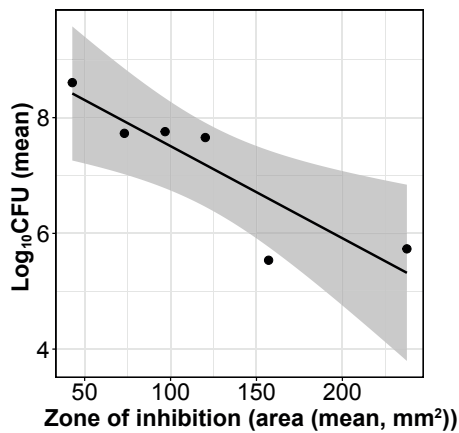


Fig. S1. CFU production and antibacterial activity is negatively correlated. The linear regression line includes the 95% confidence interval.

Strain	R.	WT			2H1A			8H1B			9H1B			2H1I			9H1A		
		1	2	3	1	2	3	1	2	3	1	2	3	1	2	3	1	2	3
WT	1	1.00	0.99	0.99	0.86	0.87	0.85	0.77	0.76	0.75	0.77	0.76	0.76	0.65	0.64	0.64	0.62	0.60	0.61
	2	0.99	1.00	0.99	0.86	0.87	0.85	0.77	0.76	0.75	0.77	0.76	0.76	0.64	0.63	0.63	0.61	0.60	0.60
	3	0.99	0.99	1.00	0.86	0.86	0.85	0.77	0.77	0.76	0.78	0.76	0.77	0.65	0.64	0.64	0.62	0.60	0.61
2H1A	1	0.86	0.86	0.86	1.00	0.99	0.99	0.96	0.96	0.95	0.96	0.96	0.96	0.78	0.77	0.78	0.76	0.75	0.77
	2	0.87	0.87	0.86	0.99	1.00	1.00	0.96	0.94	0.94	0.95	0.95	0.95	0.76	0.75	0.77	0.74	0.73	0.74
	3	0.85	0.85	0.85	0.99	1.00	1.00	0.96	0.95	0.95	0.95	0.95	0.95	0.77	0.77	0.78	0.76	0.74	0.76
8H1B	1	0.77	0.77	0.77	0.96	0.96	0.96	1.00	0.99	0.99	0.99	0.99	0.99	0.80	0.80	0.82	0.79	0.78	0.81
	2	0.76	0.76	0.77	0.96	0.94	0.95	0.99	1.00	0.99	0.99	0.99	0.99	0.79	0.79	0.80	0.78	0.76	0.79
	3	0.75	0.75	0.76	0.95	0.94	0.95	0.99	0.99	1.00	0.99	0.99	0.99	0.79	0.79	0.81	0.78	0.77	0.80
9H1B	1	0.77	0.77	0.78	0.96	0.95	0.95	0.99	0.99	0.99	1.00	1.00	0.99	0.81	0.81	0.82	0.80	0.78	0.81
	2	0.76	0.76	0.76	0.96	0.95	0.95	0.99	0.99	0.99	1.00	1.00	1.00	0.79	0.79	0.80	0.78	0.77	0.79
	3	0.76	0.76	0.77	0.96	0.95	0.95	0.99	0.99	0.99	0.99	1.00	1.00	0.78	0.78	0.80	0.78	0.76	0.79
2H1I	1	0.65	0.64	0.65	0.78	0.76	0.77	0.80	0.79	0.79	0.81	0.79	0.78	1.00	0.99	0.99	0.96	0.96	0.97
	2	0.64	0.63	0.64	0.77	0.75	0.77	0.80	0.79	0.79	0.81	0.79	0.78	0.99	1.00	0.99	0.97	0.97	0.98
	3	0.64	0.63	0.64	0.78	0.77	0.78	0.82	0.80	0.81	0.82	0.80	0.80	0.99	0.99	1.00	0.96	0.96	0.98
9H1A	1	0.62	0.61	0.62	0.76	0.74	0.76	0.79	0.78	0.78	0.80	0.78	0.78	0.96	0.97	0.96	1.00	0.99	0.99
	2	0.60	0.60	0.60	0.75	0.73	0.74	0.78	0.76	0.77	0.78	0.77	0.76	0.96	0.97	0.96	0.99	1.00	0.99
	3	0.61	0.60	0.61	0.77	0.74	0.76	0.81	0.79	0.80	0.81	0.79	0.79	0.97	0.98	0.98	0.99	0.99	1.00

Fig. S2. Pearson's correlation coefficient between each sample. This heatmap shows reproducibility between replicates of the same strain and distinction among strains similar to what is indicated by genomic rearrangements.

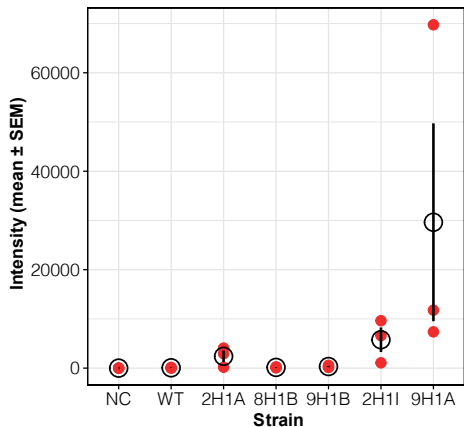


Fig. S3. Undecylprodigiosin production quantified by LC-MS/MS. No significant difference was detected among strains based one-way ANOVA followed by Tukey's tests and multiple two-sample *t* tests followed by Bonferroni correction ($P < 0.05$).

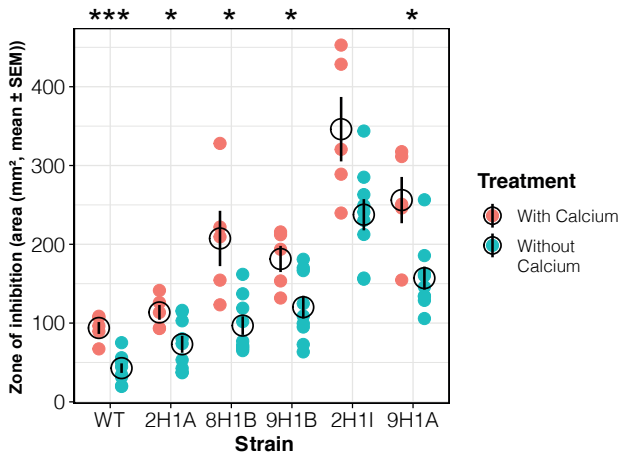


Fig. S4. The zone of inhibition against *B. subtilis* increase in most strains when overlaid media are supplemented with 20mM calcium nitrate. Asterisks indicate the statistical difference between two treatments according to Welch's *t* tests (* $P < 0.05$, *** $P < 0.001$).

Table S1. List of proteins with a VIP > 1.4 and a regression coefficient > 0 based on the PLS model using antibacterial activity (zone of inhibition) as a Y variable.

Locus tag	Coef.	VIP	Gene	Gene product
SCO0170	0.174	1.533		hypothetical protein
SCO7013	0.171	1.497		sugar-binding lipoprotein
SCO0158	0.171	1.562		oxidoreductase
SCO0299	0.170	1.515		oxidoreductase
SCO3671	0.166	1.423	<i>dnaK</i>	molecular chaperone DnaK
SCO0254	0.162	1.476		hypothetical protein
SCO3224	0.160	1.518		ABC transporter ATP-binding protein
SCO0335	0.159	1.521		hypothetical protein
SCO0257	0.158	1.493		hypothetical protein
SCO0259	0.158	1.468		alcohol dehydrogenase
SCO0137	0.157	1.466		sugar-transport protein
SCO0214	0.156	1.471		hypothetical protein
SCO1254	0.154	1.420	<i>purB</i>	adenylosuccinate lyase
SCO3132	0.152	1.519		trans-aconitate 2-methyltransferase
SCO4992	0.152	1.401		hypothetical protein
SCO2407	0.147	1.518		aldose 1-epimerase
SCO0203	0.146	1.417		two-component sensor
SCO0315	0.144	1.477		decarboxylase
SCO0361	0.144	1.472		hypothetical protein
SCO4071	0.139	1.553	<i>purC</i>	phosphoribosylaminoimidazole-succinocarbox- amide synthase
SCO3236	0.139	1.525		oxygenase
SCO2196	0.139	1.494		hypothetical protein
SCO4739	0.137	1.470		lipoprotein
SCO3222	0.136	1.473		hypothetical protein
SCO1366	0.136	1.497		hypothetical protein
SCO3229	0.136	1.507		4-hydroxyphenylpyruvic acid dioxygenase
SCO4472	0.134	1.442	<i>resA</i>	hypothetical protein
SCO2404	0.133	1.455		sugar-binding receptor
SCO3244	0.130	1.510		hypothetical protein
SCO1361	0.128	1.453		hypothetical protein

SCO1906	0.125	1.451		hypothetical protein
SCO1838	0.124	1.426		enoyl-CoA hydratase/isomerase
SCO0723	0.124	1.505		fructose transport system kinase
SCO1903	0.122	1.461		transport associated protein
SCO1138	0.122	1.441		hypothetical protein
SCO5285	0.122	1.475	<i>lon</i>	ATP-dependent protease
SCO4919	0.115	1.493		flavoprotein disulfide reductase
SCO2380	0.113	1.450		hypothetical protein
SCO3661	0.112	1.474	<i>clpB</i>	ATP-dependent protease ATP-binding subunit
SCO2887	0.111	1.460		hypothetical protein
SCO1530	0.110	1.422		hypothetical protein
SCO5059	0.109	1.463	<i>ppgK</i>	polyphosphate glucokinase
SCO4490	0.108	1.436		decarboxylase
SCO0462	0.107	1.447		oxidoreductase
SCO4956	0.105	1.433		methionine sulfoxide reductase A
SCO2262	0.102	1.430		oxidoreductase
SCO4754	0.101	1.428		transcriptional regulator
SCO3092	0.099	1.431		oxidoreductase
SCO6010	0.099	1.438		ABC transporter ATP-binding protein
SCO3945	0.098	1.453	<i>cydA</i>	cytochrome oxidase subunit I
SCO3890	0.092	1.426	<i>trxB</i>	thioredoxin reductase
SCO6026	0.090	1.404		fatty acid oxidation complex alpha-subunit
SCO5281	0.088	1.403		alpha-ketoglutarate decarboxylase
SCO1081	0.087	1.408		electron transfer flavoprotein subunit alpha

Table S2. List of proteins with a VIP > 1.4 and a regression coefficient < 0 based on the PLS model using antibacterial activity (zone of inhibition) as a Y variable.

Locus tag	Coef.	VIP	Gene	Gene product
SCO5040	-0.149	1.538		hypothetical protein
SCO4654	-0.144	1.501	<i>rpoB</i>	DNA-directed RNA polymerase subunit beta
SCO1388	-0.142	1.538		mannose-1-phosphate guanylttransferase
SCO4655	-0.133	1.428	<i>rpoC</i>	DNA-directed RNA polymerase subunit beta'
SCO6750	-0.128	1.413		isopentenyl-diphosphate delta-isomerase
SCO3328	-0.120	1.499	<i>bdtA</i>	hypothetical protein
SCO1234	-0.109	1.404	<i>ureC</i>	urease subunit alpha
SCO3144	-0.104	1.467		two-component system response regulator
SCO6638	-0.097	1.435		hypothetical protein
SCO3677	-0.096	1.419		purine phosphoribosyltransferase
SCO5629	-0.096	1.415		ATP /GTP-binding protein
SCO1908	-0.091	1.404		large hypothetical protein
SCO4568	-0.091	1.406	<i>nuoG</i>	NADH dehydrogenase subunit G
SCO7028	-0.090	1.408	<i>bxlE</i>	sugar-binding lipoprotein
SCO5176	-0.090	1.410		reductase
SCO2035	-0.090	1.425		hypothetical protein
SCO1141	-0.089	1.419		hypothetical protein
SCO7072	-0.081	1.400		hypothetical protein
SCO0932	-0.080	1.402		hypothetical protein

Table S3. List of proteins with a VIP > 1.4 and a regression coefficient > 0 based on the PLS model using CFU as a Y variable.

Locus tag	Coef.	VIP	Gene	Gene product
SCO5819	1.46E-3	1.423	<i>whiH</i>	sporulation transcription factor, WhiH
SCO6375	1.42E-3	1.452		hypothetical protein
SCO1090	1.42E-3	1.433	<i>ugpQ1</i>	phosphodiesterase
SCO2520	1.41E-3	1.408		hypothetical protein
SCO6154	1.40E-3	1.446		hypothetical protein
SCO0592	1.40E-3	1.447		hypothetical protein
SCO4159	1.39E-3	1.446	<i>glnR</i>	transcriptional regulator
SCO4239	1.39E-3	1.446		small membrane protein
SCO4768	1.38E-3	1.439	<i>bldM</i>	two-component regulator
SCO1163	1.38E-3	1.456		hypothetical protein
SCO4042	1.38E-3	1.436		hypothetical protein
SCO7073	1.37E-3	1.446		dihydroxyacetone kinase subunit DhaK
SCO3101	1.37E-3	1.414		lipoprotein
SCO3540	1.36E-3	1.466	<i>slpD</i>	proteinase
SCO5444	1.36E-3	1.450	<i>glgP</i>	glycogen phosphorylase
SCO5806	1.36E-3	1.401		hypothetical protein
SCO1611	1.36E-3	1.420		short chain dehydrogenase
SCO1612	1.36E-3	1.441		aldehyde dehydrogenase
SCO1590	1.35E-3	1.461		hypothetical protein
SCO1384	1.35E-3	1.443		hypothetical protein
SCO2522	1.35E-3	1.409		hypothetical protein
SCO3845	1.35E-3	1.451		protein phosphatase
SCO6482	1.34E-3	1.439		hypothetical protein
SCO4568	1.34E-3	1.408	<i>nuoG</i>	NADH dehydrogenase subunit G
SCO3326	1.34E-3	1.428		epimerase
SCO5028	1.34E-3	1.411		ATP-binding protein
SCO3721	1.34E-3	1.466		carbonic anhydrase
SCO2062	1.34E-3	1.413		hypothetical protein
SCO6437	1.34E-3	1.405		hypothetical protein
SCO5461	1.33E-3	1.429		hypothetical protein
SCO2035	1.33E-3	1.439		hypothetical protein

SCO0780	1.33E-3	1.404		zinc-binding oxidoreductase
SCO2088	1.33E-3	1.416	<i>murF</i>	UDP-N-acetylmuramoylalanyl-D-glutamyl-2, 6-diaminopimelate- D-alanyl-alanyl ligase
SCO2473	1.32E-3	1.470		nitrate reductase
SCO5315	1.32E-3	1.429	<i>whiE</i> , ORFVI	polyketide cyclase
SCO5803	1.32E-3	1.474	<i>lexA</i>	LexA repressor
SCO1639	1.32E-3	1.436	<i>fkpA</i>	peptidyl-prolyl cis-trans isomerase
SCO0591	1.32E-3	1.433		lysozyme
SCO1993	1.32E-3	1.443		hypothetical protein
SCO2390	1.32E-3	1.401	<i>fabF</i>	3-oxoacyl-ACP synthase
SCO7036	1.31E-3	1.412	<i>argG</i>	argininosuccinate synthase
SCO4141	1.31E-3	1.462	<i>pstC</i>	phosphate ABC transporter permease
SCO2822	1.31E-3	1.469		decarboxylase
SCO5466	1.31E-3	1.458		hydrolase
SCO2079	1.31E-3	1.400		hypothetical protein
SCO1507	1.31E-3	1.414		hypothetical protein
SCO2253	1.31E-3	1.404		hypothetical protein
SCO4774	1.30E-3	1.459		glycerol phosphate dehydrogenase
SCO5249	1.30E-3	1.456		nucleotide-binding protein
SCO4421	1.30E-3	1.417		TetR family transcriptional regulator
SCO2241	1.30E-3	1.459		glutamine synthetase
SCO4677	1.30E-3	1.468	<i>rsfA</i>	regulatory protein
SCO4881	1.29E-3	1.462		polysaccharide biosynthesis-like protein
SCO0597	1.29E-3	1.417		hypothetical protein
SCO2900	1.29E-3	1.421		hypothetical protein
SCO7057	1.28E-3	1.460		esterase
SCO5539	1.28E-3	1.420	<i>cvnB2</i>	hypothetical protein
SCO0654	1.28E-3	1.410	<i>gvpZ2</i>	hypothetical protein
SCO6714	1.28E-3	1.411		hydroxylase
SCO2813	1.28E-3	1.464		hypothetical protein
SCO4907	1.28E-3	1.428	<i>afsQ1</i>	transcriptional regulator
SCO5556	1.28E-3	1.418	<i>hupS</i>	histone-like DNA binding protein
SCO7028	1.28E-3	1.409	<i>bxlE</i>	sugar-binding lipoprotein
SCO0932	1.28E-3	1.447		hypothetical protein

SCO3887	1.27E-3	1.434	<i>parB</i>	partitioning or sporulation protein
SCO1473	1.27E-3	1.418	<i>fmt</i>	methionyl-tRNA formyltransferase
SCO5693	1.27E-3	1.416		acyl CoA dehydrogenase
SCO6014	1.27E-3	1.437		cationic amino acid transporter
SCO1141	1.27E-3	1.423		hypothetical protein
SCO1050	1.27E-3	1.426		DNA protection protein
SCO6218	1.27E-3	1.446		phosphatase
SCO4077	1.27E-3	1.425		phosphoribosylformylglycinamide synthase subunit PurS
SCO5586	1.27E-3	1.453	<i>ffh</i>	signal recognition particle protein
SCO2238	1.26E-3	1.449	<i>nadE</i>	NAD(+) synthase (glutamine-hydrolysing)
SCO2958	1.26E-3	1.460		bifunctional uroporphyrinogen-III synthetase/re- sponse regulator domain-containing protein
SCO4880	1.26E-3	1.414		transferase
SCO6059	1.26E-3	1.407		hypothetical protein
SCO5583	1.26E-3	1.462	<i>amtB</i>	ammonium transporter
SCO7072	1.25E-3	1.442		hypothetical protein
SCO3652	1.25E-3	1.404		hypothetical protein
SCO6416	1.25E-3	1.416		oxidoreductase
SCO1643	1.25E-3	1.412	<i>pcrA</i>	20S proteasome alpha-subunit
SCO5668	1.25E-3	1.406		polyamine ABC transporter ATP-binding protein
SCO0726	1.25E-3	1.417		oxidoreductase
SCO1996	1.25E-3	1.409	<i>coaE</i>	dephospho-CoA kinase
SCO2021	1.25E-3	1.430		hypothetical protein
SCO2232	1.24E-3	1.456	<i>malR</i>	maltose operon transcriptional repressor
SCO6476	1.24E-3	1.444		adenylosuccinate lyase
SCO4038	1.24E-3	1.421		deaminase
SCO5533	1.24E-3	1.419		hypothetical protein
SCO1766	1.23E-3	1.447		glycohydrolase
SCO5465	1.22E-3	1.413		hypothetical protein
SCO6637	1.22E-3	1.439		hypothetical protein
SCO0509	1.22E-3	1.410	<i>glpK2</i>	glycerol kinase
SCO0648	1.22E-3	1.426		methyltransferase
SCO4675	1.22E-3	1.416		hypothetical protein
SCO4055	1.21E-3	1.406		alcohol dehydrogenase

Appendix IV

SCO2529	1.21E-3	1.429		metalloprotease
SCO0398	1.20E-3	1.420		glycosyl transferase
SCO2140	1.19E-3	1.409		transcriptional regulator
SCO0582	1.19E-3	1.410		transcriptional regulator
SCO2385	1.19E-3	1.416		hypothetical protein
SCO1153	1.17E-3	1.424		acyl-CoA thioesterase II
SCO5585	1.17E-3	1.414	<i>glnD</i>	PII uridylyl-transferase
SCO5116	1.16E-3	1.406	<i>bldKE</i>	peptide transport system ATP-binding subunit
SCO2950	1.14E-3	1.401	<i>hup, hupA</i>	DNA-binding protein HU (hs1)

Table S4. List of proteins with a VIP > 1.4 and a regression coefficient < 0 based on the PLS model using CFU as a Y variable.

Locus tag	Coef.	VIP	Gene	Gene product
SCO2164	-1.40E-3	1.426		integral membrane efflux protein
SCO0852	-1.39E-3	1.407		aldolase
SCO2478	-1.38E-3	1.446		reductase
SCO6019	-1.38E-3	1.450		hypothetical protein
SCO6009	-1.37E-3	1.418		solute-binding protein
SCO2162	-1.37E-3	1.440		quinolinate synthetase
SCO6027	-1.36E-3	1.458		acetyl-CoA acetyltransferase
SCO5178	-1.35E-3	1.455	<i>moeB</i>	molybdopterin biosynthesis-like protein MoeZ
SCO0960	-1.34E-3	1.451		hydrolase
SCO2614	-1.34E-3	1.457	<i>fpgS</i>	folylpolyglutamate synthase
SCO2593	-1.34E-3	1.460		hypothetical protein
SCO2369	-1.33E-3	1.455		thiol-specific antioxidant protein
SCO2532	-1.33E-3	1.463		PhoH-like protein
SCO1594	-1.32E-3	1.442	<i>pheT</i>	phenylalanyl-tRNA synthetase subunit beta
SCO2013	-1.32E-3	1.444		two-component system response regulator
SCO1424	-1.31E-3	1.447		hypothetical protein
SCO3420	-1.30E-3	1.409		aldehyde dehydrogenase
SCO1296	-1.30E-3	1.433		hypothetical protein
SCO6445	-1.30E-3	1.446		inositol monophosphatase
SCO5523	-1.30E-3	1.467	<i>ilvE</i>	branched-chain amino acid aminotransferase
SCO2065	-1.29E-3	1.400		hypothetical protein
SCO6026	-1.29E-3	1.419		fatty acid oxidation complex alpha-subunit
SCO4827	-1.29E-3	1.442	<i>mdh</i>	malate dehydrogenase
SCO6148	-1.29E-3	1.445		hypothetical protein
SCO4709	-1.28E-3	1.404	<i>rplP</i>	50S ribosomal protein L16
SCO3947	-1.28E-3	1.409	<i>cydCD</i>	ABC transporter
SCO3890	-1.28E-3	1.425	<i>trxB</i>	thioredoxin reductase
SCO6740	-1.28E-3	1.437		D-amino acid oxidase
SCO1780	-1.28E-3	1.451		DNA repair protein
SCO5044	-1.28E-3	1.452	<i>fumB</i>	fumarate hydratase class I

SCO3119	-1.28E-3	1.454		hypothetical protein
SCO6102	-1.27E-3	1.404		nitrite/sulfite reductase
SCO6097	-1.27E-3	1.414	<i>cysN</i>	sulfate adenyllyltransferase subunit 1
SCO4474	-1.27E-3	1.437		hypothetical protein
SCO2179	-1.27E-3	1.440		leucyl aminopeptidase
SCO1345	-1.26E-3	1.411	<i>fabG2</i>	3-ketoacyl-ACP reductase
SCO5405	-1.26E-3	1.417		transcriptional regulator
SCO4506	-1.26E-3	1.424		hypothetical protein
SCO1081	-1.26E-3	1.426		electron transfer flavoprotein subunit alpha
SCO1905	-1.26E-3	1.426		hypothetical protein
SCO2615	-1.26E-3	1.429	<i>valS</i>	valyl-tRNA synthetase
SCO1484	-1.26E-3	1.434	<i>pyrAA</i>	carbamoyl phosphate synthase small subunit
SCO1580	-1.26E-3	1.437	<i>argC</i>	N-acetyl-gamma-glutamyl-phosphate reductase
SCO5172	-1.26E-3	1.439		hydrolase
SCO2004	-1.26E-3	1.443		formate dehydrogenase
SCO1546	-1.26E-3	1.447		aminotransferase
SCO4963	-1.25E-3	1.404		ABC transporter ATP-binding protein
SCO0909	-1.25E-3	1.405		hypothetical protein
SCO2935	-1.25E-3	1.414	<i>scrX</i>	transcriptional regulator
SCO6031	-1.25E-3	1.421	<i>hemE</i>	uroporphyrinogen decarboxylase
SCO1557	-1.25E-3	1.422		lipoprotein
SCO5024	-1.25E-3	1.424		oxidoreductase
SCO0408	-1.25E-3	1.427		methyltransferase
SCO1481	-1.25E-3	1.428	<i>pyrF</i>	orotidine 5'-phosphate decarboxylase
SCO4209	-1.25E-3	1.433	<i>pgm</i>	phosphoglyceromutase
SCO6042	-1.25E-3	1.438		hypothetical protein
SCO6264	-1.25E-3	1.439		reductase
SCO4244	-1.25E-3	1.458		hypothetical protein
SCO6279	-1.24E-3	1.406		diaminobutyrate-pyruvate aminotransferase
SCO2291	-1.24E-3	1.420	<i>axeA</i>	acetylxylen esterase
SCO1482	-1.24E-3	1.425	<i>pyrD</i>	dihydroorotate dehydrogenase 2
SCO1921	-1.24E-3	1.431		aminotransferase
SCO1661	-1.24E-3	1.442		glycerol-3-phosphate dehydrogenase
SCO6099	-1.23E-3	1.401	<i>cysC</i>	adenyllysulfate kinase

SCO3945	-1.23E-3	1.407	<i>cydA</i>	cytochrome oxidase subunit I
SCO4587	-1.23E-3	1.407		hypothetical protein
SCO4683	-1.23E-3	1.422	<i>gdhA</i>	glutamate dehydrogenase
SCO6090	-1.23E-3	1.422		antibiotic resistance macrolide glycosyltransferase
SCO6819	-1.23E-3	1.431	<i>aroA</i>	3-phosphoshikimate 1-carboxyvinyltransferase
SCO6091	-1.23E-3	1.438		hypothetical protein
SCO5520	-1.22E-3	1.405		delta-1-pyrroline-5-carboxylate dehydrogenase
SCO4186	-1.22E-3	1.411		hypothetical protein
SCO0769	-1.22E-3	1.419		aldo/keto reductase
SCO2913	-1.22E-3	1.424		hypothetical protein
SCO1223	-1.22E-3	1.426	<i>rocD</i>	ornithine aminotransferase
SCO1487	-1.21E-3	1.412	<i>pyrB</i>	aspartate carbamoyltransferase catalytic subunit
SCO4494	-1.21E-3	1.412		hypothetical protein
SCO2640	-1.21E-3	1.414	<i>asd1</i>	aspartate-semialdehyde dehydrogenase
SCO1222	-1.21E-3	1.420		hypothetical protein
SCO3877	-1.21E-3	1.424		6-phosphogluconate dehydrogenase
SCO1488	-1.21E-3	1.424	<i>pyrR</i>	bifunctional pyrimidine regulatory protein PyrR uracil phosphoribosyltransferase
SCO5976	-1.20E-3	1.408	<i>arcB</i>	ornithine carbamoyltransferase
SCO2634	-1.20E-3	1.412		hypothetical protein
SCO1570	-1.20E-3	1.415	<i>argH</i>	argininosuccinate lyase
SCO4253	-1.20E-3	1.415		hypothetical protein
SCO1578	-1.20E-3	1.420	<i>argB</i>	acetylglutamate kinase
SCO3345	-1.20E-3	1.426		dihydroxy-acid dehydratase
SCO1577	-1.20E-3	1.427	<i>argD</i>	acetylornithine aminotransferase
SCO1483	-1.20E-3	1.431	<i>pyrA</i>	carbamoyl phosphate synthase large subunit
SCO5389	-1.19E-3	1.403		hypothetical protein
SCO3096	-1.19E-3	1.421	<i>eno</i>	phosphopyruvate hydratase
SCO1579	-1.19E-3	1.422	<i>argJ</i>	bifunctional ornithine acetyltransferase/N-acetylglutamate synthase
SCO1868	-1.19E-3	1.443		hypothetical protein
SCO1523	-1.18E-3	1.413		pyridoxal biosynthesis lyase PdxS
SCO1086	-1.17E-3	1.408		hypothetical protein

Appendix IV

SCO1486	-1.16E-3	1.406	<i>pyrC</i>	dihydroorotase
SCO3127	-1.16E-3	1.408	<i>ppc</i>	phosphoenolpyruvate carboxylase
SCO3889	-1.16E-3	1.409	<i>trxA</i>	thioredoxin
SCO5554	-1.15E-3	1.408	<i>leuD</i>	isopropylmalate isomerase small subunit
SCO1916	-1.14E-3	1.406		transferase
SCO6220	-1.12E-3	1.403		hypothetical protein

Curriculum vitae

Zheren Zhang was born on 18 August 1991 in Xinyang, China. In 2008, he started a bachelor's program in veterinary medicine at South China Agricultural University in Guangzhou, China. Soon after arriving, he participated and passed one entrance examination and interview, allowing him to be enrolled in Dingying class specializing in animal science. Since 2010, he worked as an intern in the laboratory of Prof. dr. Mei Hong, studying the functions of drug transporter proteins in animals. After spending two years on bench work, he obtained a bachelor's degree with distinction. Later, he decided to move abroad for the master's program in microbial biotechnology and health at Leiden University after receiving the Leiden University Excellence Scholarship. Upon arrival in January 2013, he started an internship under the supervision of Dr. Daniel Rozen and Prof. dr. Dennis Claessen. During the next two years, he completed two research projects where he revisited a known phenomenon in *Streptomyces coelicolor*, genomic instability. According to his preliminary results, he wrote a successful proposal to fund his doctoral studies from the China Scholarship Council. In March 2015, he initiated his Ph.D. under the supervision of Dr. Daniel Rozen, Prof. dr. Dennis Claessen and Prof. dr. Gilles van Wezel and the majority of his Ph.D. work is presented in this thesis. Zheren will soon join the laboratory of Prof. dr. Stuart West at the Department of Zoology, University of Oxford (United Kingdom).

List of publications

- Z. Zhang**, B. Claushuis, D. Claessen, D. E. Rozen. Mutational meltdown of microbial altruists in *Streptomyces coelicolor* colonies. *bioRxiv* (2020).
- Z. Zhang**, C. Du, F. de Barsey, M. Liem, A. Liakopoulos, G. P. van Wezel, Y. H. Choi, D. Claessen, D. E. Rozen. Antibiotic production in *Streptomyces* is organized by a division of labor through terminal genomic differentiation. *Science Advances* (2020).
- Z. Zhang**, D. Claessen, D. E. Rozen. Understanding microbial divisions of labor. *Frontiers in Microbiology* (2016).
- K. Ramijan, **Z. Zhang**, G. P. van Wezel, D. Claessen. Genome rearrangements and megaplasmid loss in the filamentous bacterium *Kitasatospora viridifaciens* are associated with protoplast formation and regeneration. *Antonie van Leeuwenhoek* (2020).
- K. Ramijan. E. Ultee, J. Willemse, **Z. Zhang**, J. A. J. Wondergem, A. van der Meij, D. Heinrich, A. Briegel, G. P. van Wezel, D. Claessen. Stress-induced formation of cell wall-deficient cells in filamentous actinomycetes. *Nature Communications* (2018).
- S. Westhoff, T. M. van Leeuwe, O. Qachach, **Z. Zhang**, G. P. van Wezel, D. E. Rozen. The evolution of no-cost resistance at sub-MIC concentrations of streptomycin in *Streptomyces coelicolor*. *The ISME Journal* (2017).
- X. Liu, J. Huang, Y. Sun, K. Zhan, **Z. Zhang**, M. Hong. Identification of multiple binding sites for substrate transport in bovine organic anion transporting polypeptide 1a2. *Drug Metabolism and Disposition* (2013).
- Y. Yu, X. Liu, **Z. Zhang**, Y. Xiao, M. Hong. Cloning and functional characterization of the pig (*Sus scrofa*) organic anion transporting polypeptide 1a2. *Xenobiotica* (2013).